NACA RM A9G18

NACA

RESEARCH MEMORANDUM

EFFECTS OF SYSTEMATIC CHANGES OF TRAILING-EDGE ANGLE AND LEADING-EDGE RADIUS ON THE VARIATION WITH MACH NUMBER OF THE AERODYNAMIC CHARACTERISTICS OF A 10-PERCENT-CHORD-THICK NACA AIRFOIL SECTION

By James L. Summers and Donald J. Graham

Ames Aeronautical Laboratory
Moffett Field, Calif.

NATIONAL ADVISORY COMMITTEE
FOR AERONAUTICS

WASHINGTON
September 26, 1949

NATIONAL ADVISORY COMMITTEE FOR AERONAUTICS

RESEARCH MEMORANDUM

EFFECTS OF SYSTEMATIC CHANGES OF TRAILING-EDGE ANGLE AND LEADING-EDGE RADIUS ON THE VARIATION WITH MACH NUMBER OF THE AERODYNAMIC CHARACTERISTICS OF A 10-PERCENT-CHORD-THICK NACA AIRFOIL SECTION

By James L. Summers and Donald J. Graham

SUMMARY

The results of a wind-tunnel investigation of the effects of variation of trailing-edge angle and leading-edge radius on the aerodynamic characteristics of a 10-percent-chord-thick airfoil section at Mach numbers from 0.3 to 0.9 are presented. The corresponding Reynolds number range of the investigation is from approximately 1,000,000 to 2,000,000.

The variation of section lift coefficient with Mach number at low and moderate angles of attack is indicated to be little affected by trailing-edge-angle variation within the limits of 18° and 6° and by leading-edge-radius variation within the limits of 1.10 and 0.27 percent of the airfoil chord. The maximum section lift coefficient at Mach numbers above 0.7 is increased significantly by decreases in either the trailing-edge angle or the leading-edge radius. The section lift-curve slope is almost uniformly increased at Mach numbers below that corresponding to the break in lift (approximately 0.8 Mach number) by reductions in these two parameters.

The Mach number of drag divergence is adversely affected at low section lift coefficients by reductions in the trailing-edge angle and the leading-edge radius; the trailing-edge angle exerts considerably the greater effect. The variation of section drag coefficient with section lift coefficient is generally more favorable at Mach numbers above 0.6 for the profiles with the smaller trailing-edge angles.

Section moment coefficients are not significantly affected by variation of either the trailing-edge angle or the leading-edge radius within the limits of the present investigation.

INTRODUCTION

A great amount of interest has been displayed recently in the influence of two parameters of airfoil geometry, the trailing-edge angle

and the leading-edge radius, on the variation of the aerodynamic characteristics of airfoil sections with Mach number. B. Göthert, in reference 1, demonstrated a significant effect of trailing-edge-angle variation on the lift characteristics of two airfoil sections at high subsonic Mach numbers. Göthert also showed an appreciable effect of leading-edge-radius variation on the drag characteristics of an airfoil section at supercritical Mach numbers. Various other experimental investigations have also indicated the influence of the trailing-edge angle, particularly with respect to the variation with Mach number of the effectiveness of a trailing-edge control surface (reference 2). These latter cases, however, constitute more or less isolated observations of a phenomenon, no correlation being possible because the trailing-edge angle was not the sole variable. Göthert's work represents the only available study of the effects of systematic, if not altogether rational, variations of the two shape parameters. It is of somewhat limited value, however, in that only two basic airfoil sections were investigated, one of which, the NACA 23015, is generally considered unsuitable for most high Mach number applications.

To amplify the information on the subject, a program of airfoil tests has been undertaken in the Ames 1- by 3-1/2-foot high-speed wind tunnel with the objective of determining for several thickness-chord ratios the separate effects of systematic changes in the trailing-edge angle and the leading-edge radius on the aerodynamic characteristics of an airfoil section at high subsonic Mach numbers. The base profile is of the modified NACA 4-digit series (see reference 3) with the maximum thickness at the 40-percent-chord station. The thickness-chord ratios range from 4 to 10 percent. The present report presents the results of the tests for the thickness-chord ratio of 10 percent.

NOTATION

c_d	section drag coefficient
$c_{d_{min}}$	minimum section drag coefficient
c_l	section lift coefficient
$c_{l_{max}}$	maximum section lift coefficient
$c_{m_{c/4}}$	section pitching-moment coefficient about the quarter-chord point
M	Mach number
R	Reynolds number
V	free-stream velocity, feet per second

a_o section lift-curve slope at zero lift coefficient, per degree

c airfoil chord, feet

v local velocity, feet per second

Δv_a increment in local velocity corresponding to additional type of load distribution, feet per second

x distance along chord, fractions of chord

y distance perpendicular to chord, fractions of chord

α_o section angle of attack, degrees

DESCRIPTION OF AIRFOILS

The airfoil sections presently investigated are listed in the following table:

NACA airfoil designation	Trailing-edge angle (deg)	Leading-edge radius (percent chord)
0010-1.10 40/1.575	17.9	1.10
0010-1.10 40/1.051	12	1.10
0010-1.10 40/0.524	6	1.10
0010-0.70 40/1.575	17.9	.70
0010-0.70 40/1.051	12	.70
0010-0.70 40/0.524	6	.70
0010-0.27 40/1.575	17.9	.27
0010-0.27 40/1.051	12	.27
0010-0.27 40/0.524	6	.27

The airfoil numbering system is the same as that employed by Göthert in reference 1. The first group of four digits in the above numbering system has the same significance as the designation given in reference 4: The first digit indicates the camber in percent of the chord; the second, the position of the camber in tenths of the chord from the leading edge; and the last two, the maximum thickness in percent of the chord. The decimal number following the dash is the leading-edge-radius index; the leading-edge radius as a fraction of the airfoil chord is given by the product of the radius index and the square of the thickness-chord ratio. The radius index of 1.10 is normal for the commonly used NACA 4-digit-series airfoil sections. The two digits immediately preceding the virgule represent the position of maximum

thickness in percent of the chord from the leading edge. The last decimal number is the trailing-edge-angle index, the angle being twice the arc tangent of the product of the angle index and the thickness-chord ratio. The trailing-edge-angle index of 1.575 is considered normal for the NACA 4-digit-series airfoil sections with maximum thickness at 40 percent of the chord. (See reference 3.)

The airfoil-thickness forms are defined by two equations (given in reference 3 and reproduced below). The ordinates from the leading edge to the position of maximum thickness are given by the equation

$$y = a_0\sqrt{x} + a_1x + a_2x^2 + a_3x^3$$

The ordinates from the position of maximum thickness to the trailing edge are given by the equation

$$y = d_0 + d_1(1-x) + d_2(1-x)^2 + d_3(1-x)^3$$

The coefficients of the equations are determined as described in reference 3. The coefficient a_0 is equal to the square root of twice the leading-edge radius and the coefficient d_1 is equal to the tangent of one-half of the trailing-edge angle. By means of the two equations the leading-edge radius and the trailing-edge angle can be specified independently. The nature of these equations is such that changes in the trailing-edge angle also result in minor alterations of the airfoil-thickness distribution forward of the maximum-thickness position.

The coordinates of the airfoil sections tested are given in tables I to IX. The airfoil profiles and theoretical pressure distributions are illustrated in figure 1.

APPARATUS AND TESTS

The tests were made in the Ames 1- by 3-1/2-foot high-speed wind tunnel, a low-turbulence two-dimensional-flow wind tunnel.

The airfoil models were of 6-inch chord and were constructed of aluminum alloy. The models entirely spanned the short dimension of the wind-tunnel test section. Two-dimensional flow was preserved through the use of contoured sponge-rubber gaskets compressed between the model ends and the tunnel walls (to prevent end leakage).

Measurements of lift, drag, and quarter-chord pitching moment were made at Mach numbers from 0.3 to as high as 0.9 for each of the models at angles of attack increasing by 1° or 2° increments from -2° to 12°. This range of angles of attack was sufficient to encompass the lift stall at all but the highest Mach numbers. The Reynolds number variation with Mach number for the tests is illustrated in figure 2.

Lift and pitching moments were evaluated by a method similar to that described in reference 5 from integrations of the pressure reactions on the tunnel walls of the forces on the airfoils. Drag values were determined from wake-survey measurements utilizing a rake of total-head tubes.

ACCURACY OF MEASUREMENT

The several sources of error affecting the results presented herein are listed below with estimates of their magnitudes. In no cases are the inaccuracies sufficiently large to affect the significance of the results.

Previous comparisons of drag coefficients measured in the Ames 1- by 3-1/2-foot high-speed wind tunnel with values more accurately established from tests in other facilities indicate a maximum error of the order of 5 percent in the determination of the drag coefficient. The instrument used to measure lift and pitching moment is inaccurate for small values of force and moment by virtue of large instrument tares. It is difficult to assess the magnitude of error in measurement from this source because it is not likely to be consistent.

The angle of attack is established by reference to a pair of selected points on the surface of the profile by means of an adjustable template. Errors inherent in airfoil fabrication and in the initial setting of this template to the reference points can cause a maximum error of 0.1° in the angle of attack. In addition, the instrument employed to measure the angular setting can be read only to be the nearest 0.1°; the possibility of an additional error in angle of attack of 0.05° exists from this cause.

RESULTS AND DISCUSSION

Section lift, drag, and quarter-chord pitching-moment coefficients are presented as functions of Mach number at constant angles of attack in figures 3, 4, and 5, respectively. The angles of attack indicated in the figures represent nominal values only, being subject to the experimental errors discussed in the preceding section. The failure to realize zero lift at zero incidence for all of the profiles (fig. 3) is due to a combination of the previously discussed inaccuracies of measurement. The characteristics have been corrected for tunnel-wall interference by the methods of reference 6. The dashed portions of the curves shown in the figures at the higher Mach numbers serve to indicate the region of possible influence of wind-tunnel choking effects on the results.

From figures 3, 4, and 5, no striking differences in aerodynamic characteristics are observed to result from the variation of either the

trailing-edge angle or the leading-edge radius. The Mach number of lift divergence is sensibly the same for all of the trailing-edge angles and leading-edge radii investigated. At the lower angles of attack the Mach number for which the section drag coefficient abruptly increases, the drag-divergence Mach number , increases with increasing trailing-edge angle. Increasing the leading-edge radius is indicated to increase slightly the drag-divergence Mach number. The rate of increase of drag coefficient with Mach number above that for drag divergence does not appear to be affected by changes in either parameter. No significant differences in the variation of section pitching-moment coefficient with Mach number are indicated for the various trailing-edge angles and leading-edge radii.

At an angle of attack of 8°, nearly all the profiles investigated exhibited an abrupt decrease in the section drag coefficient followed by a rapid rise in drag as the Mach number is increased from 0.65 to 0.75 (fig. 4). An abrupt increase in the section lift coefficient is seen to accompany this decrease in section drag coefficient (fig. 3). This phenomenon has been observed in previous airfoil tests and is believed to be the result of an abrupt transition from a type of flow associated with low Reynolds numbers to that representative of moderately large Reynolds numbers. Schlieren photographs (fig. 6) of the flow about the NACA 0010-1.10 40/1.051 airfoil section at 8° angle of attack tend to support this belief in indicating that a marked change in the boundary-layer flow occurs between the Mach numbers of 0.707 and 0.731. Similar changes were noted for the other airfoil sections (in this general region) at Mach numbers near these values.

In figure 7, section lift coefficient as a function of section angle of attack is plotted at constant Mach number for the various profiles. The only outstanding difference in the characteristics of the profiles is in the magnitude of the maximum section lift coefficient at Mach numbers above 0.7; the value of this parameter increases with progressive decreases in both the trailing-edge and the leading-edge radius. This characteristic is more clearly indicated in figures 8 and 9, which illustrate the variations with Mach number of maximum section lift coefficient and section lift-curve slope for the several combinations of trailing-edge angle and leading-edge radius. The greatest gain in maximum section lift coefficient with decreasing trailing-edge angle is observed for the profile with the normal leading-edge radius (1.10-percent c). The most favorable maximum lift characteristics are realized for the NACA 0010-0.70 40/0.524 section, however.

At the lower Mach numbers, the maximum section lift coefficients are probably not quantitatively representative of full-scale characteristics by virtue of the relatively low Reynolds numbers of the present investigation. The results of the investigation of reference 7

have indicated, however, that, at Mach numbers above approximately 0.6, Reynolds number effects on maximum lift coefficient are of small significance and Mach number effects predominate. It is therefore believed that the present conclusions drawn with respect to the effects of trailing-edge-angle and leading-edge-radius variation on the maximum section lift coefficient at supercritical Mach numbers are valid for full-scale conditions.

With reference again to figures 8 and 9, no important difference in the variation of section lift-curve slope with Mach number is seen to result from the variation of either the trailing-edge angle or the leading-edge radius. In general, the magnitude of the section lift-curve slope is increased appreciably at Mach numbers below that corresponding to the lift break by decreases in either or both the trailing-edge angle and the leading-edge radius.

Section drag coefficient as a function of section lift coefficient at constant Mach number is shown in figure 10 for the profiles investigated. The minimum section drag coefficient at Mach numbers above 0.7 is adversely affected by decreases in the trailing-edge angle. (See fig. 11). From the data of figure 12, the leading-edge radius is observed to have a less pronounced effect, the largest values of minimum section drag coefficient being realized for the smallest leading-edge radius. The higher drag coefficients in each of these figures for the NACA 0010-0.27 40/0.524 section at Mach numbers below that for drag divergence are believed to result from inaccuracies in the determination of the instrument tare for the test of this profile, a factor which becomes of increasingly less significance with increasing magnitude of the drag coefficient. The poorer minimum drag characteristics of the airfoil sections with the smaller trailing-edge angles are somewhat offset by a generally more favorable variation of drag coefficient with lift coefficient at Mach numbers greater than 0.6.

Section pitching-moment coefficient is plotted in figure 13 as a function of section lift coefficient at constant Mach number. No outstanding differences are observed to result from the variation of either the trailing-edge angle or the leading-edge radius.

CONCLUSIONS

The results of a wind-tunnel investigation of the effects of systematic variations of trailing-edge angle and leading-edge radius on the variation with Mach number of the aerodynamic characteristics of a 10-percent-chord-thick symmetrical airfoil section with maximum thickness at 40 percent of the chord indicate the following:

1. The variation of section lift coefficient with Mach number at low and moderate angles of attack is little affected by trailing-edge-angle variation within the limits of 18° and 6°, and by leading-edge-radius variation within the limits of 1.10 and 0.27 percent of the airfoil chord.

2. The maximum section lift coefficient at Mach numbers above 0.7 increases with decreases in either the trailing-edge angle or the leading-edge radius. In the present investigation, the most favorable variation of maximum section lift coefficient with Mach number was realized with a leading-edge radius of 0.7 percent of the chord and a trailing-edge angle of 6°.

3. The section lift-curve slope is almost uniformly increased at Mach numbers below that for the lift break (approximately 0.8 Mach number) by decreases in either the trailing-edge angle or the leading-edge radius.

4. At low section lift coefficients, the drag-divergence Mach number is adversely affected by reductions in the trailing-edge angle and the leading-edge radius, the former having the predominant effect. For the normal leading-edge radius of the sections investigated, the drag-divergence Mach number at zero lift was approximately 0.05 higher for the normal profile trailing-edge angle of 17.9° than for the 6° angle.

5. The variation of section drag coefficient with section lift coefficient is generally more favorable at Mach numbers above 0.6 for the airfoil sections with the smaller trailing-edge angles.

6. Section pitching-moment characteristics are not significantly affected by variations of either the trailing-edge angle or the leading-edge radius within the limits of the present investigation.

Ames Aeronautical Laboratory,
National Advisory Committee for Aeronautics,
Moffett Field, Calif.

REFERENCES

1. Göthert, B.: German High Speed Wind Tunnel Results collected by B. Göthert with comments by W. A. Mair, RAE TN AERO 1684, August 1945.

2. Stevenson, David B., and Adler, Alfred A.: High-Speed Wind-Tunnel Tests of an NACA 0009-64 Airfoil Having a 33.4-Percent-Chord Flap with an Overhang 20.1 Percent of the Flap Chord. NACA TN 1417, 1947.

3. Stack, John, and von Doenhoff, Albert E.: Tests of 16 Related Airfoils at High Speeds. NACA Rep. 492, 1934.

4. Jacobs, Eastman N., Ward, Kenneth E., and Pinkerton, Robert M.: The Characteristics of 78 Related Airfoil Sections from Tests in the Variable-Density Wind Tunnel. NACA Rep. 460, 1933.

5. Abbott, Ira H., von Doenhoff, Albert E., and Stivers, Louis S., Jr.: Summary of Airfoil Data. NACA Rep. 824, 1945.

6. Allen, H. Julian, and Vincenti, Walter G.: Wall Interference in a Two-Dimensional-Flow Wind Tunnel, With Consideration of the Effect of Compressibility. NACA Rep. 782, 1944.

7. Spreiter, John R., and Steffen, Paul J.: Effect of Mach and Reynolds Numbers on Maximum Lift Coefficient. NACA TN 1044, 1946.

TABLE I.- COORDINATES AND THEORETICAL PRESSURE DISTRIBUTIONS FOR THE NACA 0010-1.10 40/1.575 AIRFOIL SECTION

x (percent c)	y (percent c)	$(v/V)^2$	v/V	$\Delta v_a/V$
0	0	0	0	2.324
1.25	1.511	1.108	1.053	1.286
2.5	2.044	1.245	1.116	.966
5.0	2.722	1.286	1.134	.690
7.5	3.178	1.277	1.130	.556
10	3.533	1.269	1.127	.475
15	4.056	1.261	1.123	.377
20	4.411	1.248	1.117	.316
30	4.856	1.244	1.116	.241
40	5.000	1.242	1.115	.193
50	4.856	1.231	1.110	.155
60	4.433	1.211	1.101	.126
70	3.733	1.155	1.074	.098
80	2.767	1.089	1.043	.072
90	1.556	.980	.990	.045
95	.856	.912	.955	.030
100	.100	0	0	0

L.E. radius: 1.10-percent chord

TABLE II.- COORDINATES AND THEORETICAL PRESSURE DISTRIBUTIONS FOR THE NACA 0010-1.10 40/1.051 AIRFOIL SECTION

x (percent c)	y (percent c)	$(v/V)^2$	v/V	$\Delta v_a/V$
0	0	0	0	2.385
1.25	1.466	1.170	1.082	1.304
2.5	1.966	1.250	1.118	.955
5.0	2.589	1.246	1.116	.674
7.5	3.009	1.239	1.113	.546
10	3.337	1.228	1.108	.466
15	3.845	1.216	1.103	.370
20	4.240	1.228	1.108	.313
30	4.791	1.254	1.120	.242
40	5.000	1.267	1.126	.194
50	4.783	1.245	1.116	.157
60	4.197	1.177	1.085	.123
70	3.338	1.111	1.054	.095
80	2.305	1.037	1.018	.070
90	1.193	.932	.965	.044
95	.638	.861	.928	.030
100	.100	0	0	0
L.E. radius: 1.10-percent chord				

TABLE III.- COORDINATES AND THEORETICAL PRESSURE DISTRIBUTIONS FOR THE NACA 0010-1.10 40/0.524 AIRFOIL SECTION

x (percent c)	y (percent c)	$(v/V)^2$	v/V	$\Delta v_a/V$
0	0	0	0	2.530
1.25	1.425	1.175	1.084	1.294
2.5	1.889	1.268	1.126	.957
5.0	2.454	1.240	1.117	.677
7.5	2.836	1.225	1.107	.541
10	3.140	1.202	1.096	.460
15	3.639	1.188	1.090	.366
20	4.064	1.203	1.097	.310
30	4.725	1.274	1.129	.244
40	5.000	1.299	1.140	.195
50	4.709	1.268	1.126	.150
60	3.962	1.189	1.090	.122
70	2.943	1.067	1.033	.092
80	1.836	.986	.993	.067
90	.827	.919	.959	.040
95	.416	.859	.927	.028
100	.100	0	0	0

L.E. radius: 1.10-percent chord

TABLE IV.- COORDINATES AND THEORETICAL PRESSURE DISTRIBUTIONS FOR THE NACA 0010-0.70 40/1.575 AIRFOIL SECTION

x (percent c)	y (percent c)	$(v/V)^2$	v/V	$\Delta v_a/V$
0	0	0	0	2.763
1.25	1.279	1.038	1.019	1.270
2.5	1.782	1.152	1.073	.942
5.0	2.460	1.210	1.100	.674
7.5	2.949	1.226	1.107	.547
10	3.338	1.235	1.112	.469
15	3.926	1.244	1.116	.374
20	4.347	1.254	1.120	.315
30	4.848	1.257	1.121	.240
40	5.000	1.246	1.116	.191
50	4.856	1.230	1.109	.154
60	4.433	1.197	1.094	.124
70	3.733	1.155	1.075	.097
80	2.767	1.087	1.043	.071
90	1.556	.993	.997	.045
95	.856	.888	.943	.030
100	.100	0	0	0
L.E. radius: 0.70-percent chord				

NACA

TABLE V.- COORDINATES AND THEORETICAL PRESSURE DISTRIBUTIONS FOR THE NACA 0010-0.70 40/1.051 AIRFOIL SECTION

x (percent c)	y (percent c)	$(v/V)^2$	v/V	$\Delta v_a/V$
0	0	0	0	2.859
1.25	1.239	1.085	1.042	1.307
2.5	1.705	1.166	1.080	.955
5.0	2.326	1.187	1.090	.677
7.5	2.776	1.198	1.094	.549
10	3.141	1.202	1.096	.471
15	3.721	1.222	1.105	.377
20	4.172	1.237	1.112	.318
30	4.783	1.263	1.124	.245
40	5.000	1.281	1.132	.196
50	4.783	1.253	1.119	.156
60	4.197	1.196	1.094	.125
70	3.338	1.118	1.058	.095
80	2.305	1.037	1.018	.070
90	1.193	.955	.977	.043
95	.638	.861	.928	.028
100	.100	0	0	0

L.E. radius: 0.70-percent chord

NACA

TABLE VI.- COORDINATES AND THEORETICAL PRESSURE DISTRIBUTIONS FOR THE NACA 0010-0.70 40/0.524 AIRFOIL SECTION

x (percent c)	y (percent c)	$(v/V)^2$	v/V	$\Delta v_a/V$
0	0	0	0	3.007
1.25	1.198	1.105	1.051	1.329
2.5	1.628	1.173	1.083	.968
5.0	2.191	1.178	1.085	.681
7.5	2.602	1.169	1.081	.549
10	2.943	1.163	1.079	.469
15	3.515	1.186	1.089	.377
20	3.995	1.217	1.103	.320
30	4.717	1.276	1.130	.248
40	5.000	1.305	1.142	.199
50	4.709	1.274	1.129	.158
60	3.962	1.182	1.087	.123
70	2.943	1.071	1.035	.092
80	1.836	1.001	1.000	.066
90	.827	.909	.953	.039
95	.416	.825	.909	.023
100	.100	0	0	0

L.E. radius: 0.70-percent chord

TABLE VII.– COORDINATES AND THEORETICAL PRESSURE DISTRIBUTIONS FOR THE NACA 0010–0.27 40/1.575 AIRFOIL SECTION

x (percent c)	y (percent c)	$(v/V)^2$	v/V	$\Delta v_a/V$
0	0	0	0	3.857
1.25	.944	.892	.944	1.282
2.5	1.400	1.011	1.005	.950
5.0	2.078	1.113	1.055	.688
7.5	2.611	1.167	1.080	.564
10	3.044	1.200	1.095	.486
15	3.744	1.238	1.113	.389
20	4.244	1.256	1.121	.327
30	4.833	1.265	1.124	.249
40	5.000	1.253	1.119	.197
50	4.856	1.235	1.111	.159
60	4.433	1.205	1.098	.127
70	3.733	1.157	1.076	.100
80	2.767	1.089	1.044	.073
90	1.556	.990	.995	.045
95	.856	.910	.954	.030
100	.100	0	0	0

L.E. radius: 0.27–percent chord

TABLE VIII.- COORDINATES AND THEORETICAL PRESSURE DISTRIBUTIONS FOR THE NACA 0010-0.27 40/1.051 AIRFOIL SECTION

x (percent c)	y (percent c)	$(v/V)^2$	v/V	$\Delta v_a/V$
0	0	0	0	4.044
1.25	.905	.933	.966	1.316
2.5	1.321	1.020	1.010	.940
5.0	1.941	1.092	1.045	.674
7.5	2.434	1.135	1.065	.562
10	2.852	1.168	1.081	.476
15	3.539	1.214	1.102	.382
20	4.074	1.241	1.114	.323
30	4.769	1.284	1.133	.248
40	5.000	1.287	1.134	.197
50	4.783	1.250	1.118	.157
60	4.197	1.196	1.094	.124
70	3.338	1.123	1.060	.095
80	2.305	1.042	1.021	.069
90	1.193	.958	.979	.042
95	.638	.882	.939	.025
100	.100	0	0	0
L.E. radius: 0.27-percent chord				

TABLE IX.- COORDINATES AND THEORETICAL PRESSURE DISTRIBUTIONS FOR THE NACA 0010-0.27 40/0.524 AIRFOIL SECTION

x (percent c)	y (percent c)	$(v/V)^2$	v/V	$\Delta v_a/V$
0	0	0	0	4.175
1.25	.864	.953	.976	1.308
2.5	1.244	1.018	1.009	.948
5.0	1.807	1.077	1.038	.678
7.5	2.259	1.105	1.051	.549
10	2.654	1.134	1.065	.476
15	3.333	1.173	1.083	.382
20	3.898	1.219	1.104	.325
30	4.703	1.278	1.130	.252
40	5.000	1.304	1.142	.204
50	4.709	1.275	1.129	.160
60	3.962	1.181	1.087	.124
70	2.943	1.089	1.044	.094
80	1.836	.991	.996	.068
90	.827	.894	.945	.042
95	.416	.850	.922	.027
100	.100	0	0	0
L.E. radius: 0.27-percent chord				

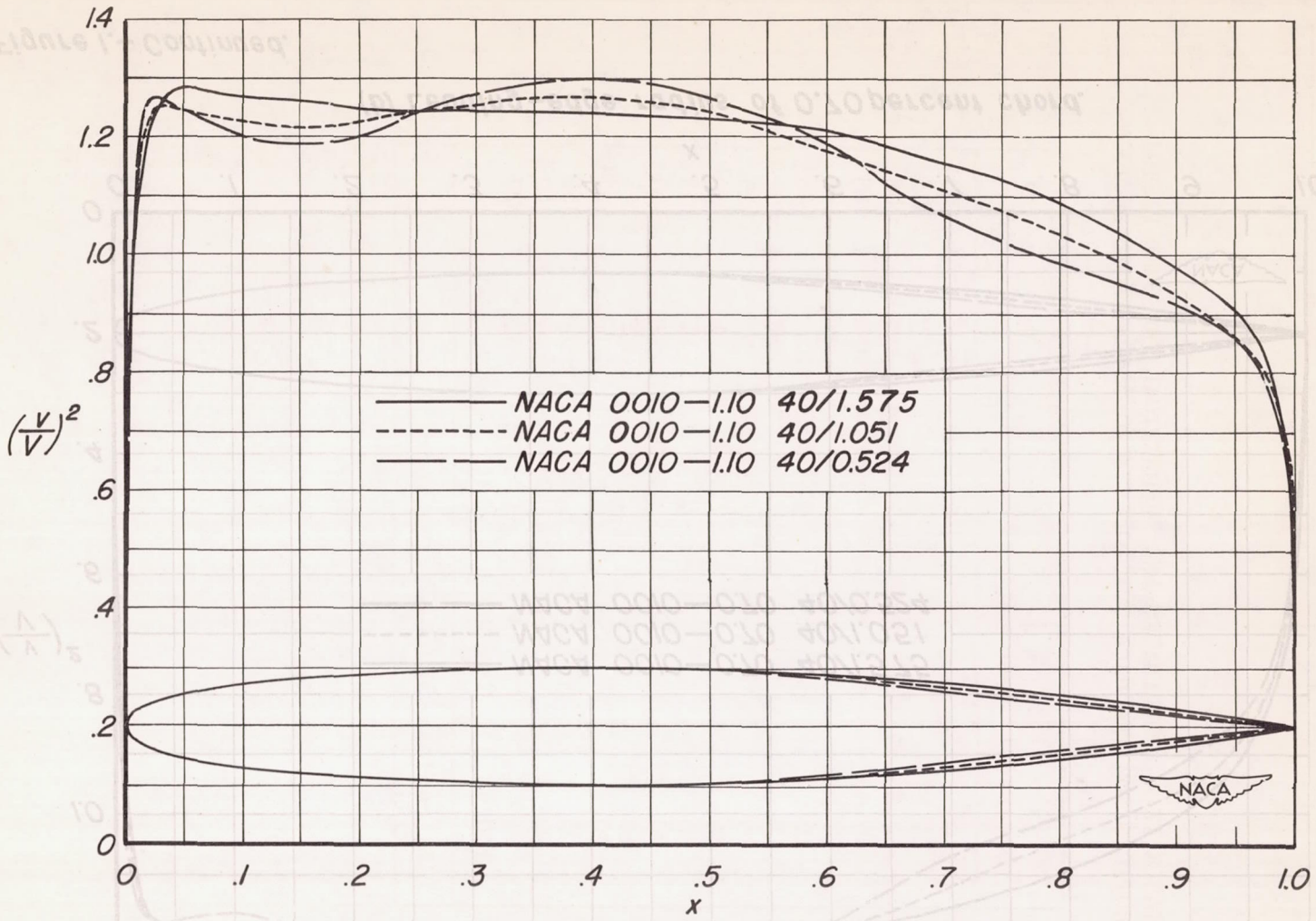

(a) Leading-edge radius of 1.10 percent chord.

Figure 1.- Airfoil profiles and theoretical pressure distributions.

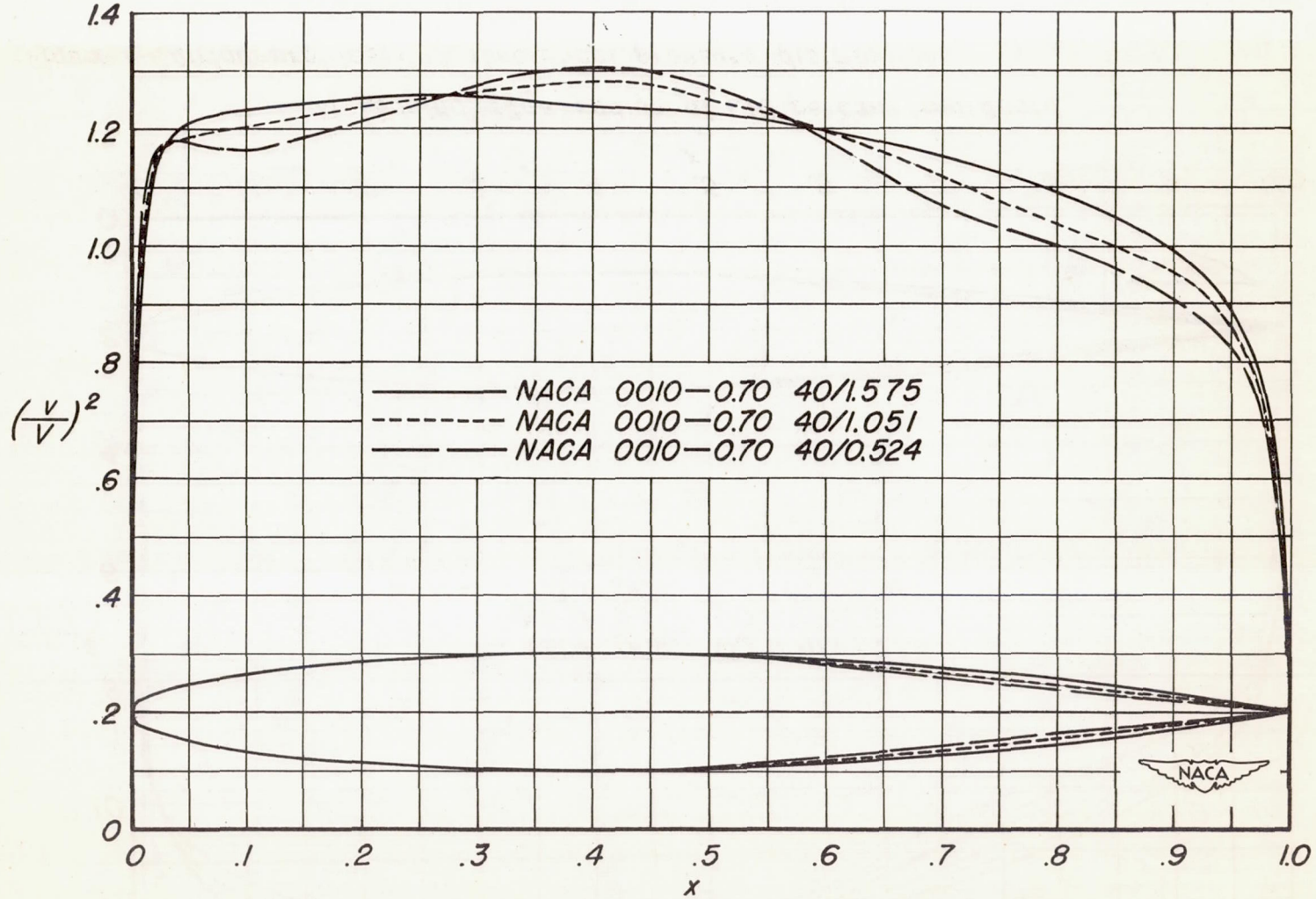

(b) Leading-edge radius of 0.70 percent chord.

Figure 1.- Continued.

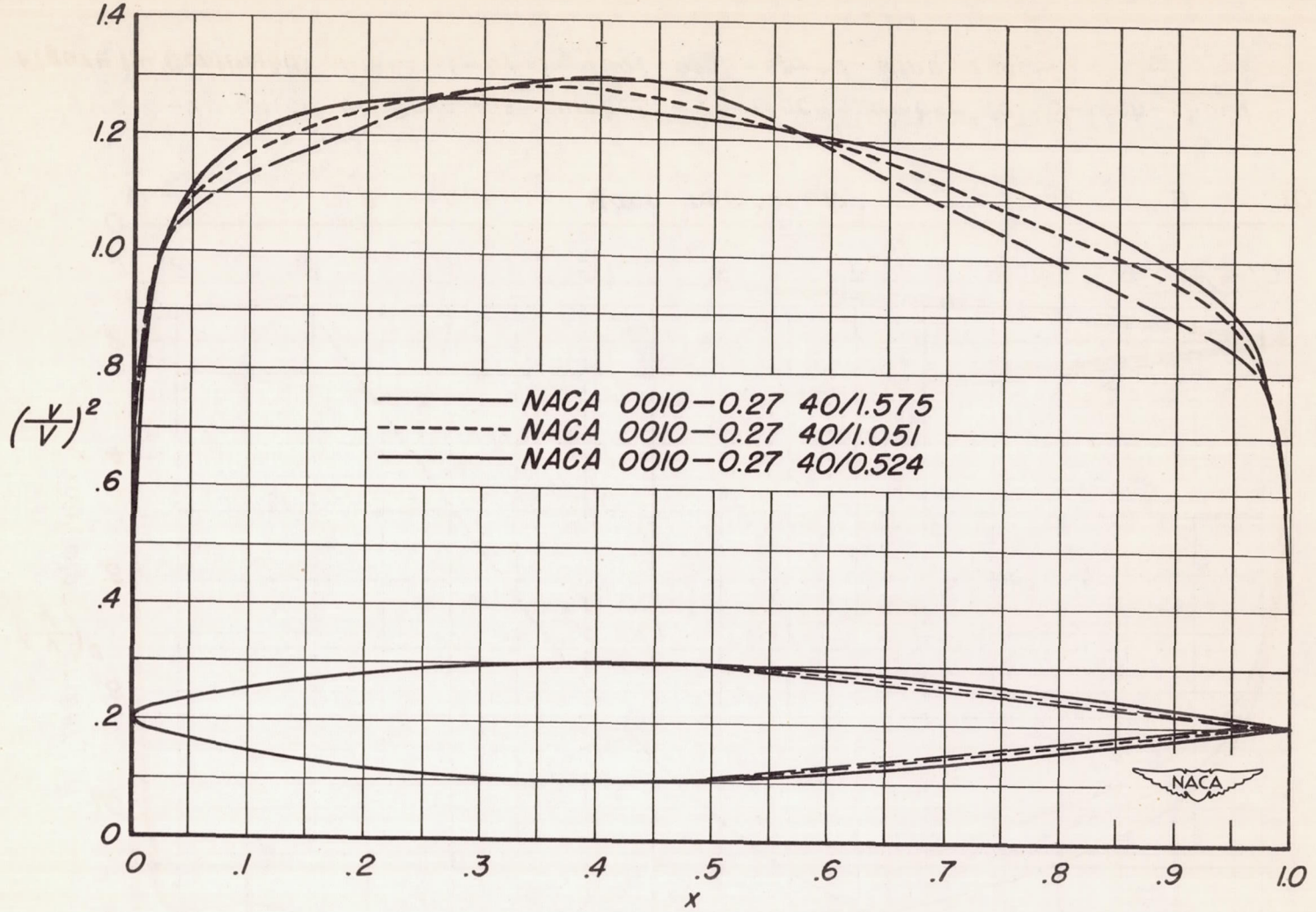

(c) Leading-edge radius of 0.27 percent chord.

Figure 1.- Concluded.

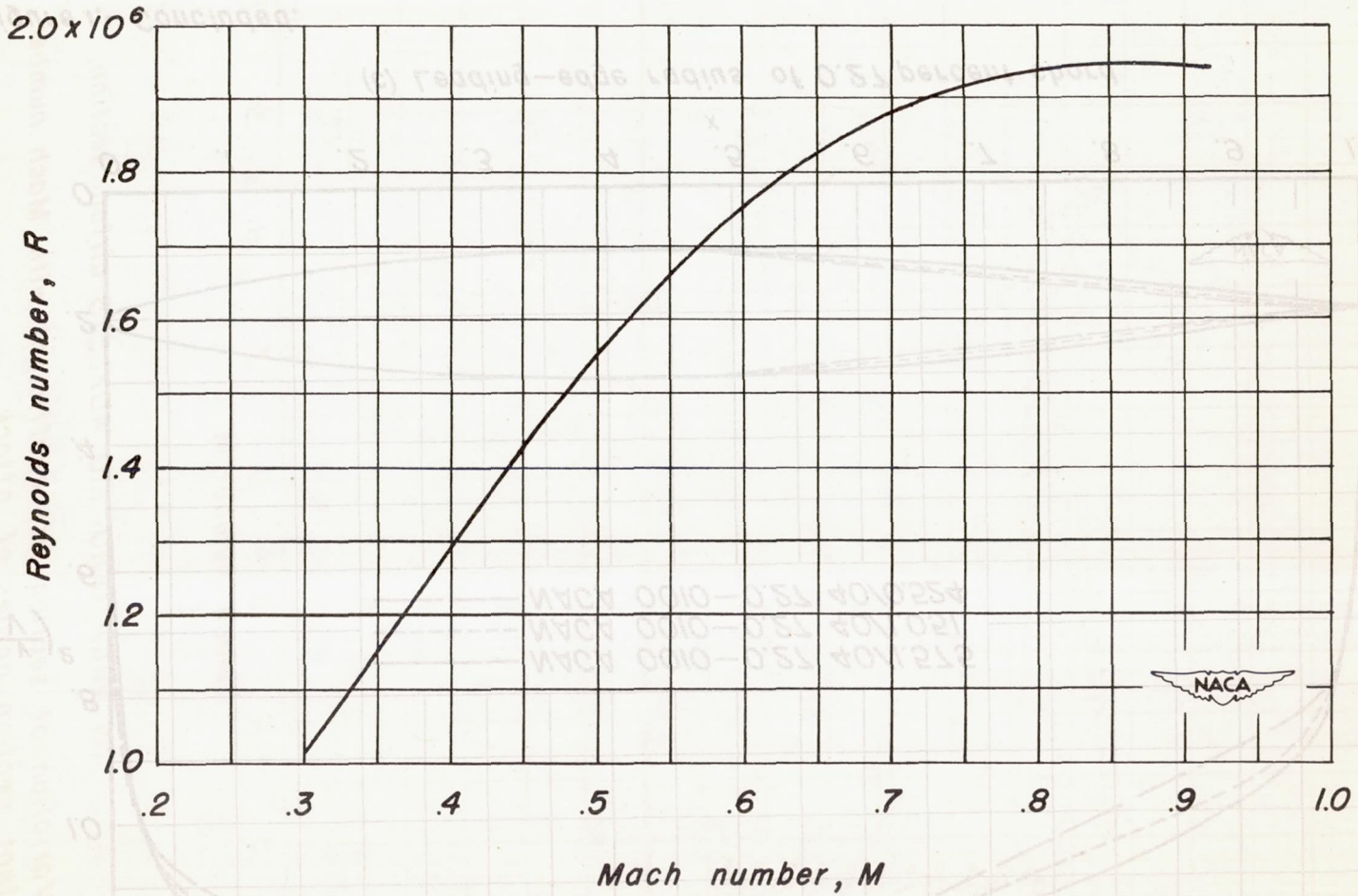

Figure 2.–Variation of Reynolds number with Mach number for 6-inch-chord airfoils in the Ames 1-by 3 $\frac{1}{2}$-foot high-speed wind tunnel.

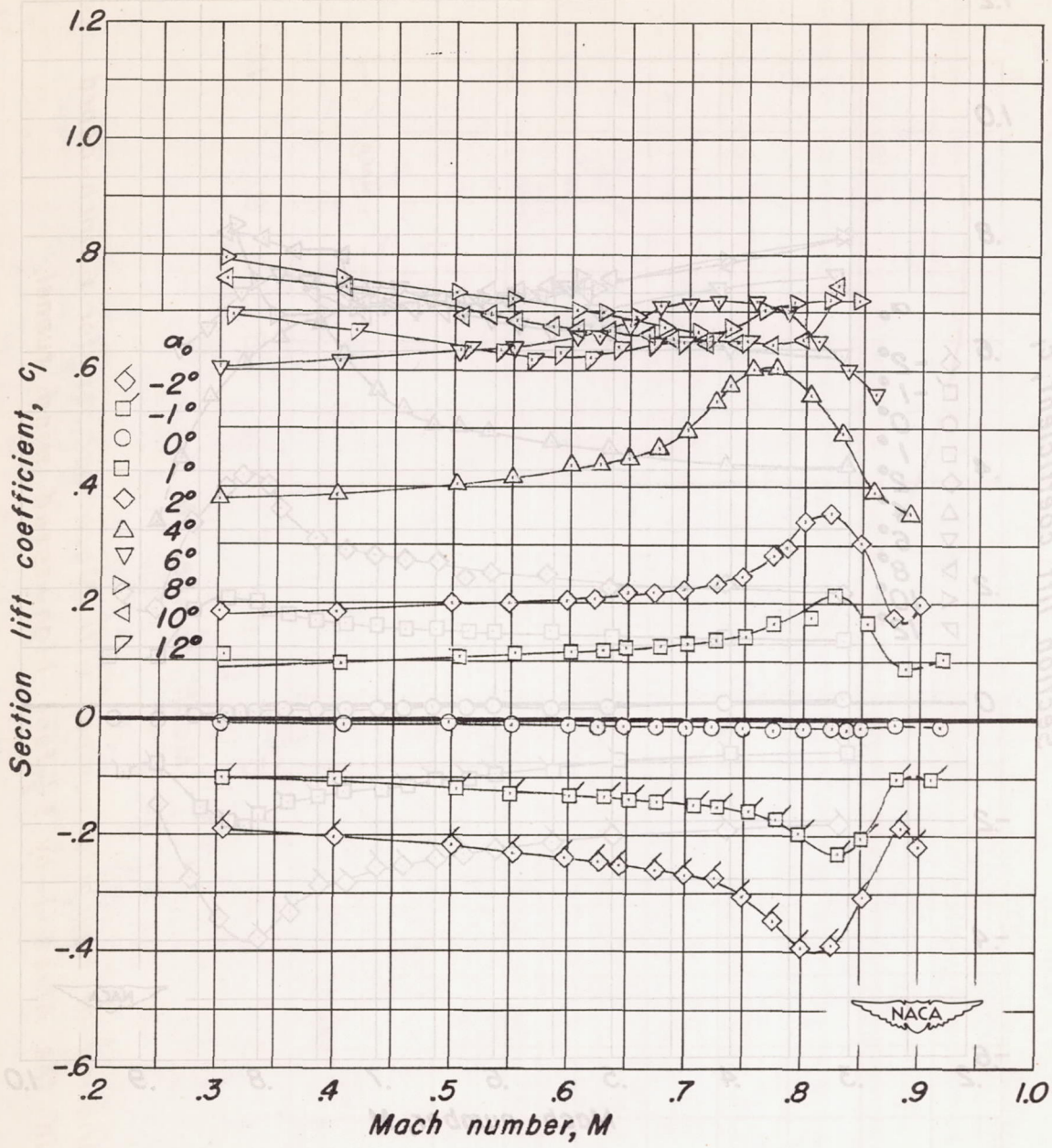

(a) NACA 0010-1.10 40/1.575 airfoil section.

Figure 3.- Variation of section lift coefficient with Mach number at constant section angles of attack.

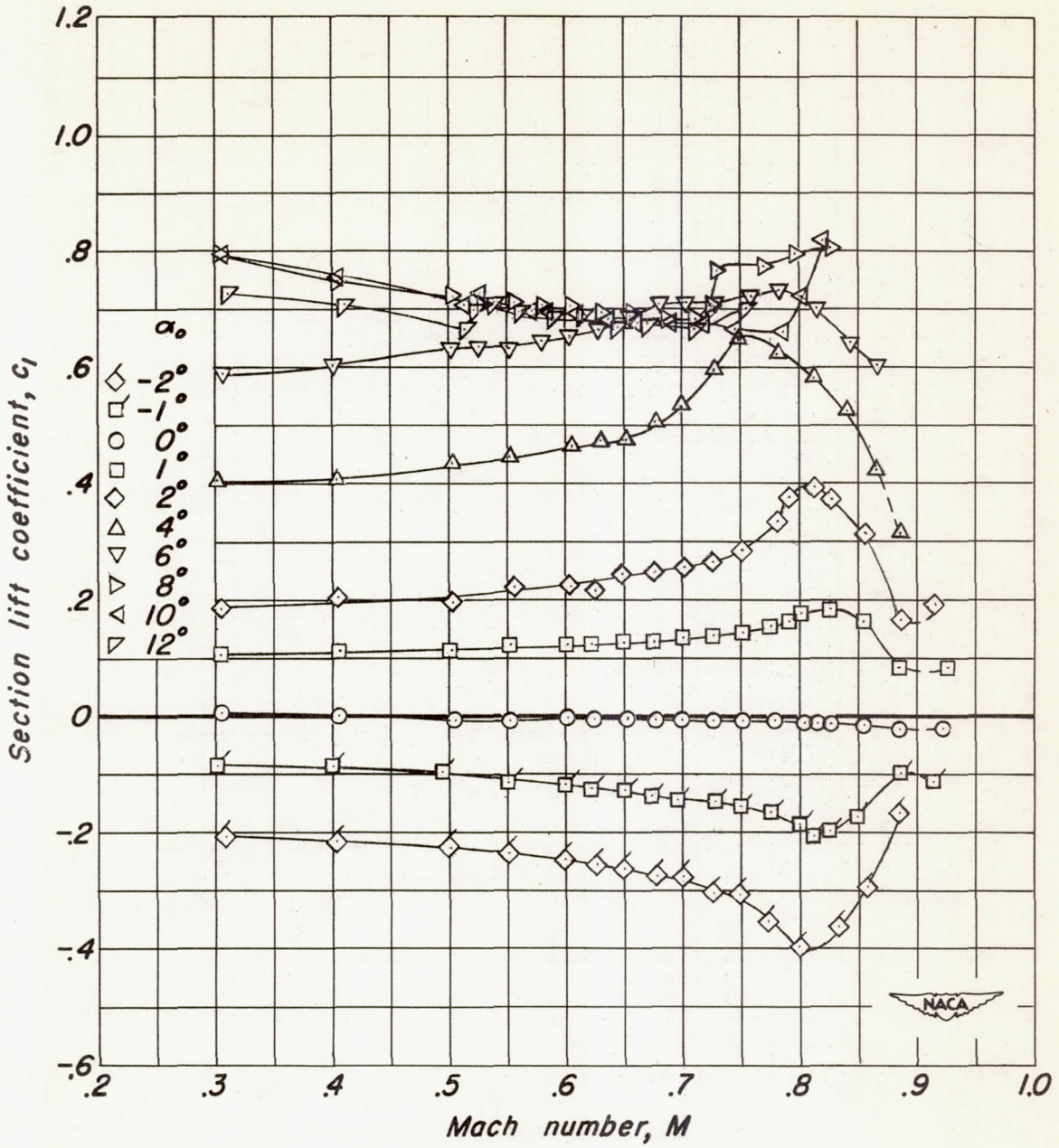

(b) NACA 0010-1.10 40/1.051 airfoil section.

Figure 3.- Continued.

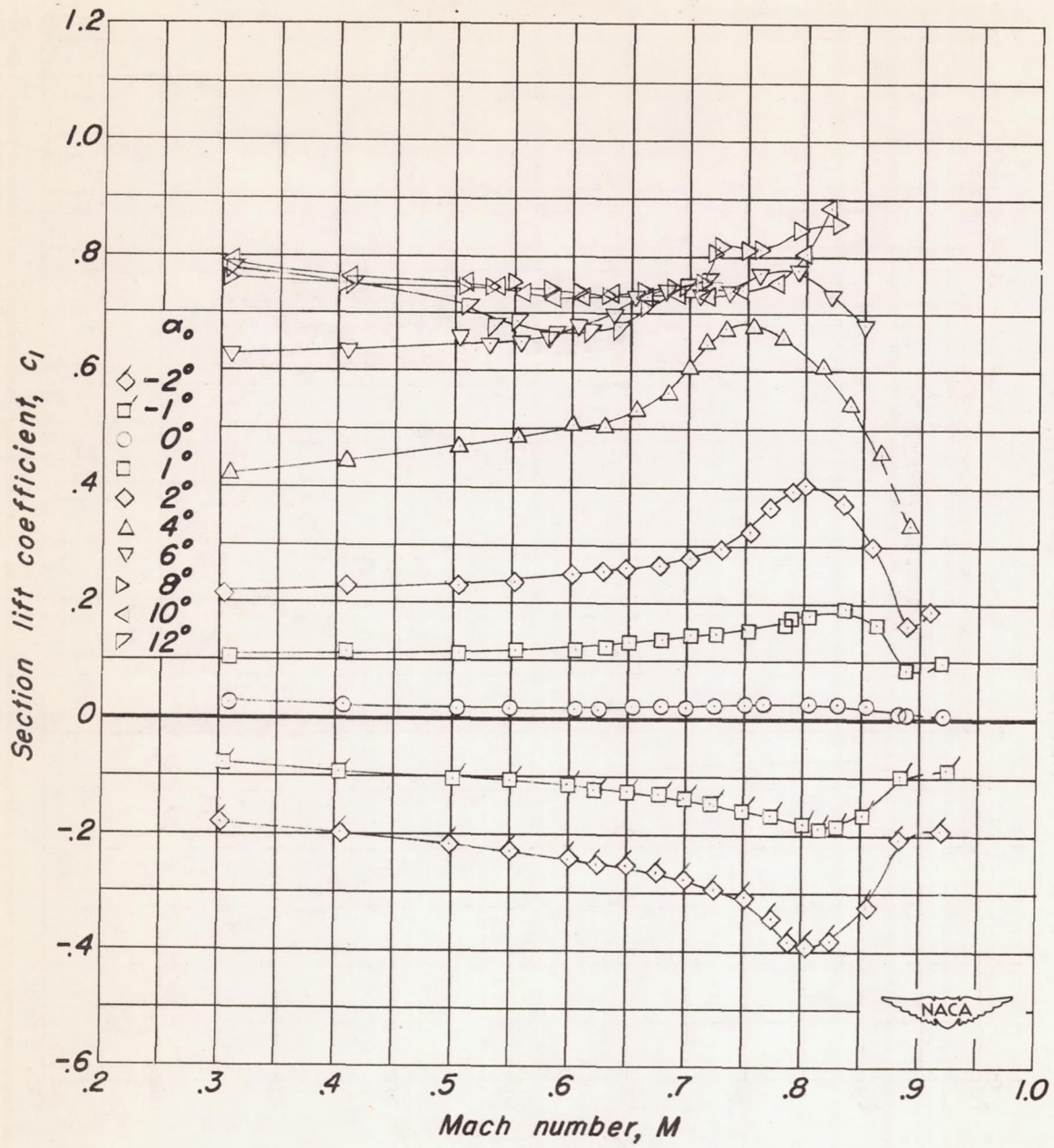

(c) NACA 0010-1.10 40/0.524 airfoil section.

Figure 3.- Continued.

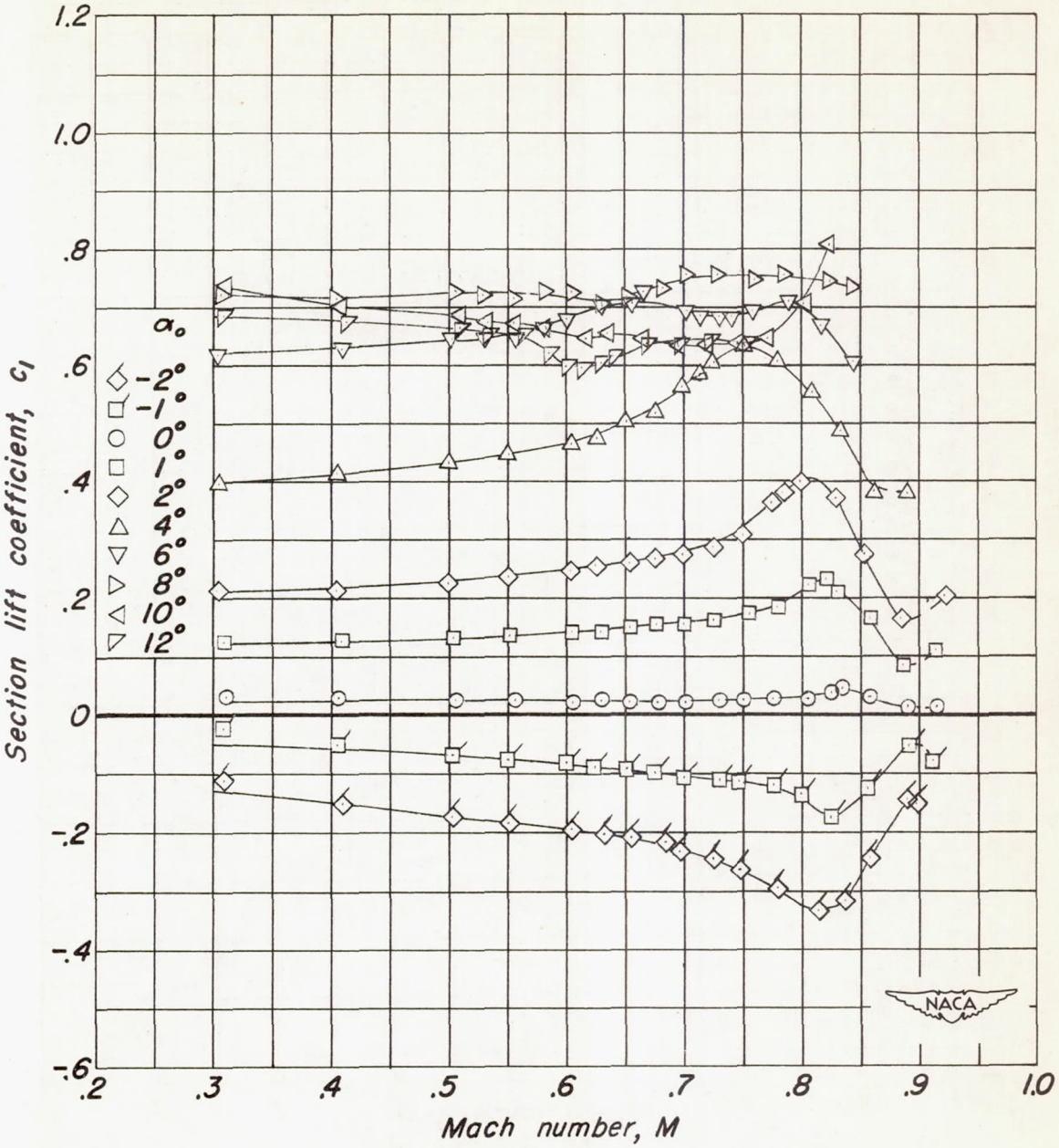

(d) NACA 0010-0.70 40/1.575 airfoil section.

Figure 3.- Continued.

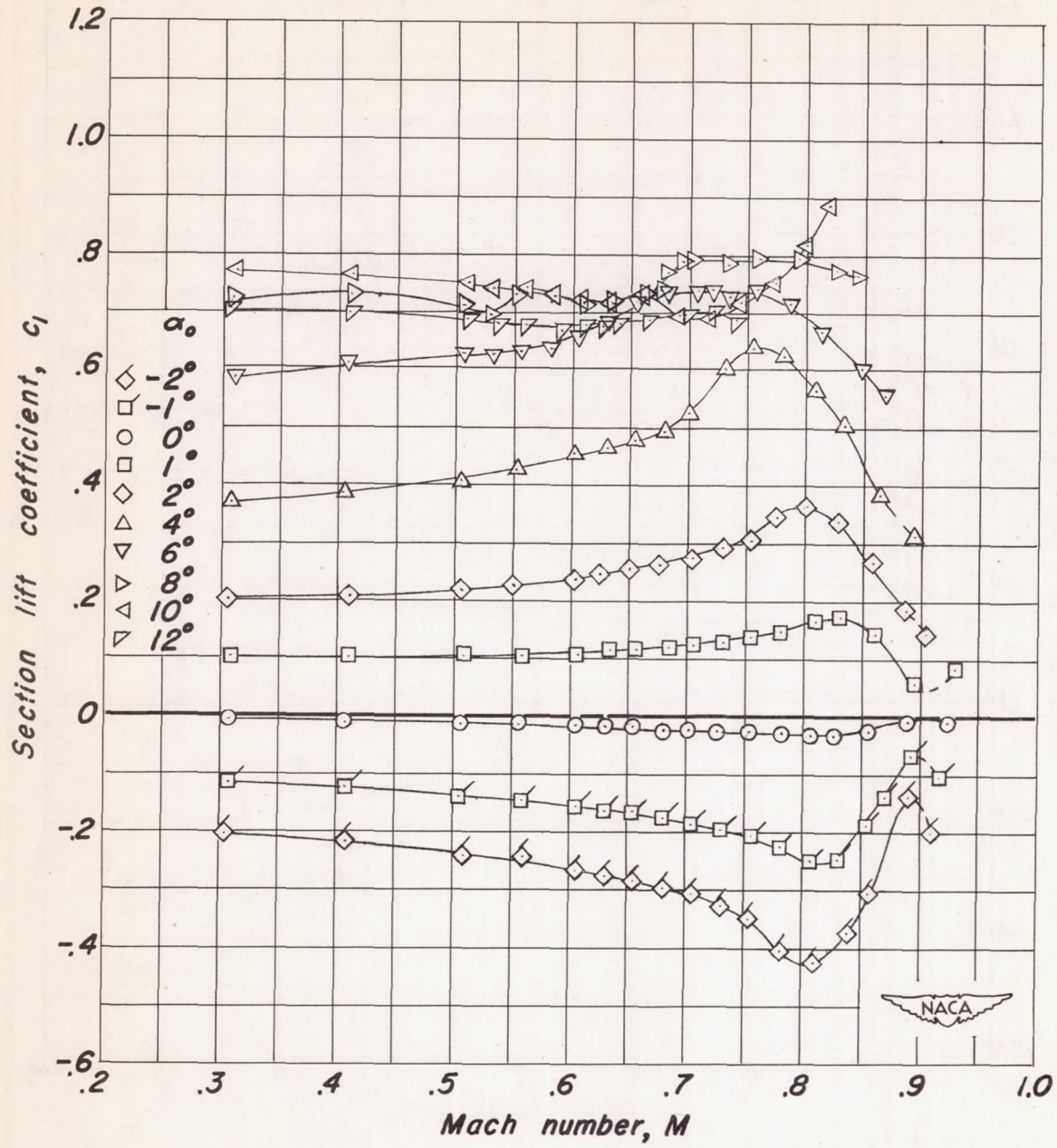

(e) NACA 0010-0.70 40/1.051 airfoil section.

Figure 3.- Continued.

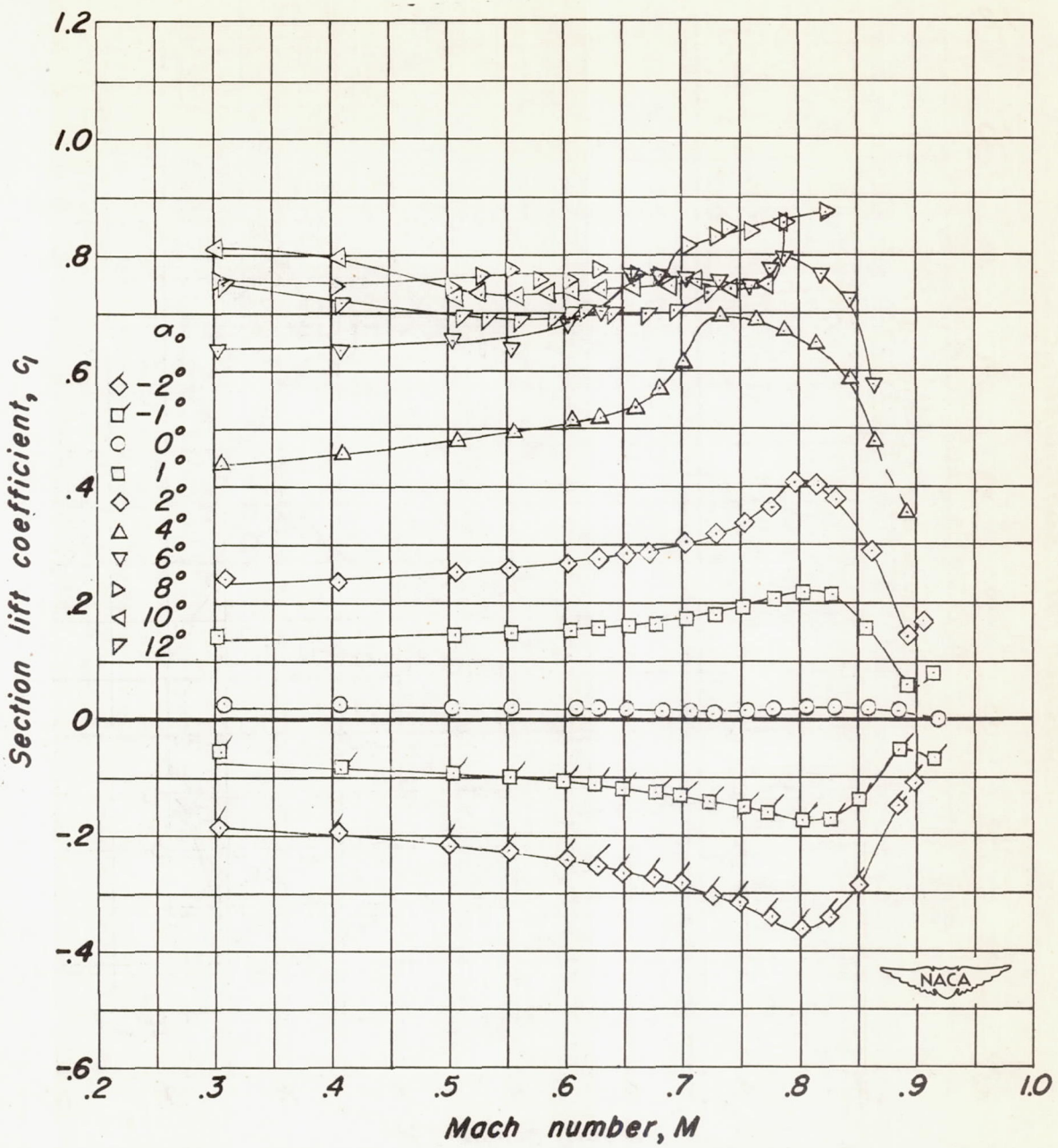

(f) NACA 0010-0.70 40/0.524 airfoil section.

Figure 3.- Continued.

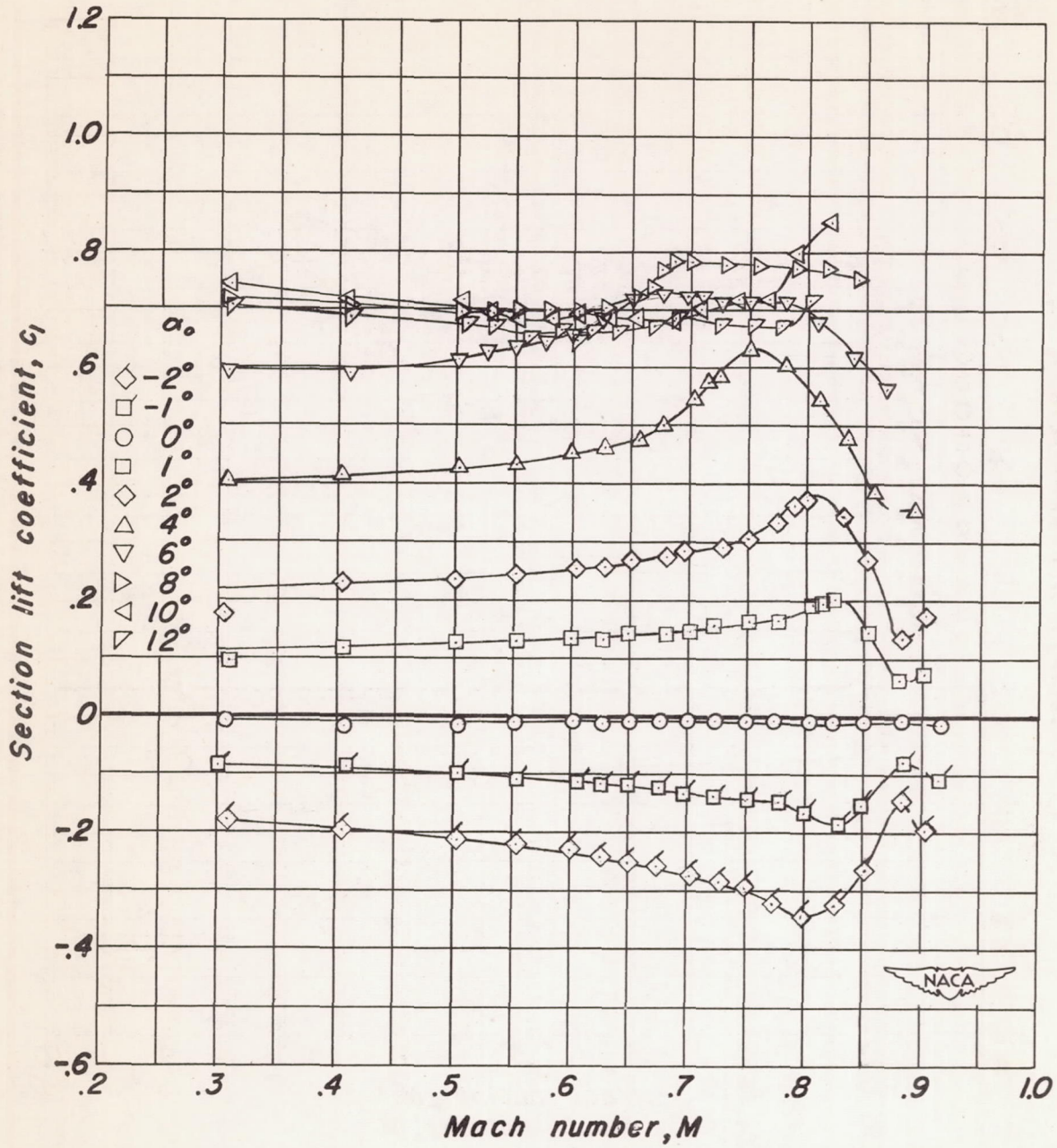

(g) NACA 0010-0.27 40/1.575 airfoil section.

Figure 3.- Continued.

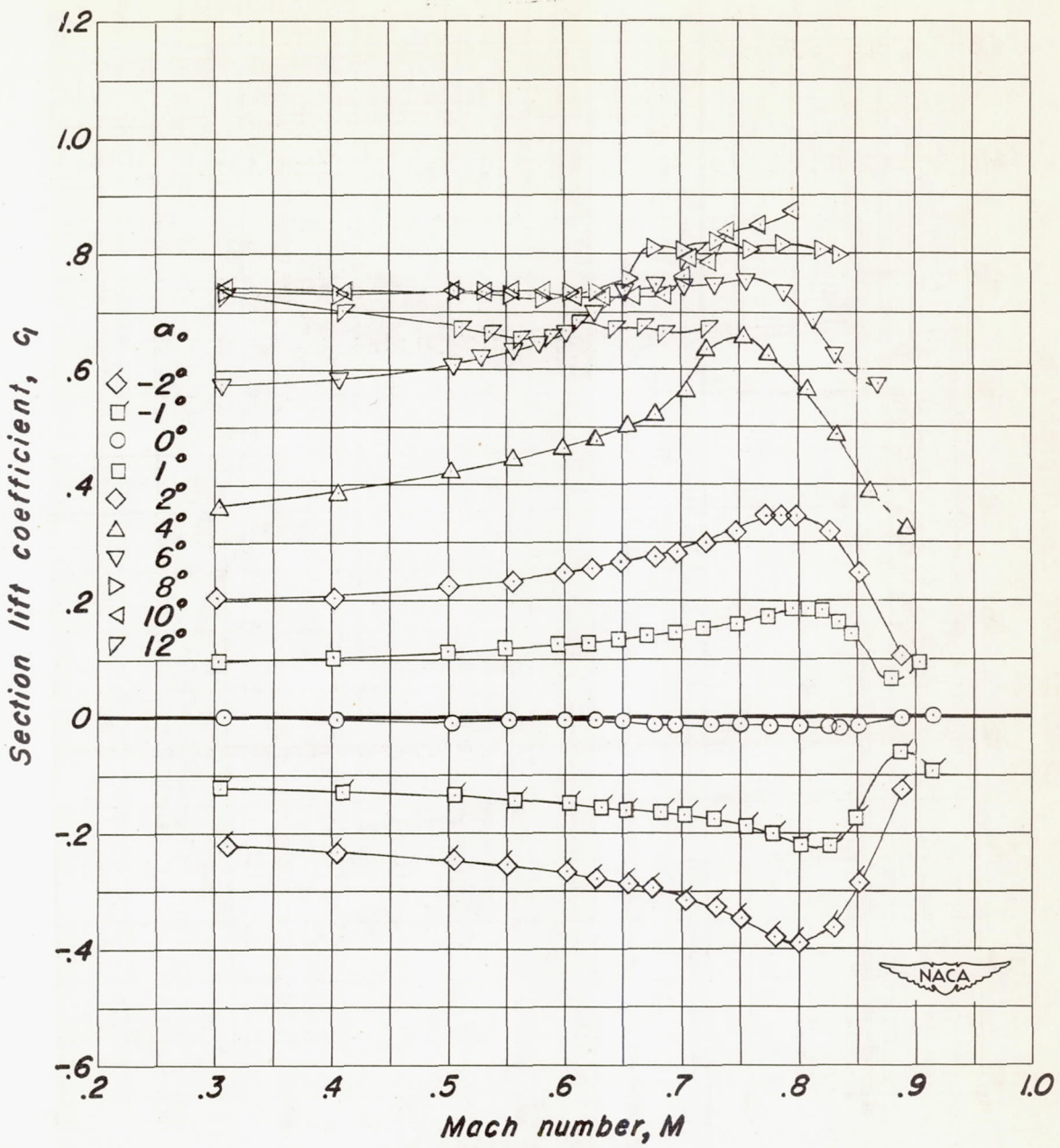

(h) NACA 0010-0.27 40/1.051 airfoil section.

Figure 3.- Continued.

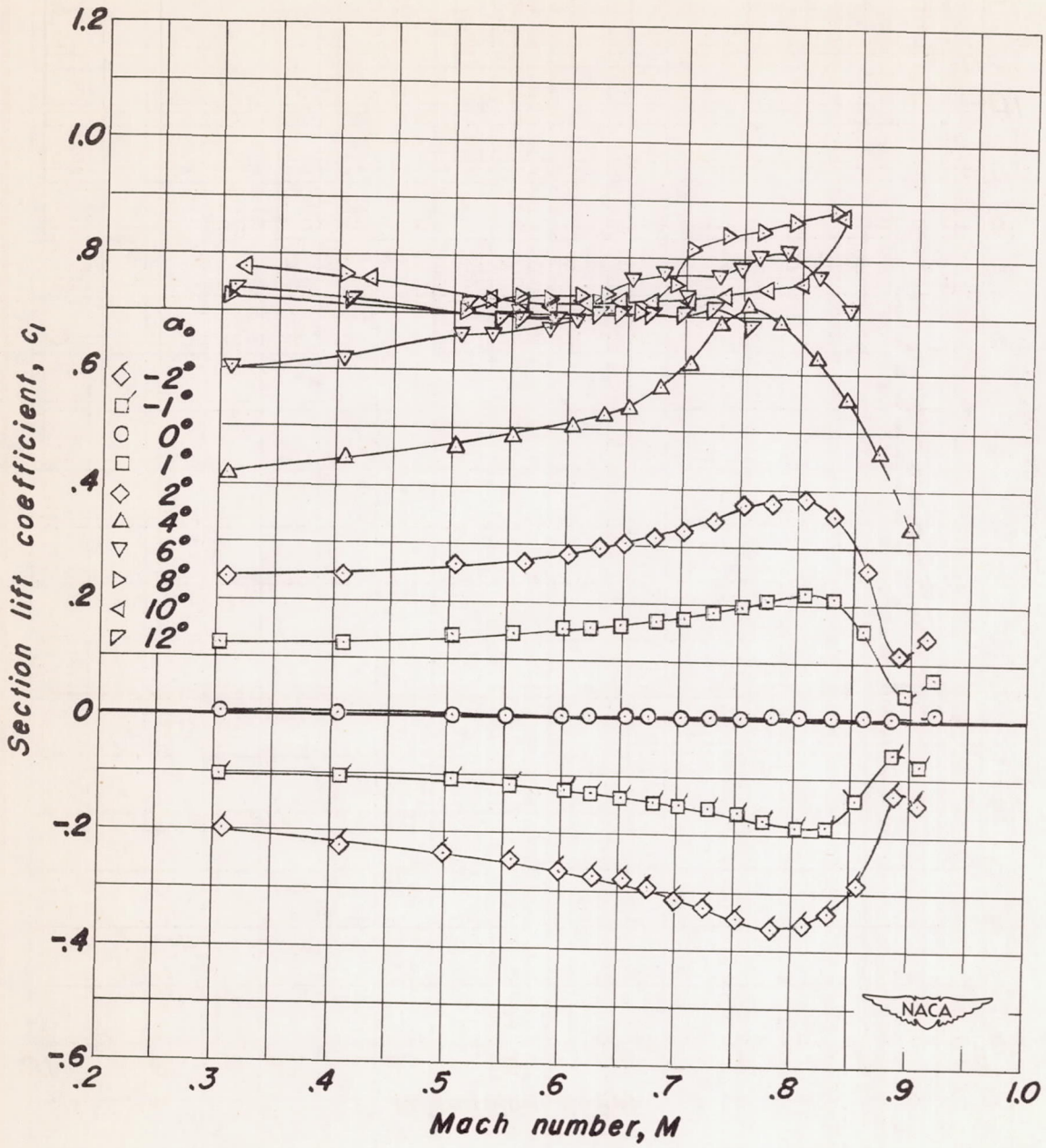

(i) NACA 0010-0.27 40/0.524 airfoil section.

Figure 3.- Concluded.

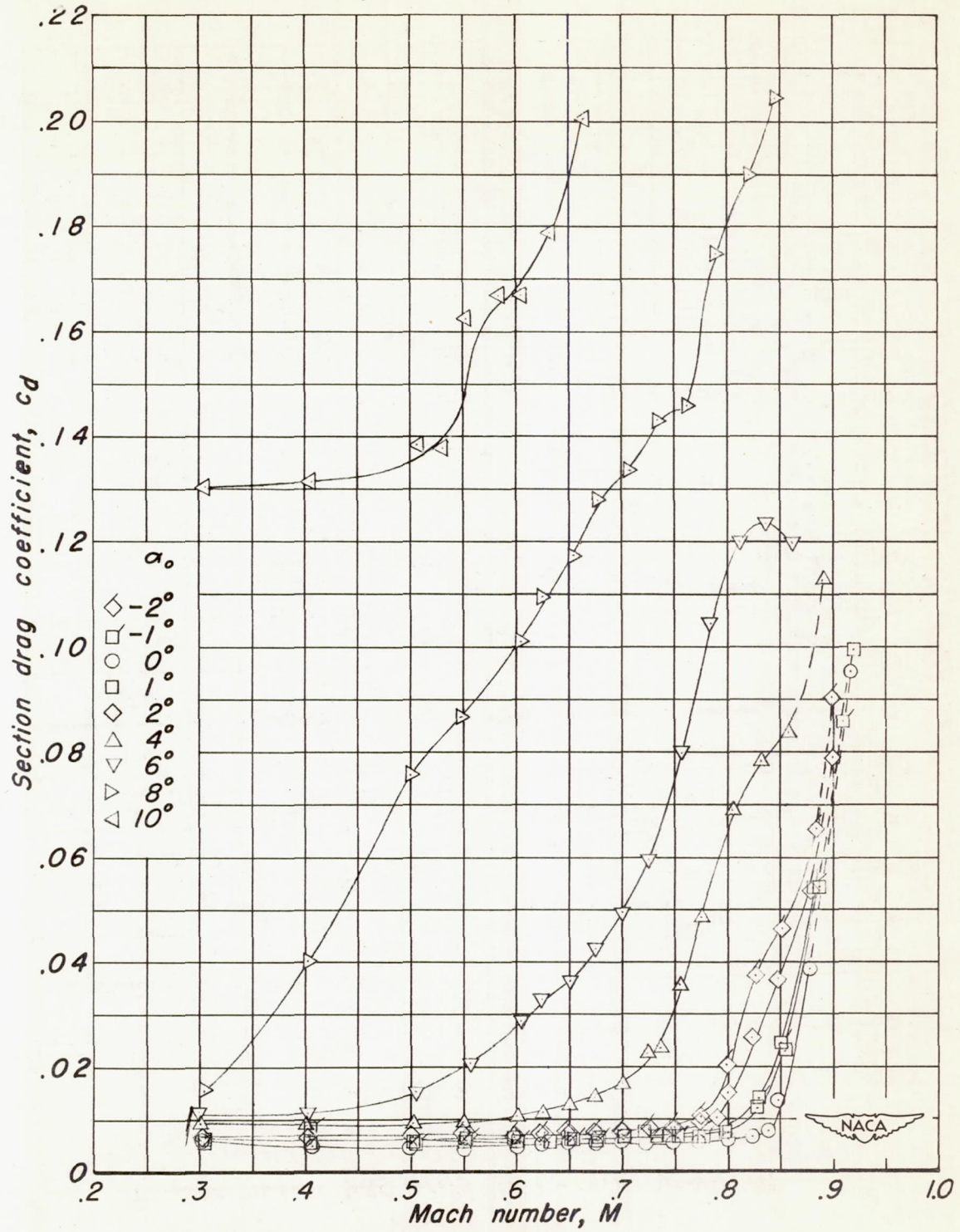

(a) NACA 0010-1.10 40/1.575 airfoil section.

Figure 4.- Variation of section drag coefficient with Mach number at constant section angles of attack.

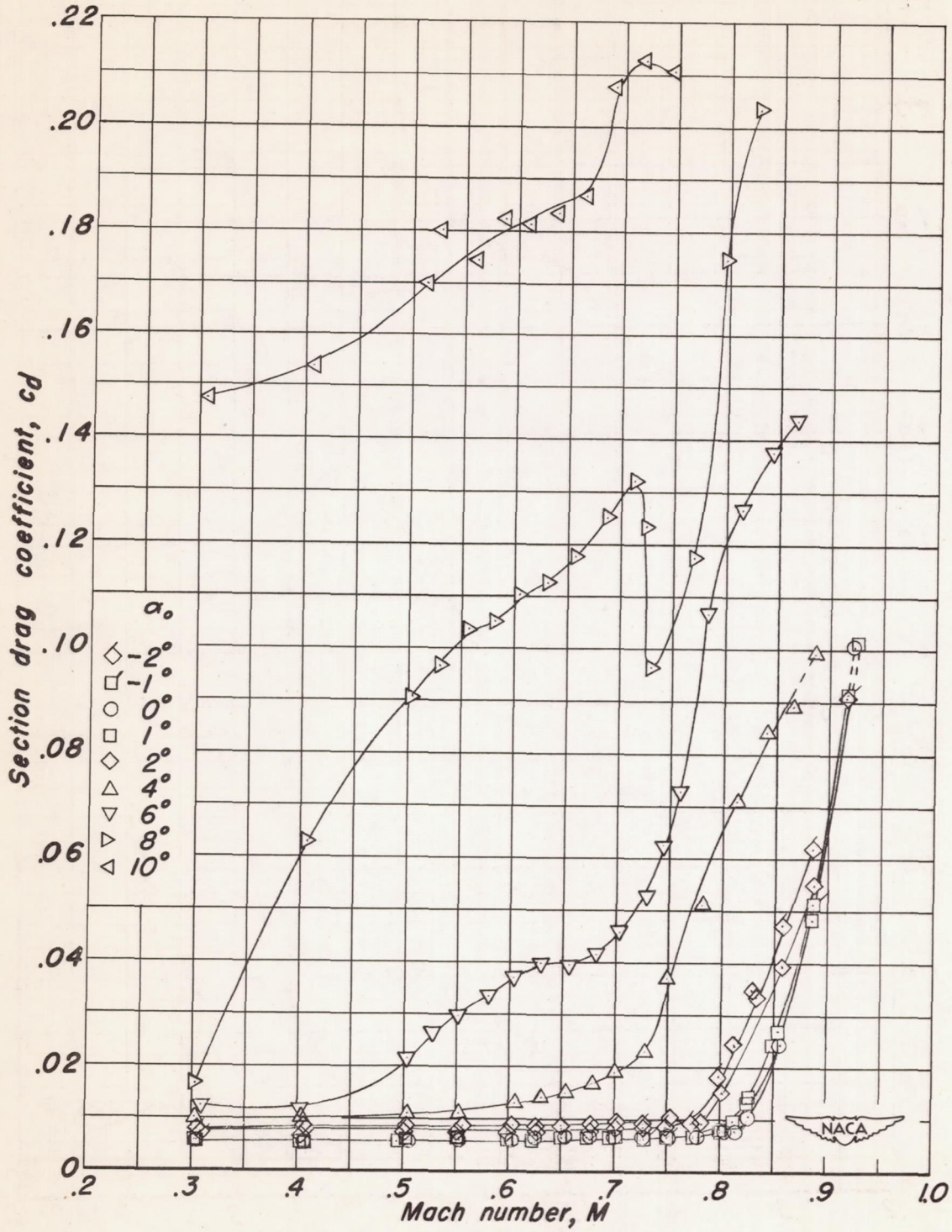

(b) NACA 0010-1.10 40/1.051 airfoil section.

Figure 4.- Continued.

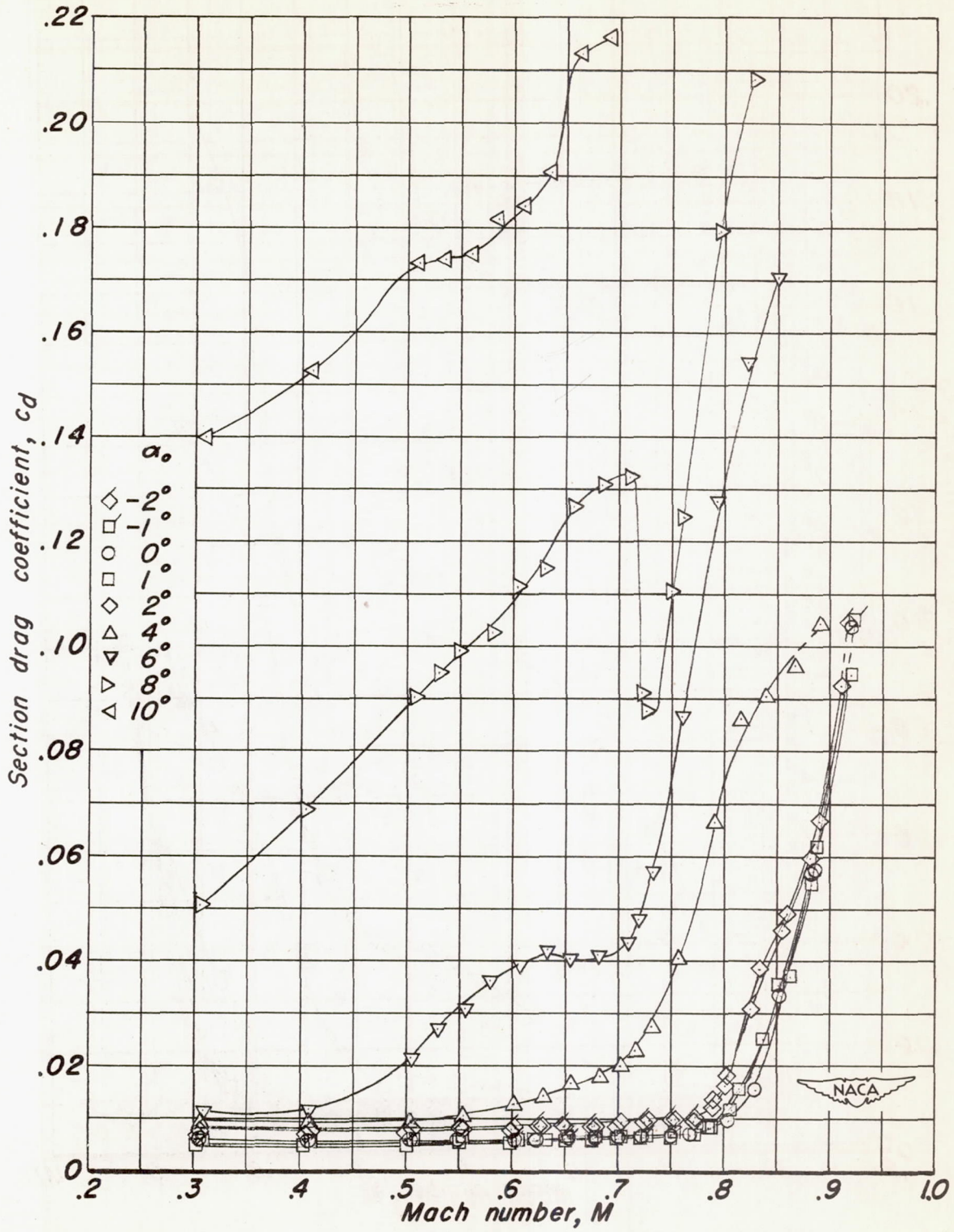

(c) NACA 0010-1.10 40/0.524 airfoil section.

Figure 4.- Continued.

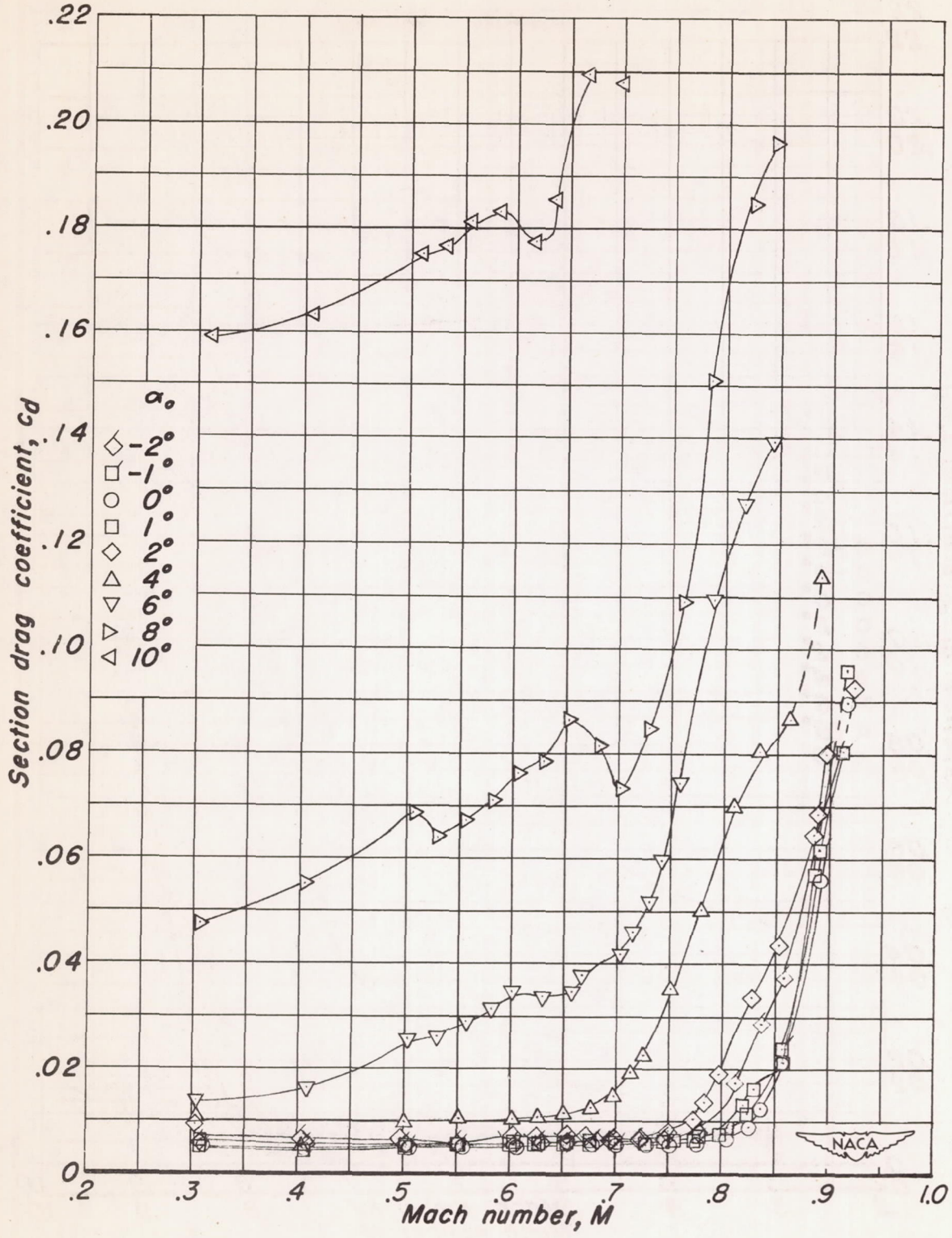

(d) NACA 0010-0.70 40/1.575 airfoil section.

Figure 4.- Continued.

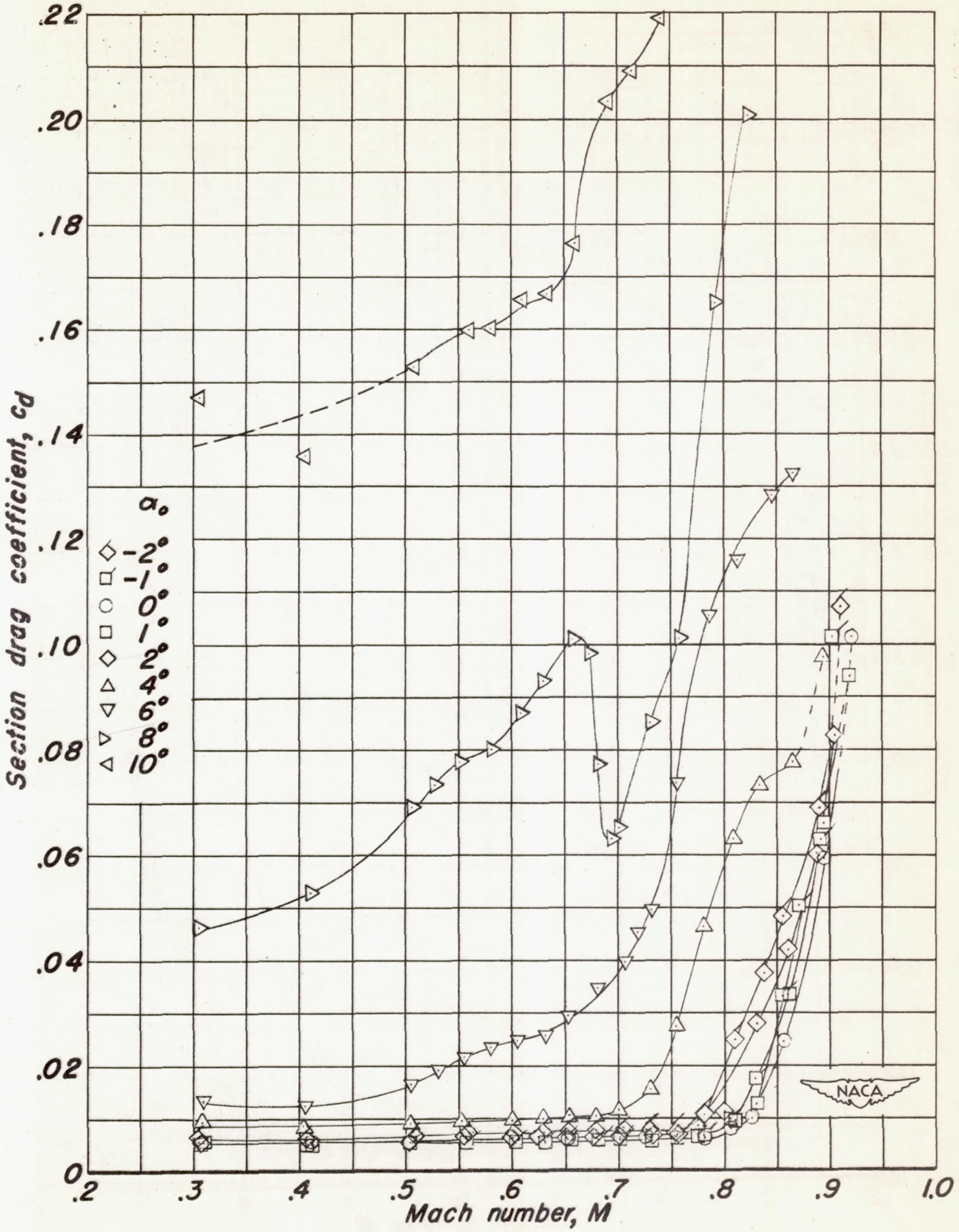

(e) NACA 0010-0.70 40/1.051 airfoil section.

Figure 4.- Continued.

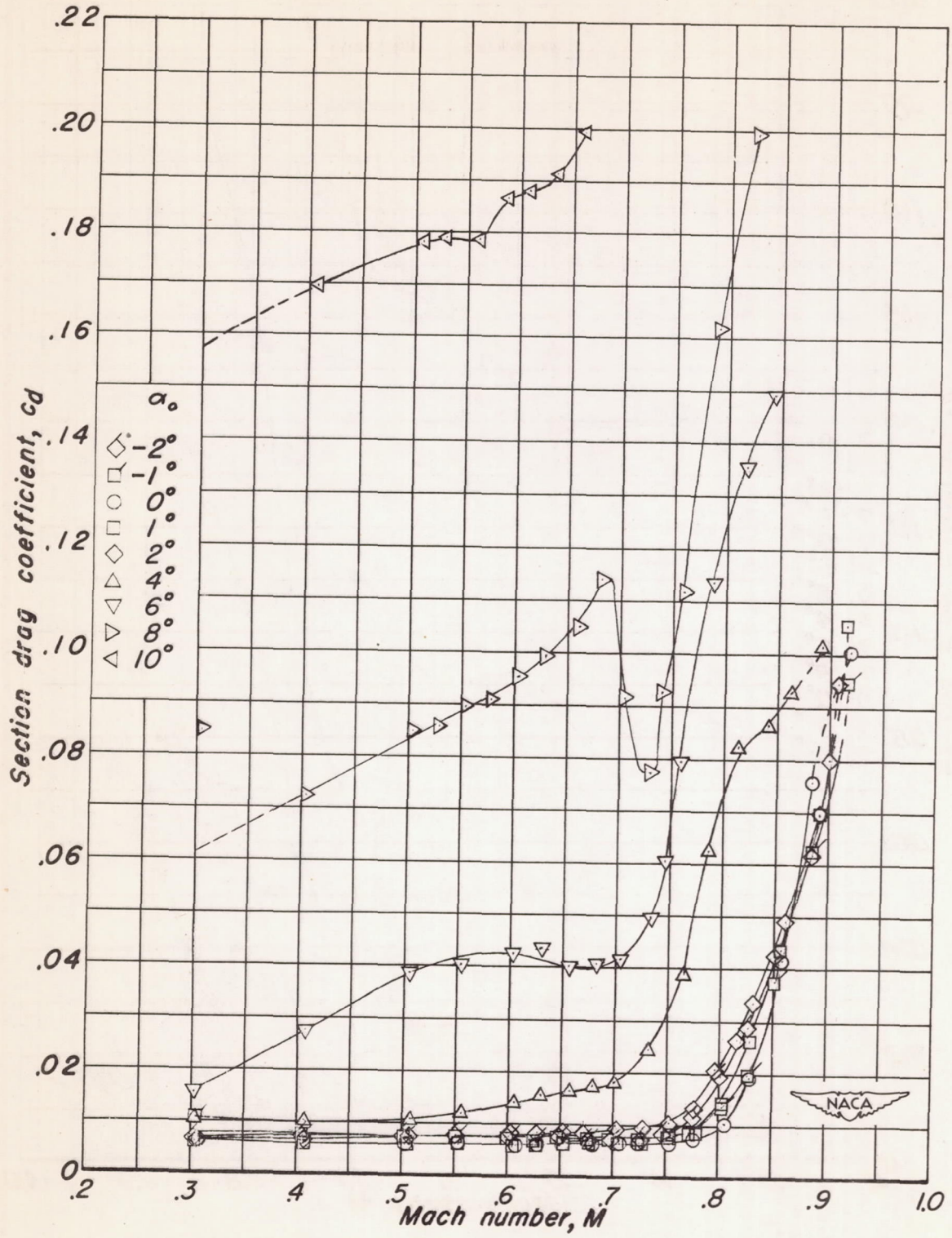

(f) NACA 0010-0.70 40/0.524 airfoil section.

Figure 4.- Continued.

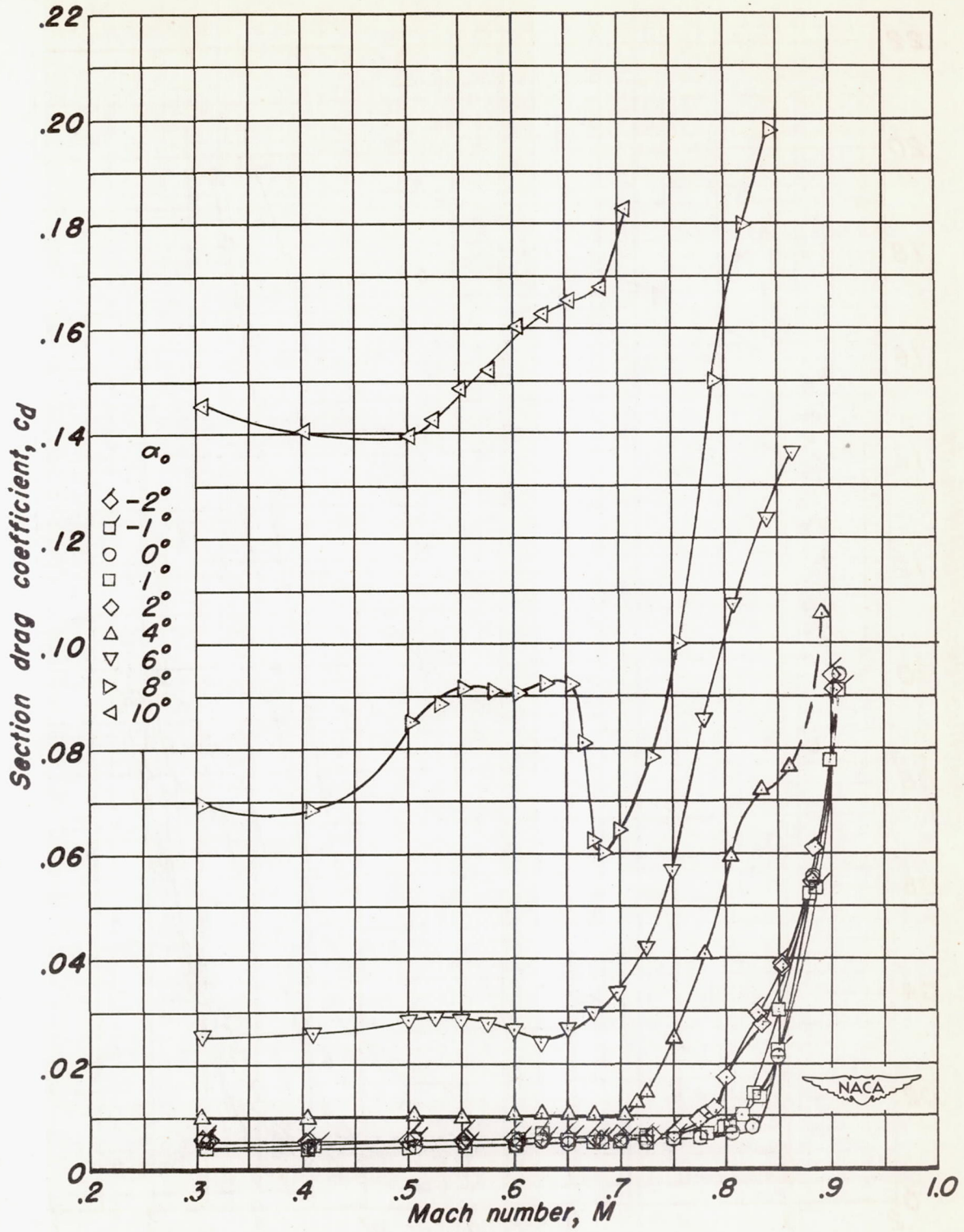

(g) NACA 0010-0.27 40/1.575 airfoil section.

Figure 4.- Continued.

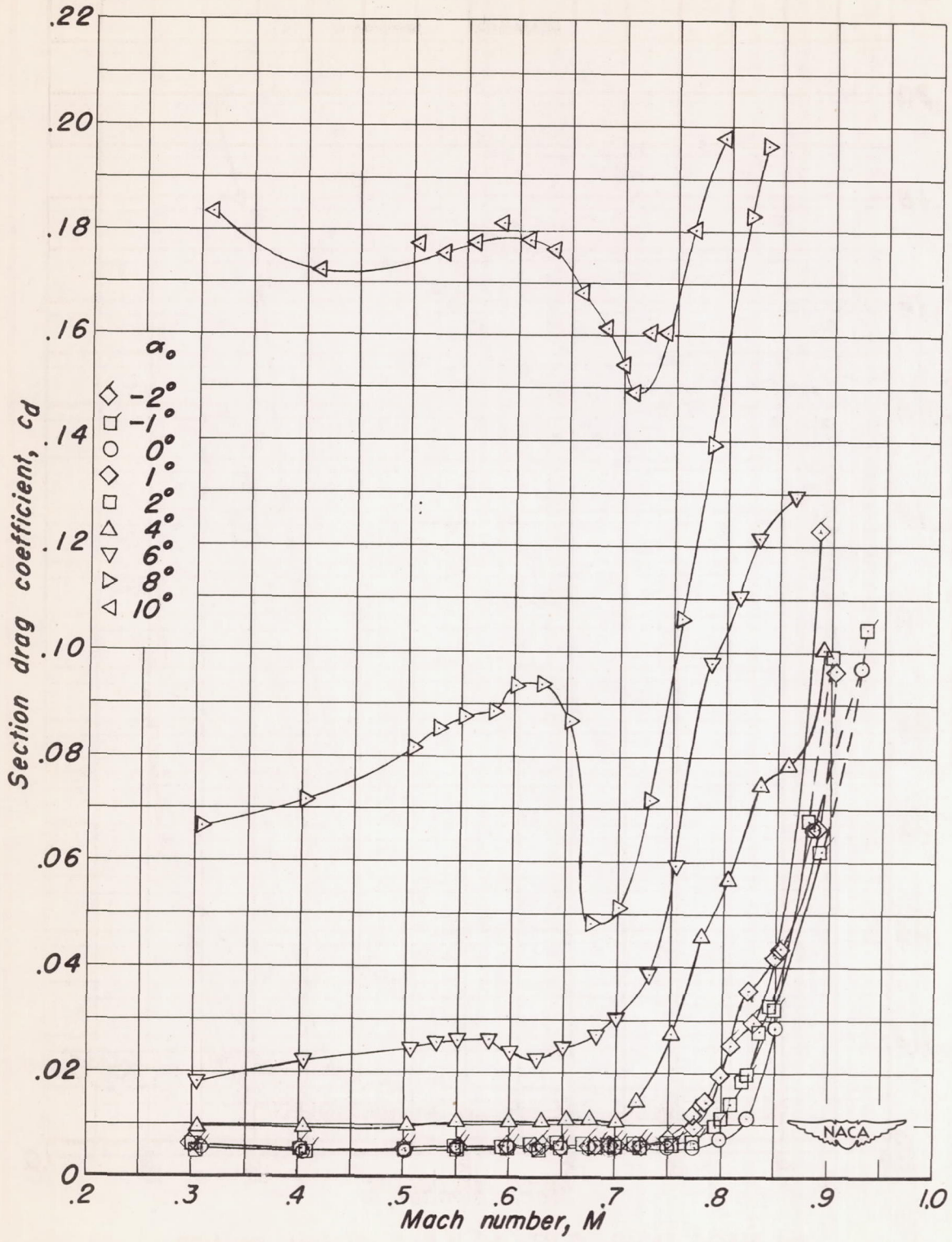

(h) NACA 0010-0.27 40/1.051 airfoil section.

Figure 4.-Continued.

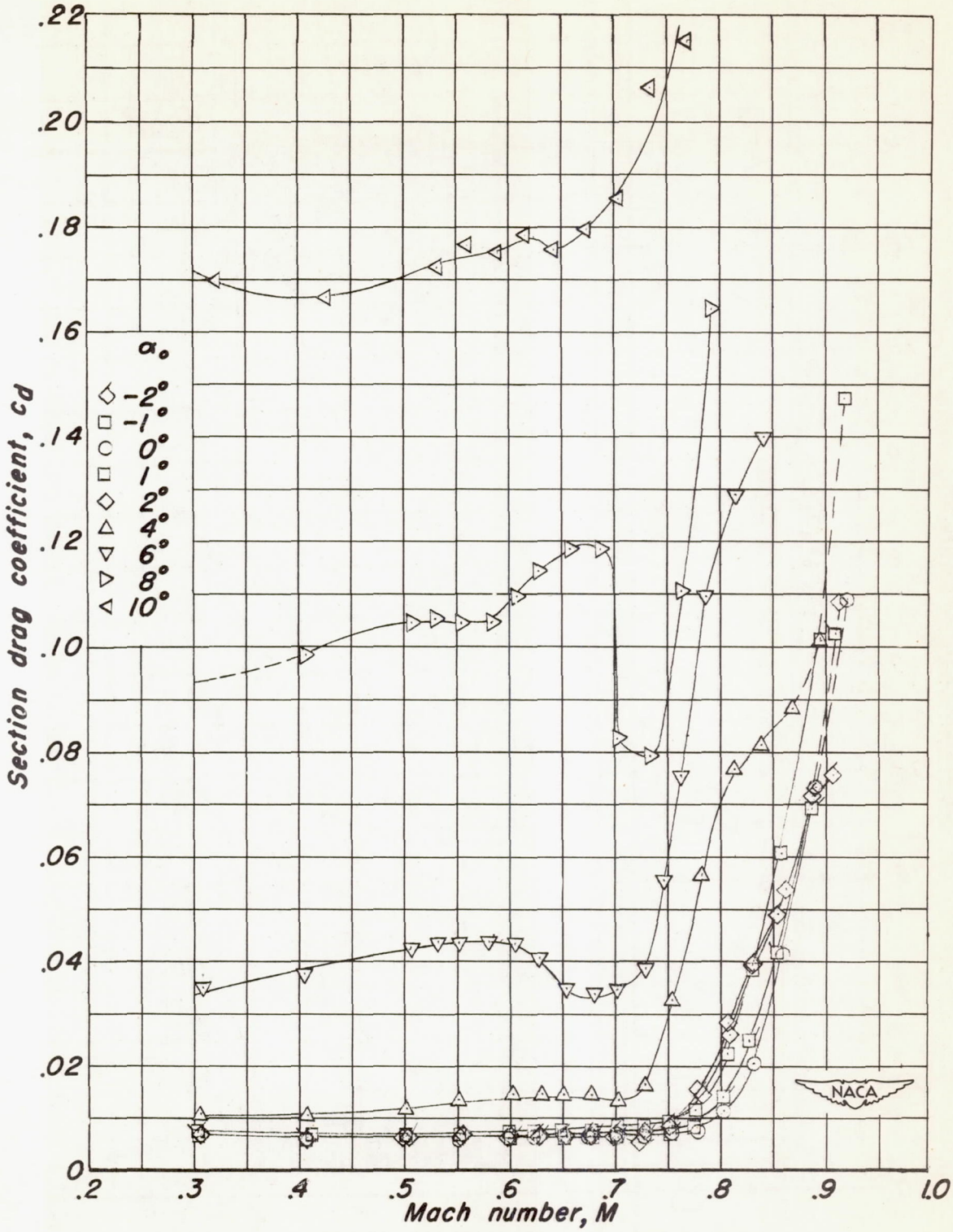

(i) NACA 0010-0.27 40/0.524 airfoil section.

Figure 4.- Concluded.

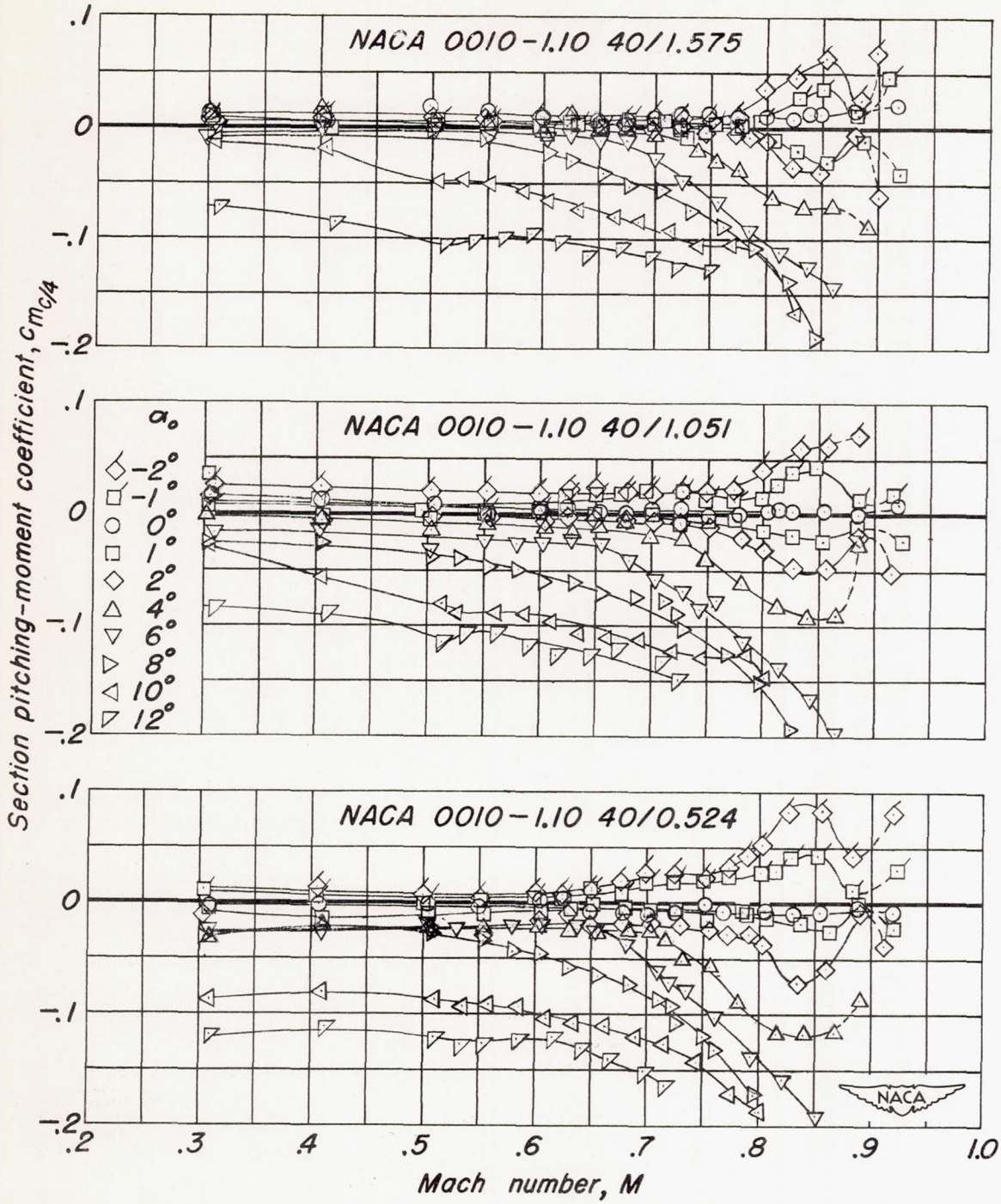

(a) Leading-edge radius of 1.10 percent chord.

Figure 5.-Variation of section pitching-moment coefficient with Mach number at constant section angles of attack.

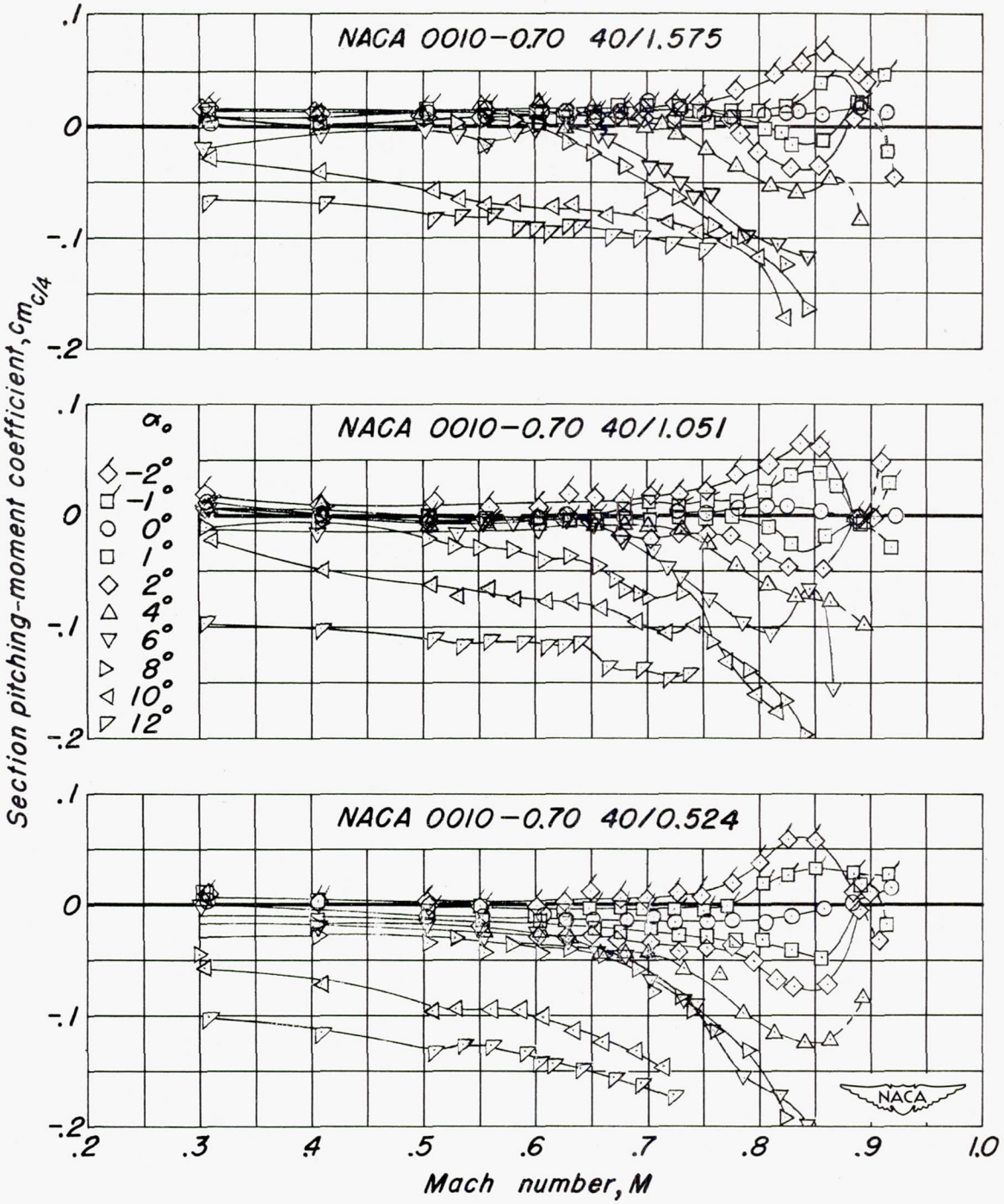

(b) Leading-edge radius of 0.70 percent chord.

Figure 5.- Continued.

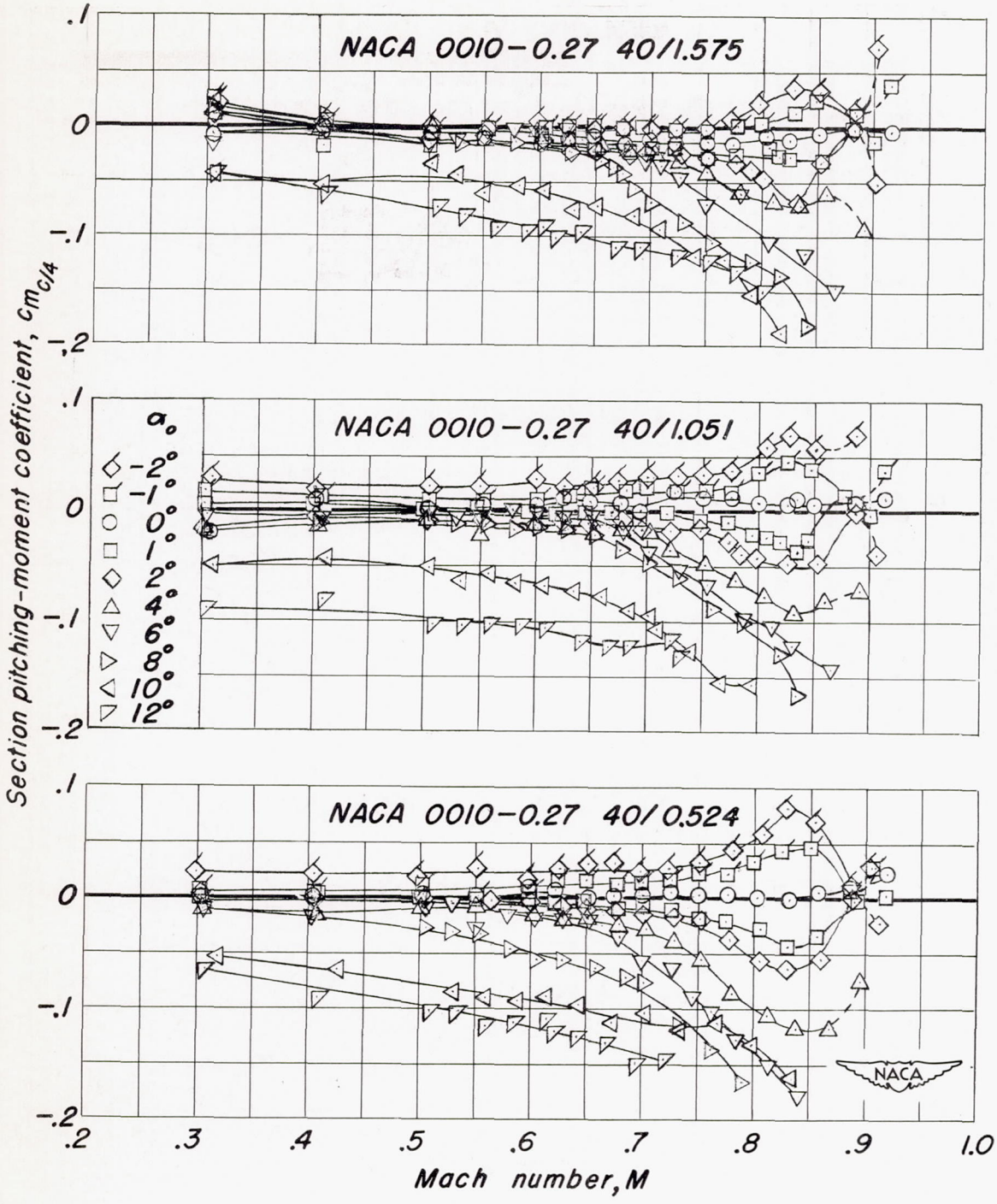

(c) Leading-edge radius of 0.27 percent chord.

Figure 5.- Concluded.

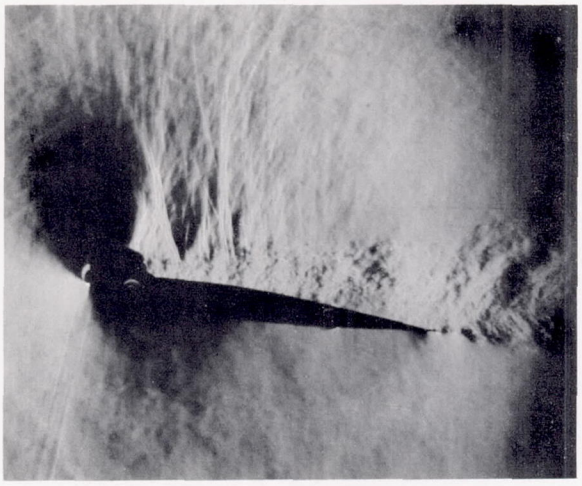

(a) 0.707 Mach number.

NACA
A-14206

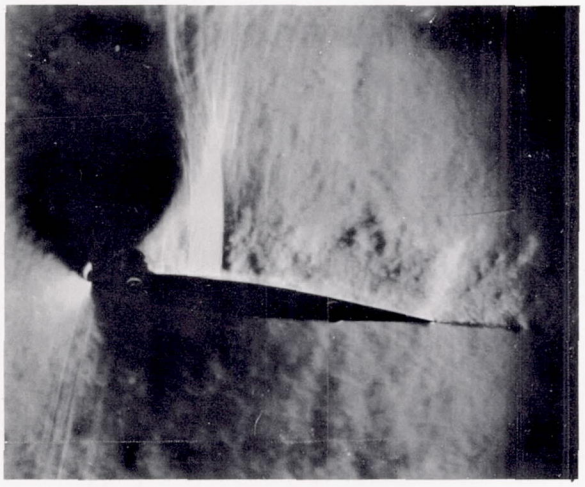

(b) 0.731 Mach number.

NACA
A-14207

Figure 6.– Schlieren photographs of the NACA 0010-1.10 40/1.051 airfoil section at 8° of attack.

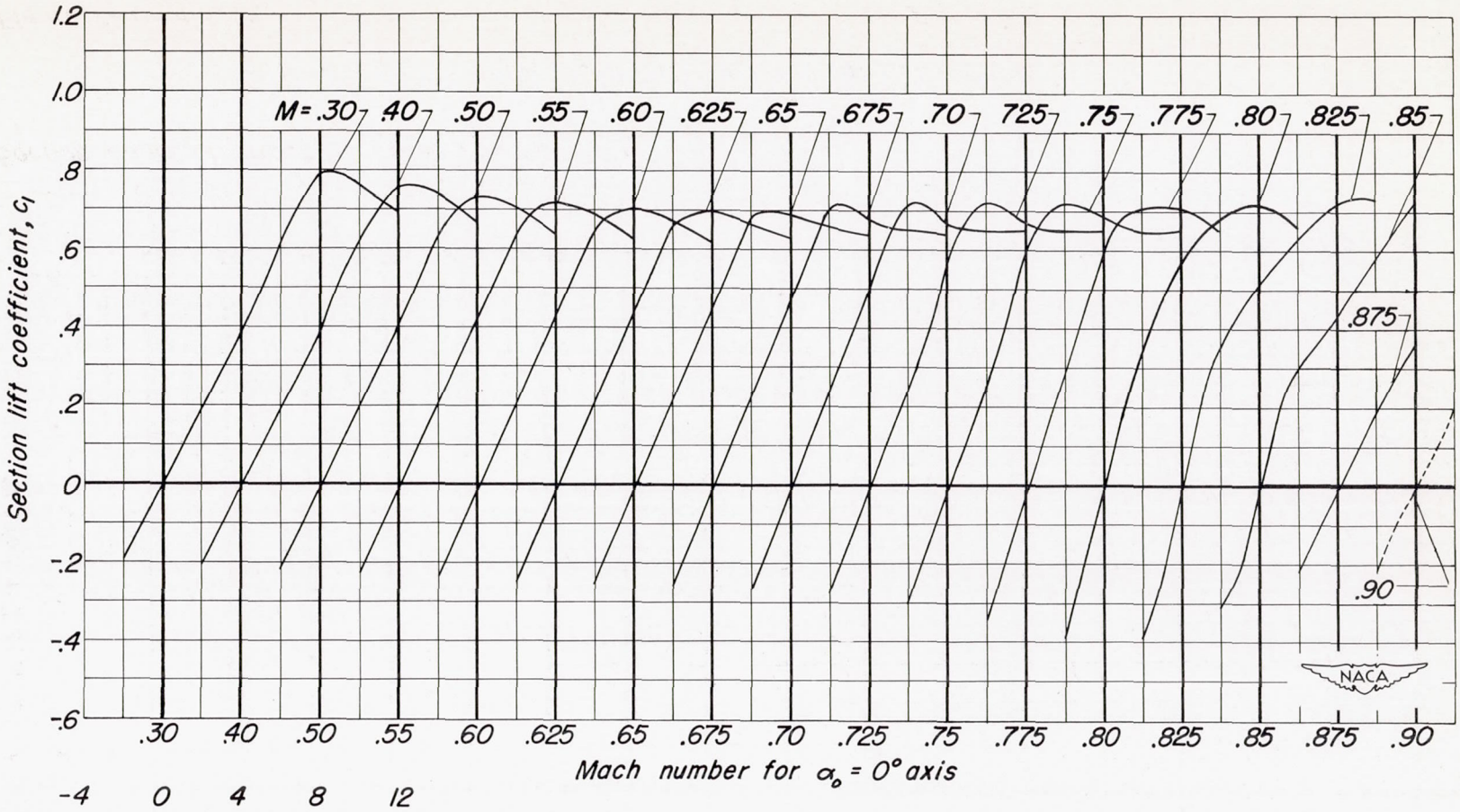

(a) NACA 0010-1.10 40/1.575 airfoil section.

Figure 7.- Variation of section lift coefficient with section angle of attack at various Mach numbers.

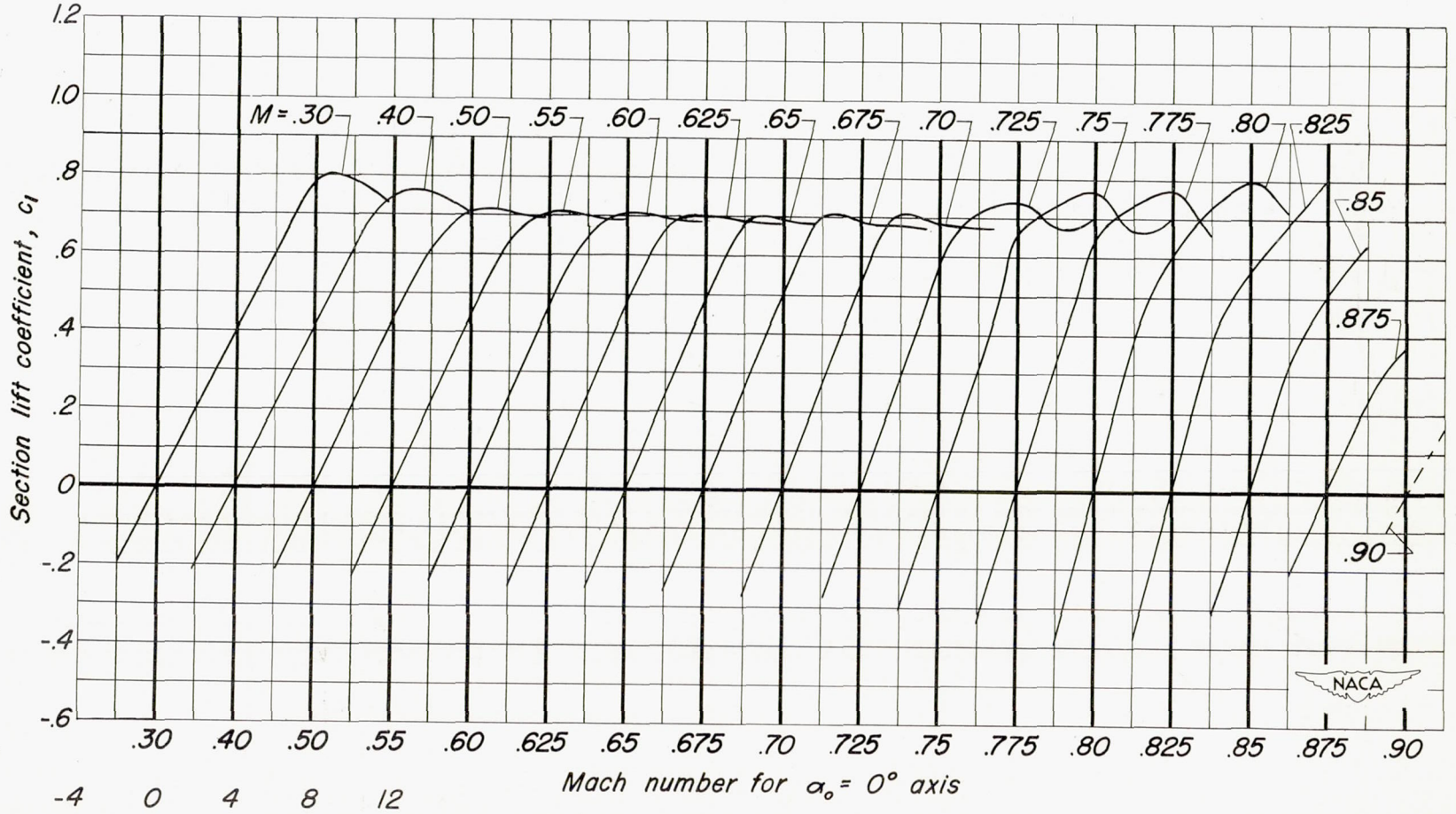

(b) NACA 0010-1.10 40/1.051 airfoil section.

Figure 7.- Continued.

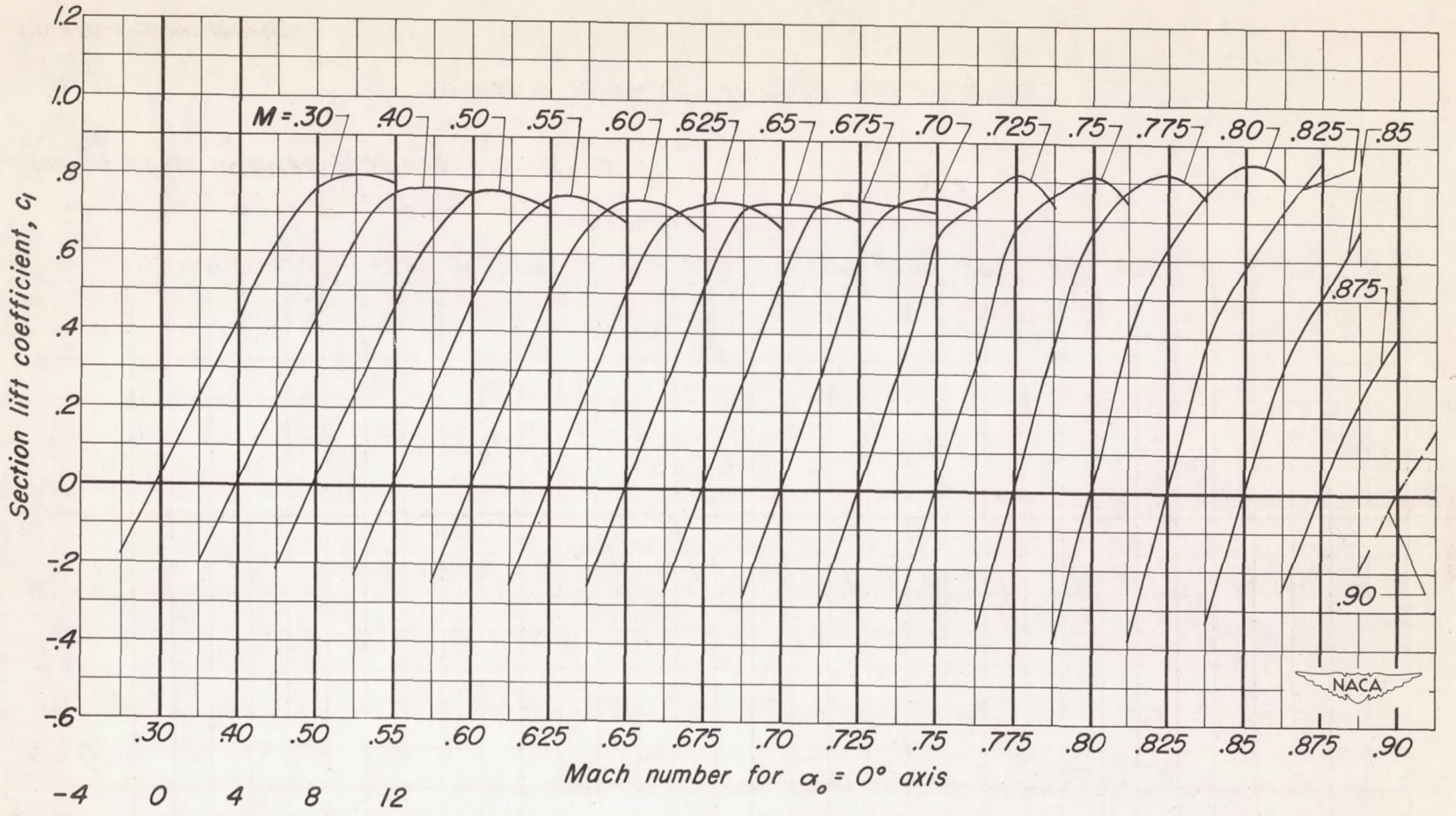

(c) NACA 0010-1.10 40/0.524 airfoil section.

Figure 7.- Continued.

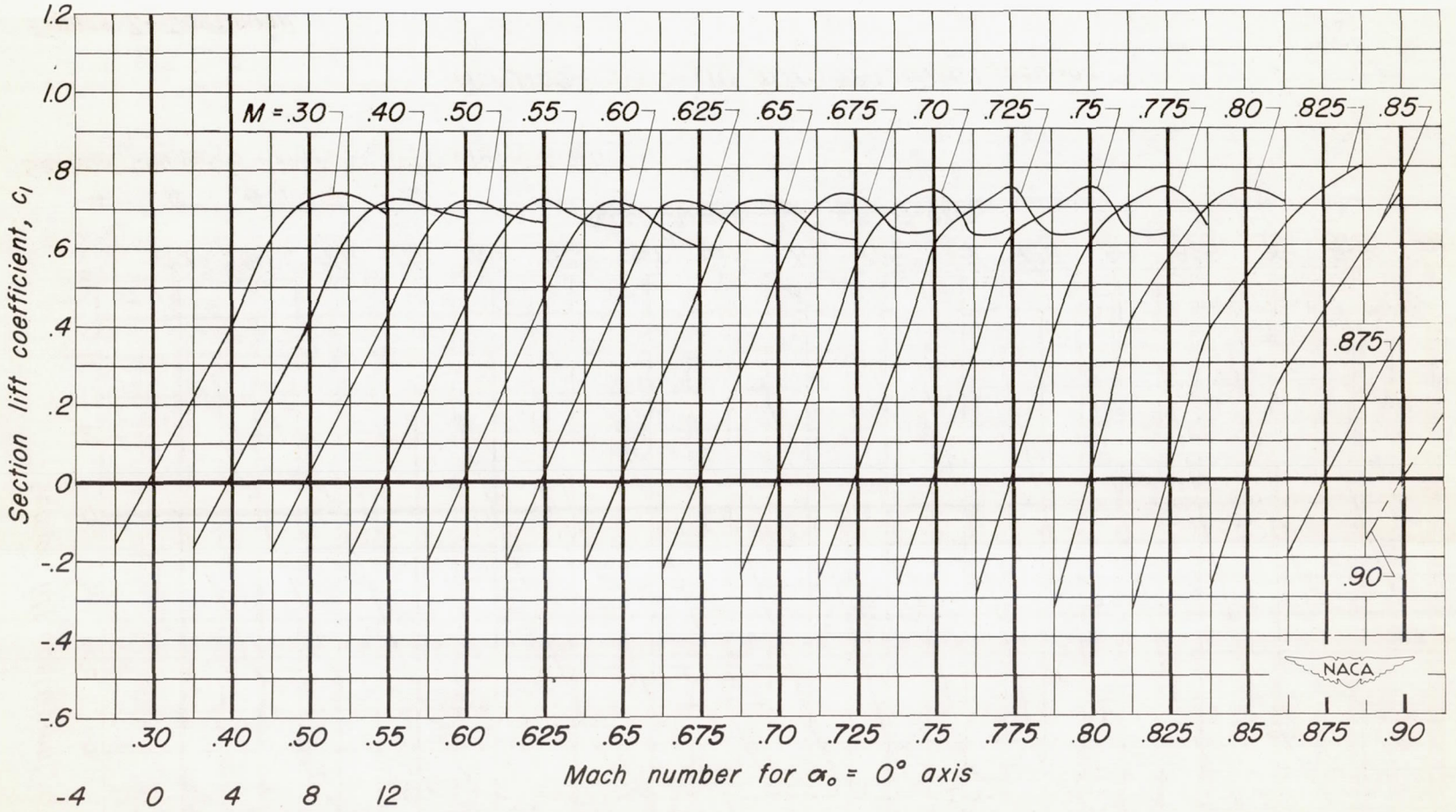

(d) NACA 0010-0.70 40/1.575 airfoil section.

Figure 7.- Continued.

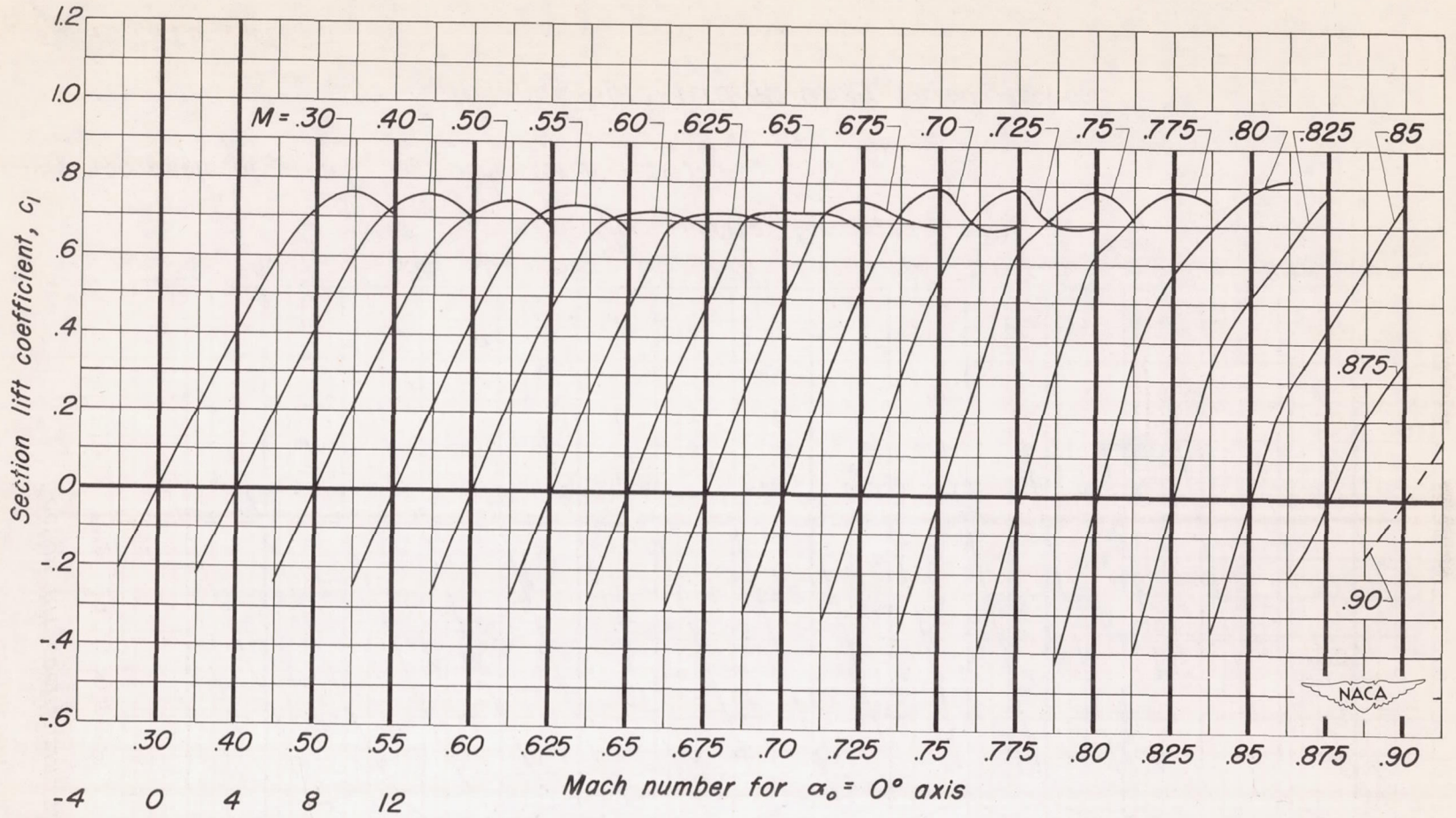

(e) NACA 0010–0.70 40/1.051 airfoil section.

Figure 7.– Continued.

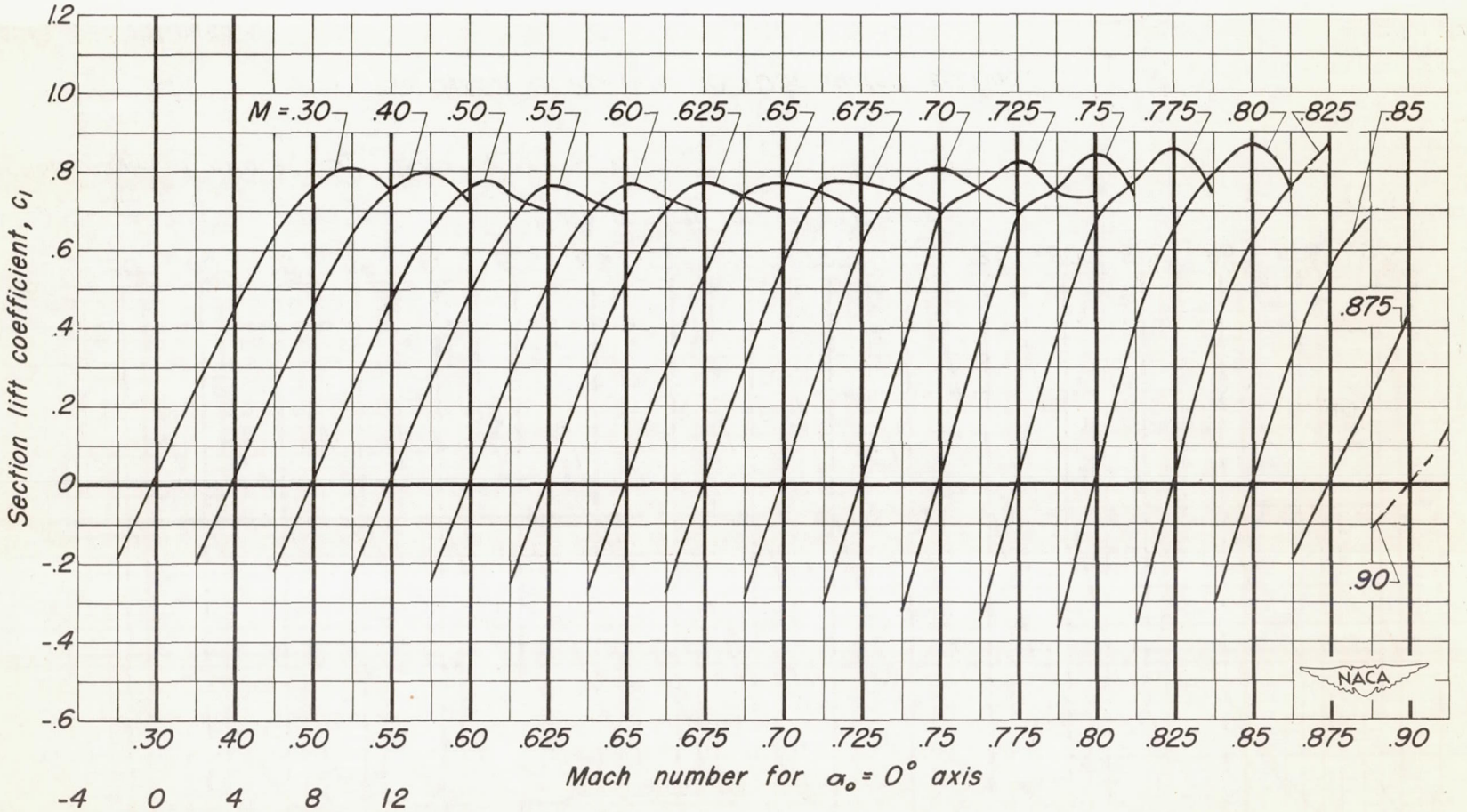

(f) NACA 0010-0.70 40/0.524 airfoil section.

Figure 7.- Continued.

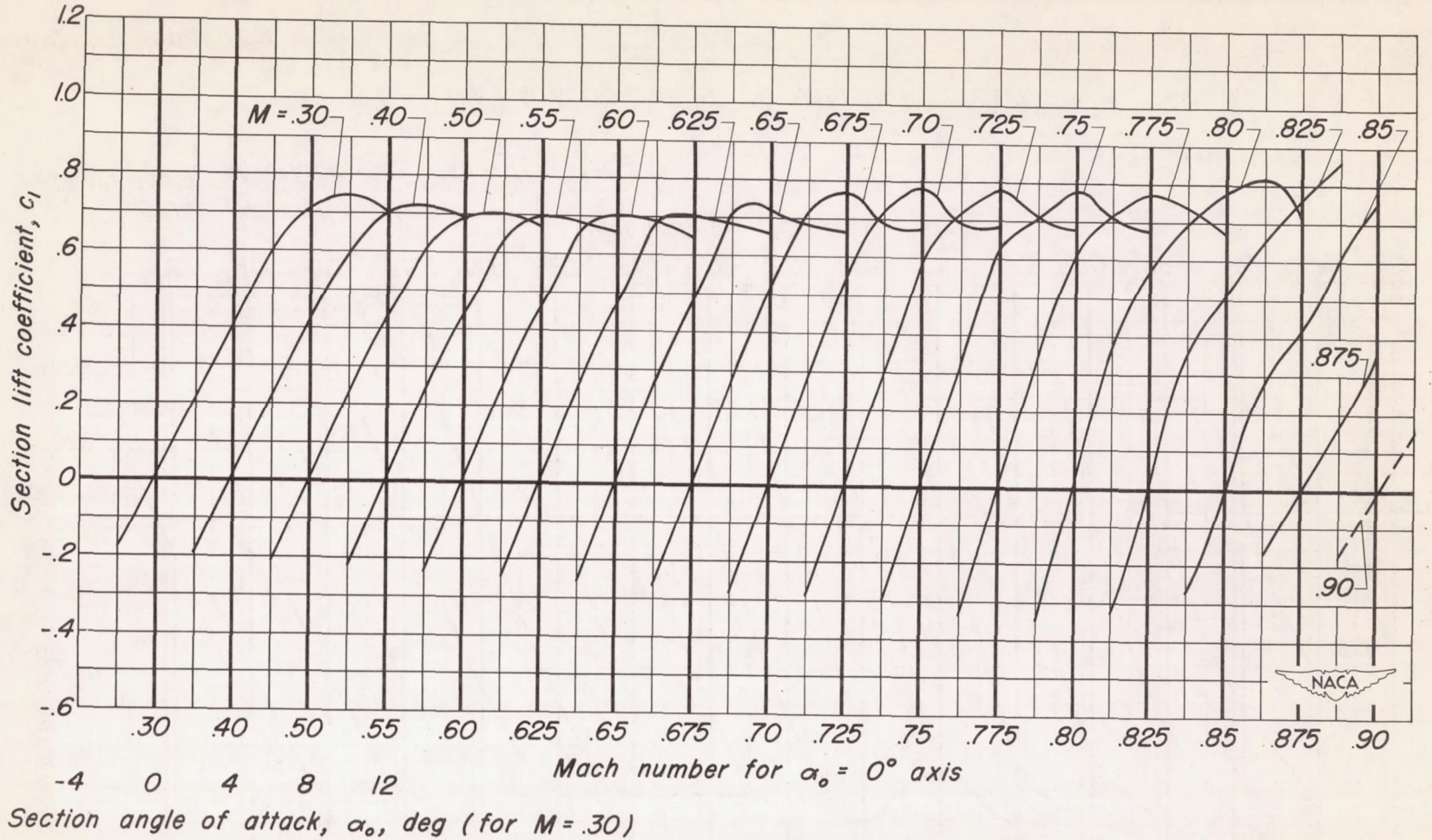

(g) NACA 0010-0.27 40/1.575 airfoil section.

Figure 7.- Continued.

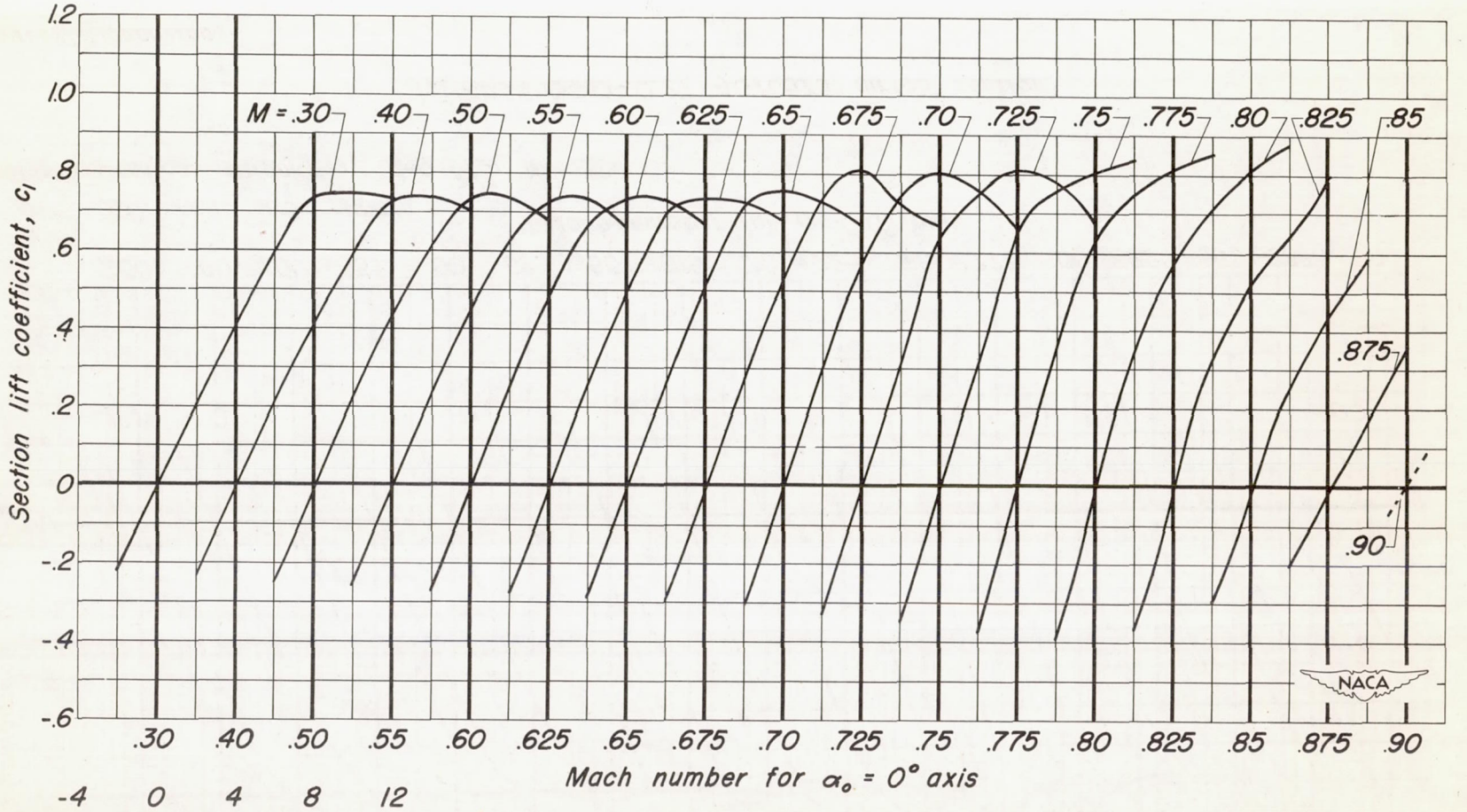

(h) NACA 0010-0.27 40/1.051 airfoil section.

Figure 7.-Continued.

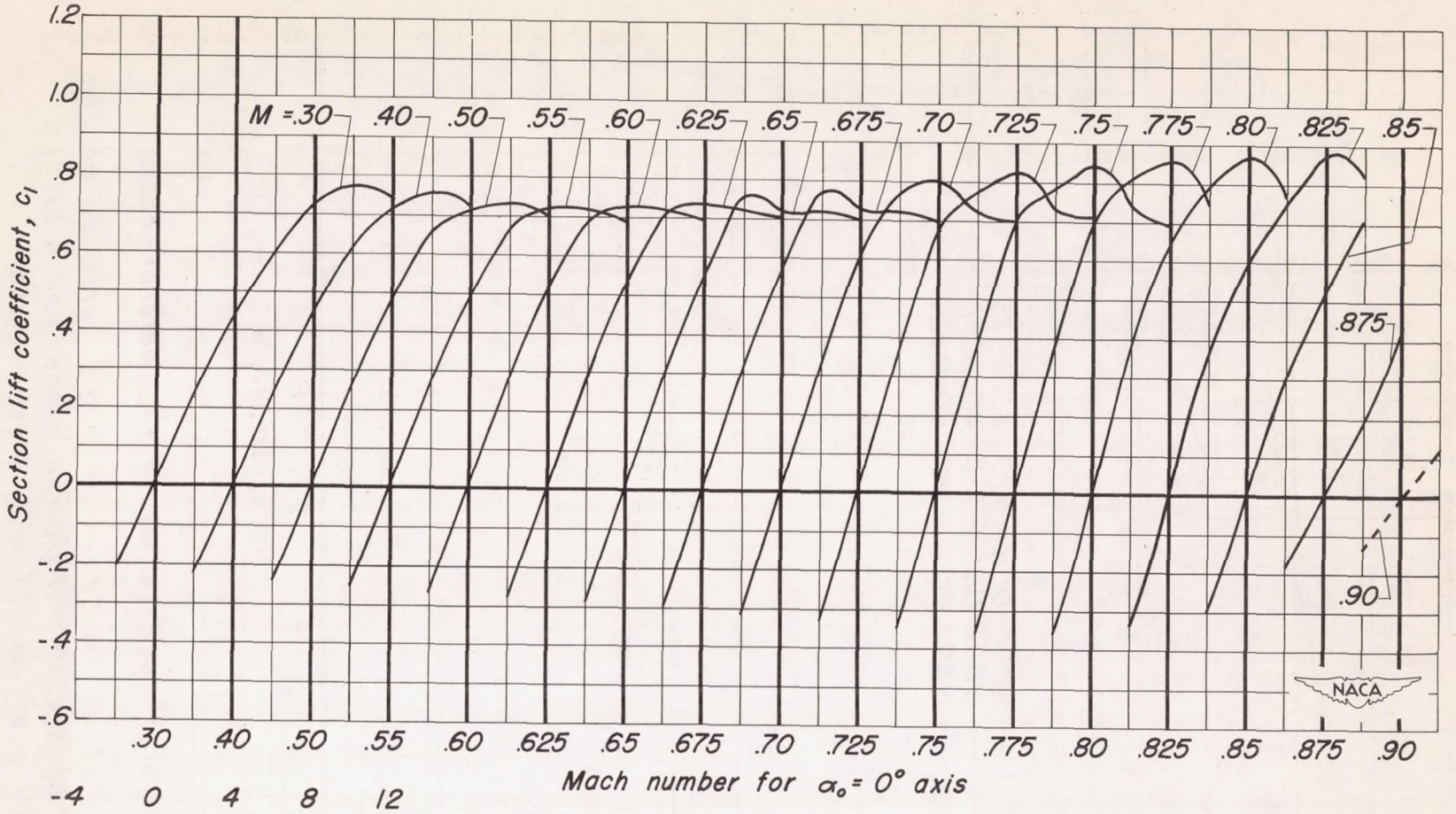

(i) NACA 0010-0.27 40/0.524 airfoil section.

Figure 7.- Concluded.

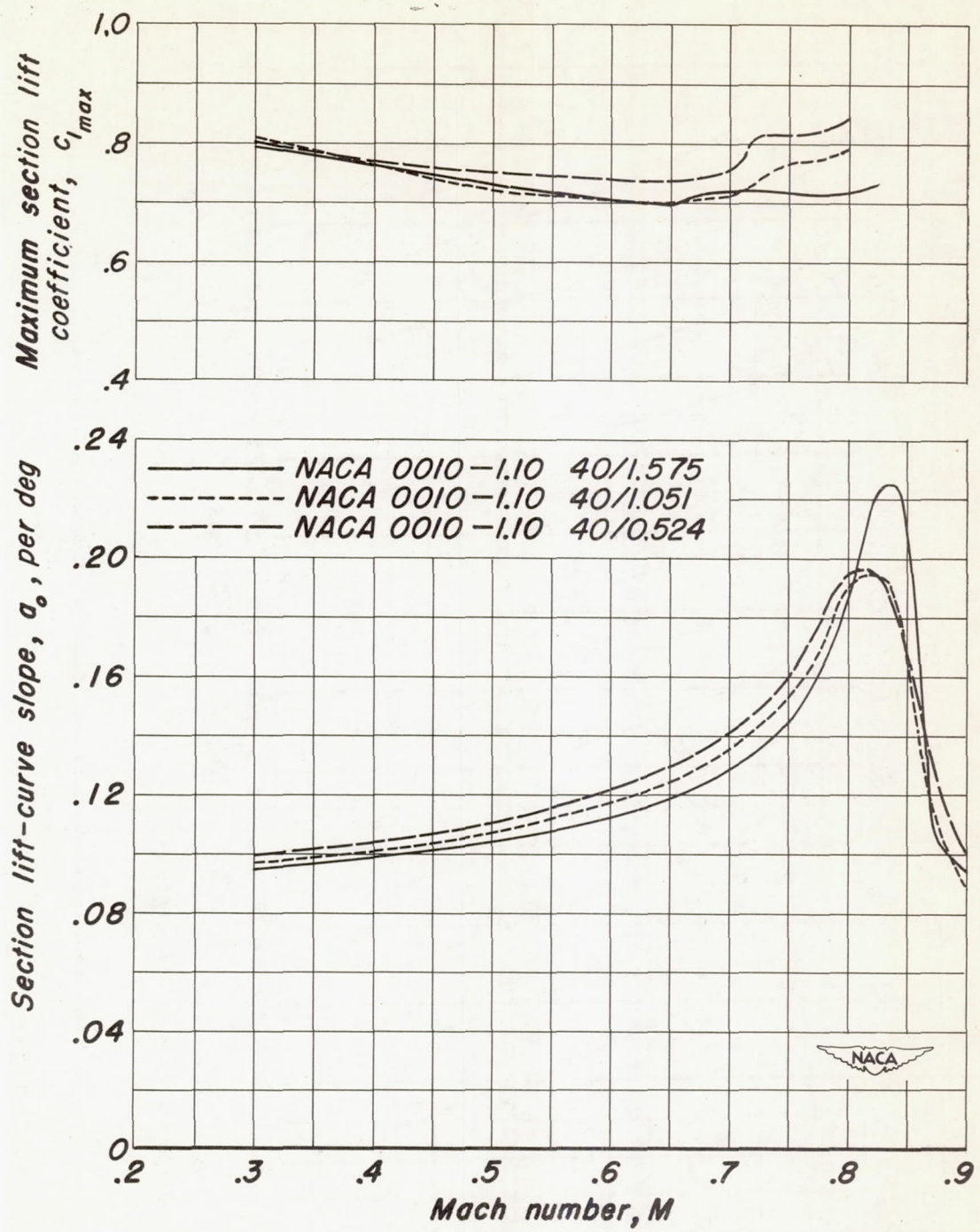

(a) Leading-edge radius of 1.10 percent chord.

Figure 8.- Effect of trailing-edge angle variation on the variation of section lift-curve slope and maximum section lift coefficient with Mach number.

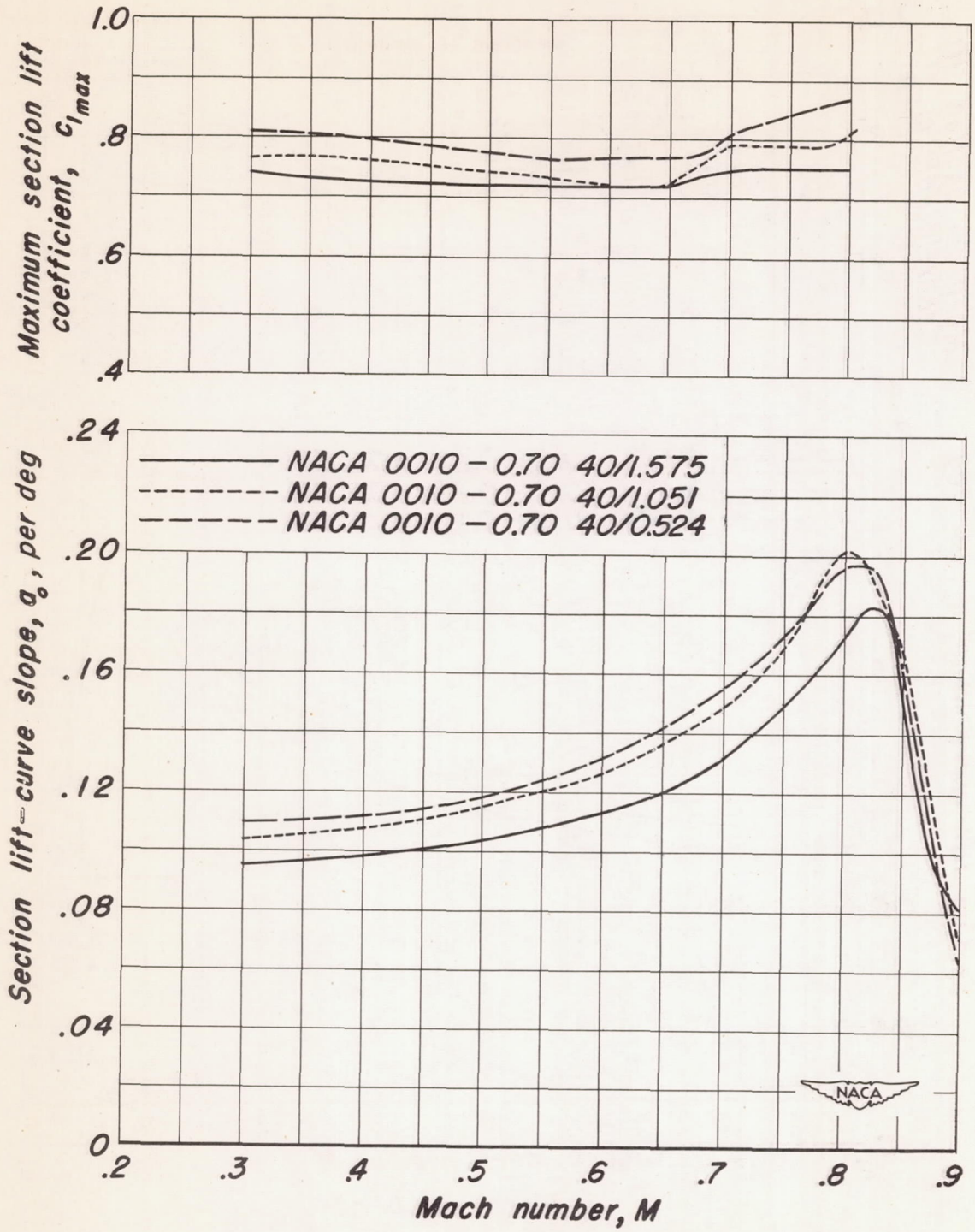

(b) Leading-edge radius of 0.70 percent chord.

Figure 8.– Continued.

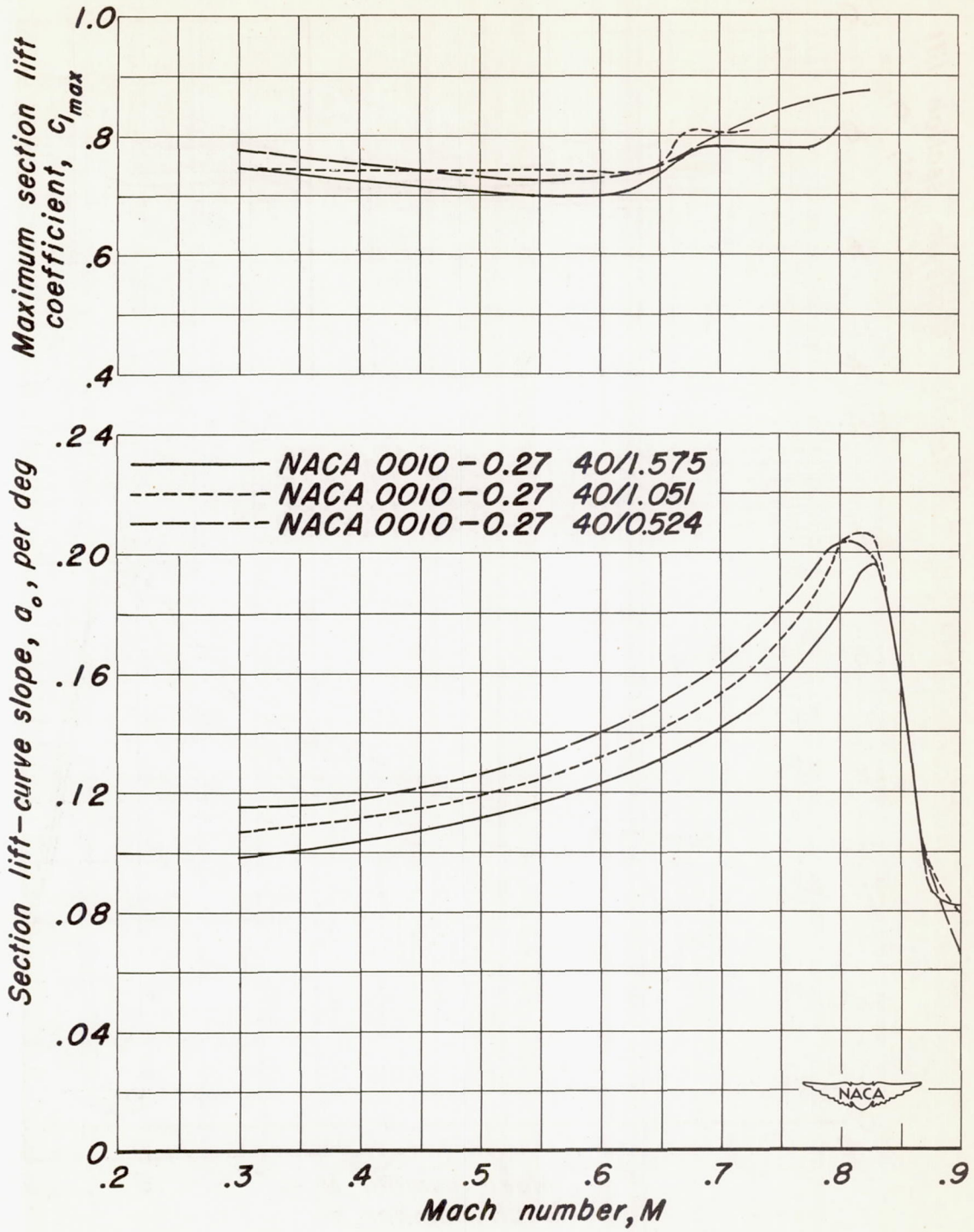

(c) Leading-edge radius of 0.27 percent chord.

Figure 8.-Concluded.

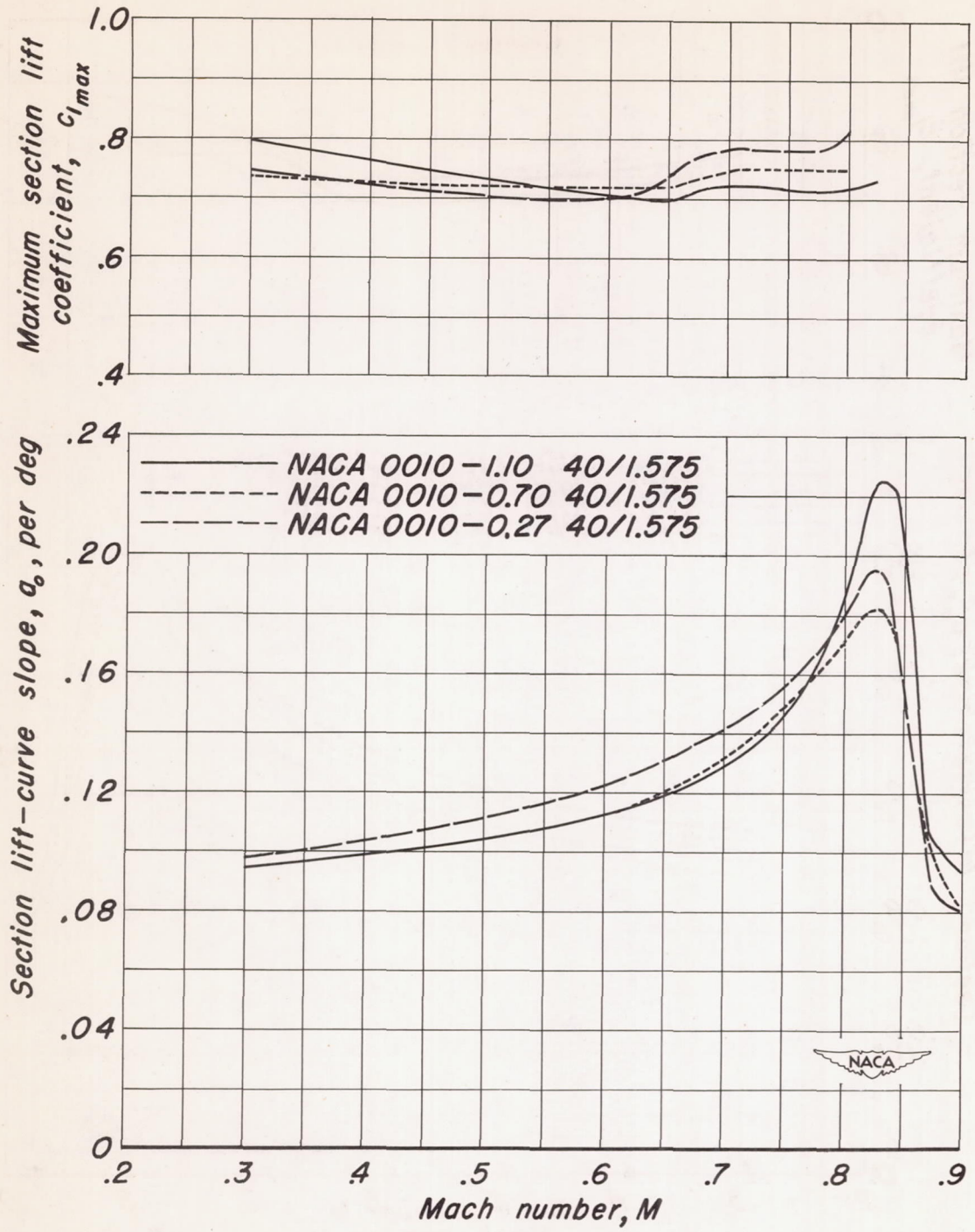

(a) Trailing-edge angle of 17.9°.

Figure 9.- Effect of leading-edge radius variation on the variation of section lift-curve slope and maximum section lift coefficient with Mach number.

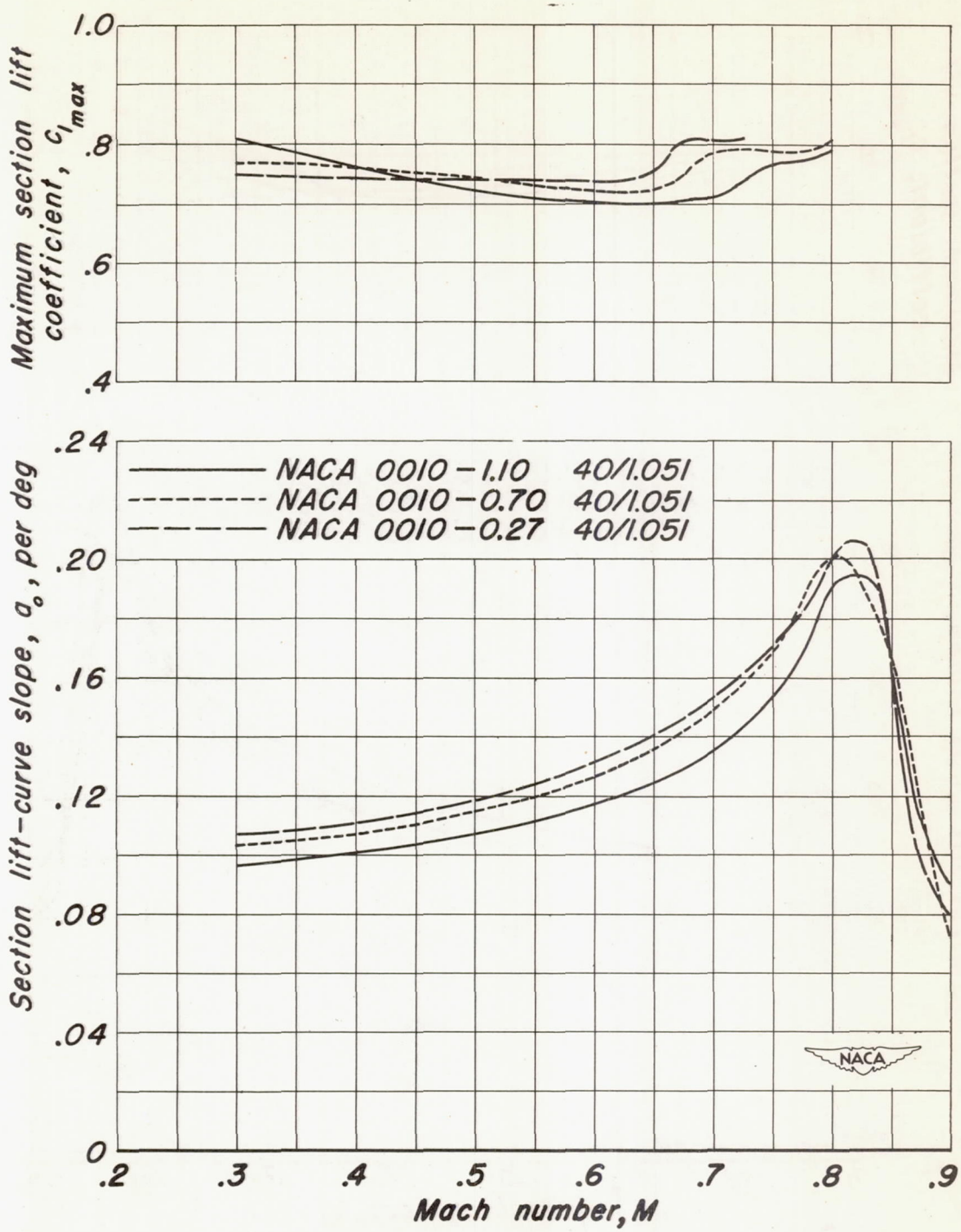

(b) Trailing-edge angle of 12.0°.

Figure 9.- Continued.

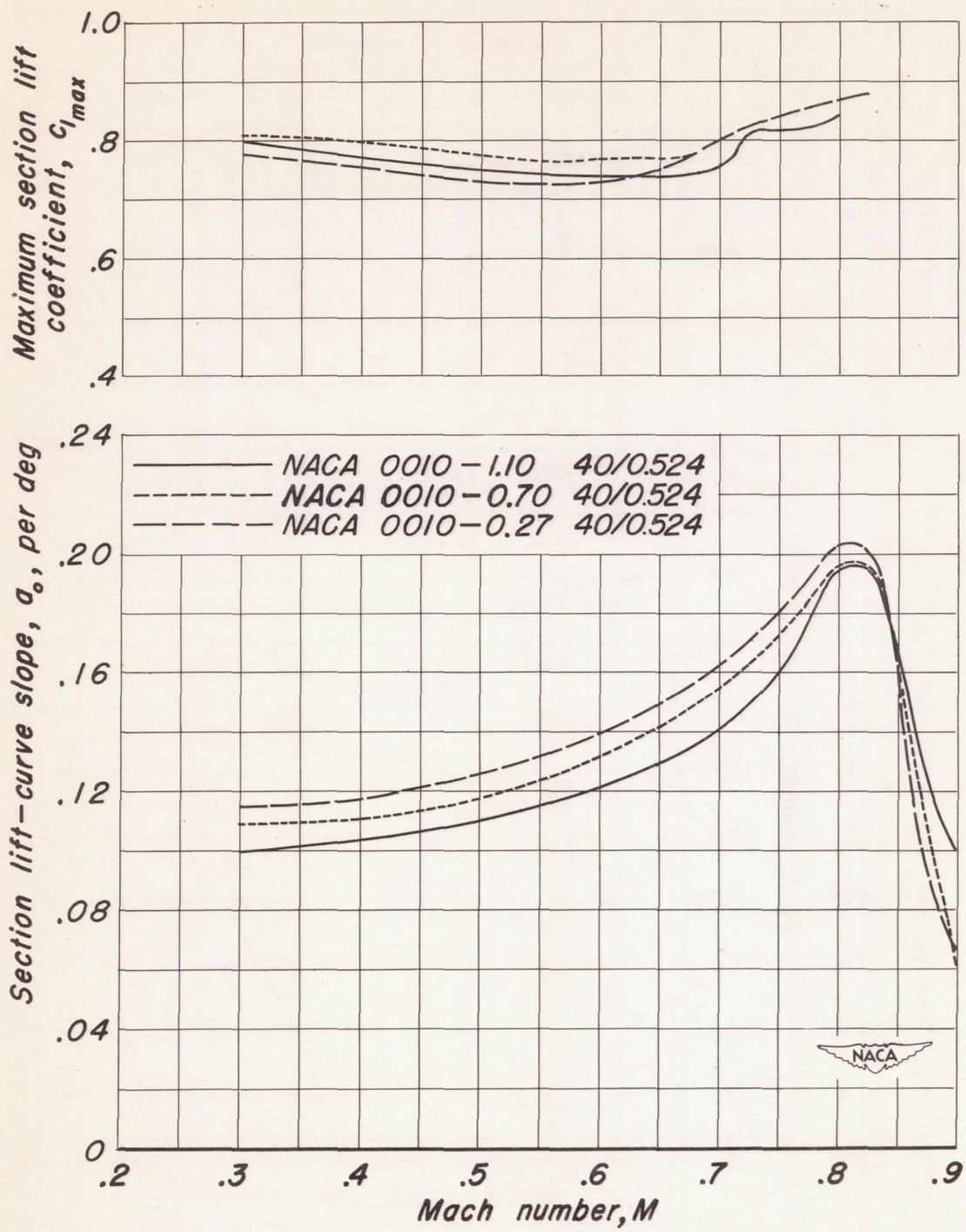

(c) Trailing-edge angle of 6.0°.

Figure 9.- Concluded.

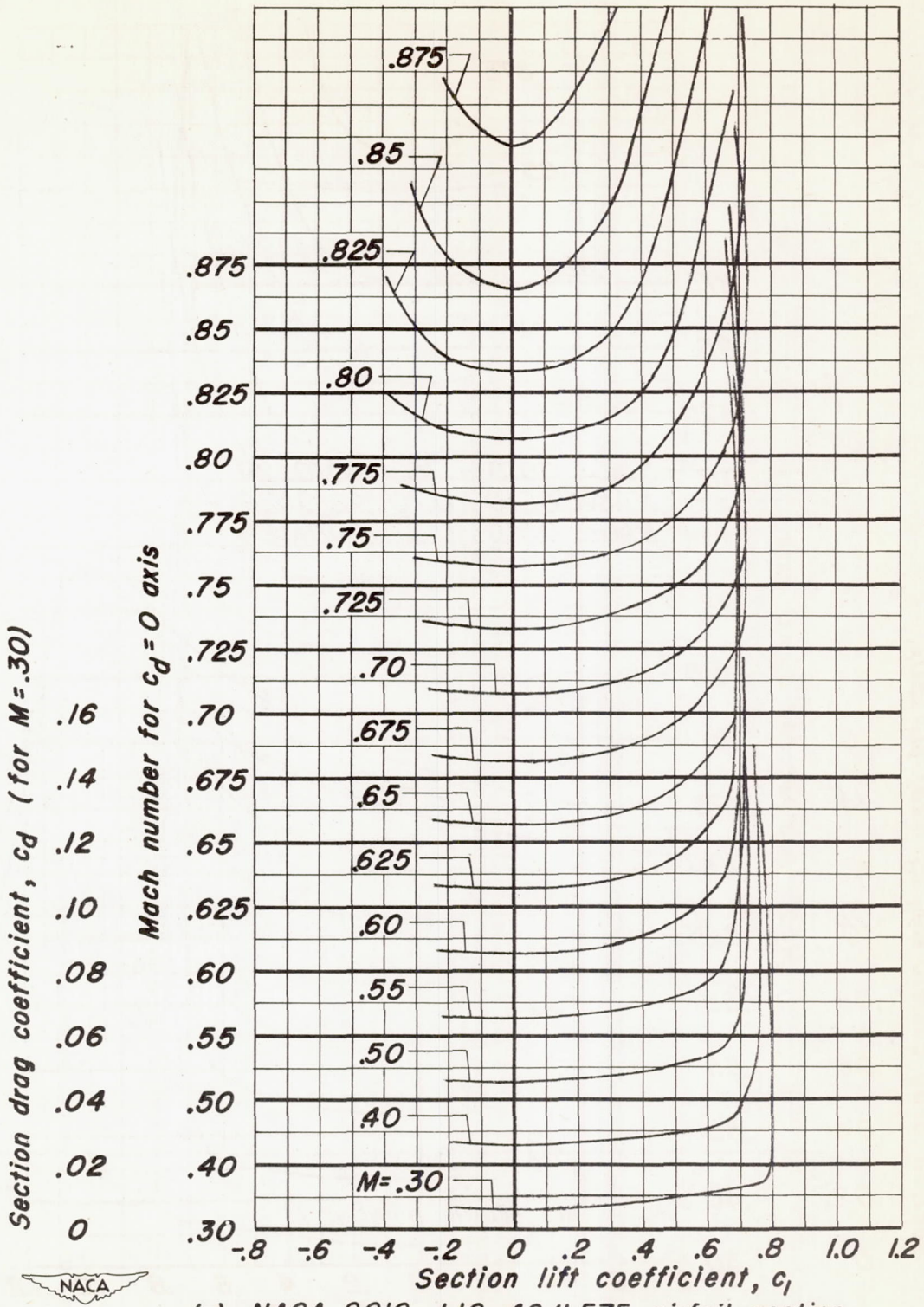

(a) NACA 0010-1.10 40/1.575 airfoil section.

Figure 10.- Variation of section drag coefficient with section lift coefficient at various Mach numbers.

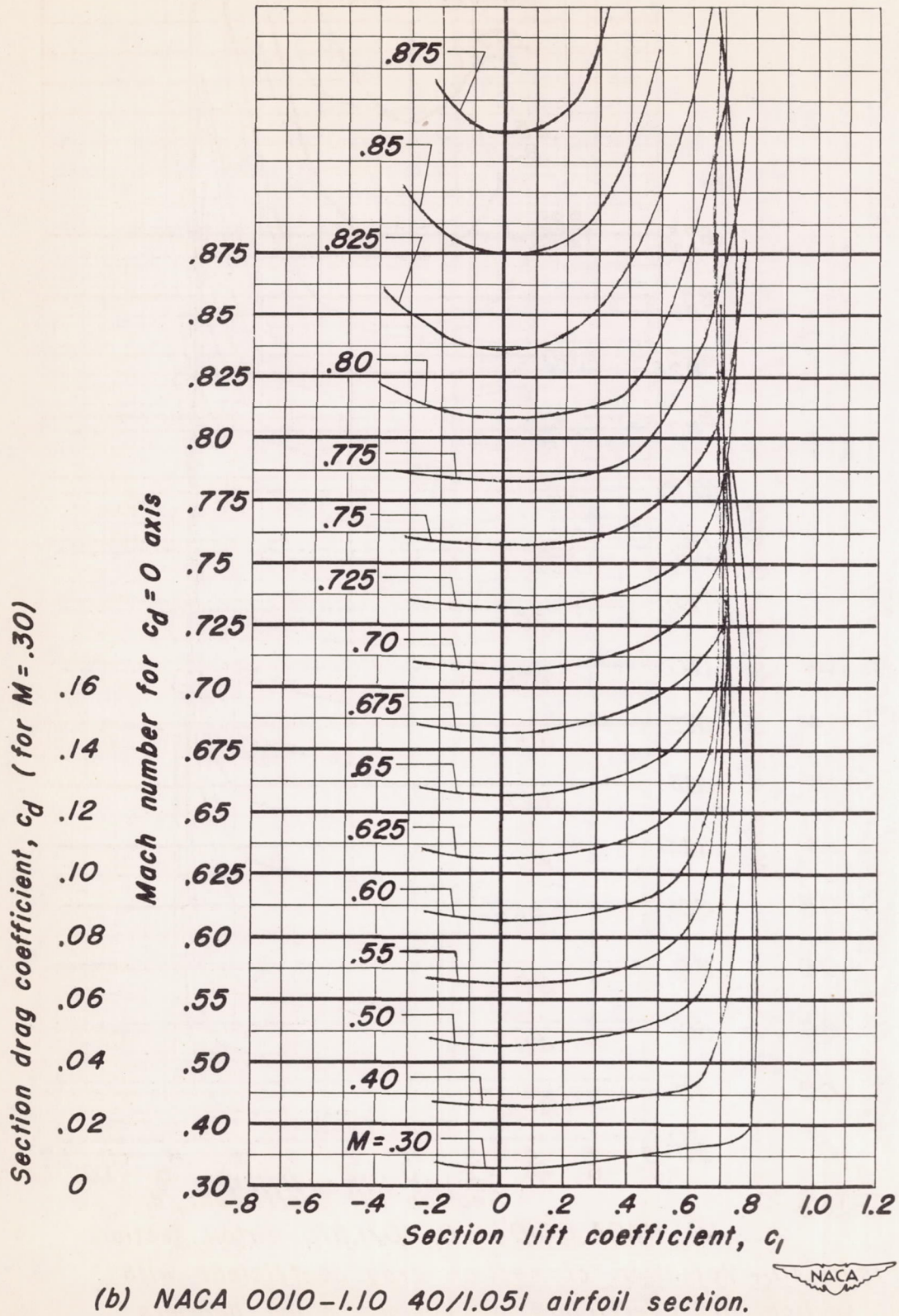

(b) NACA 0010-1.10 40/1.051 airfoil section.

Figure 10.- Continued.

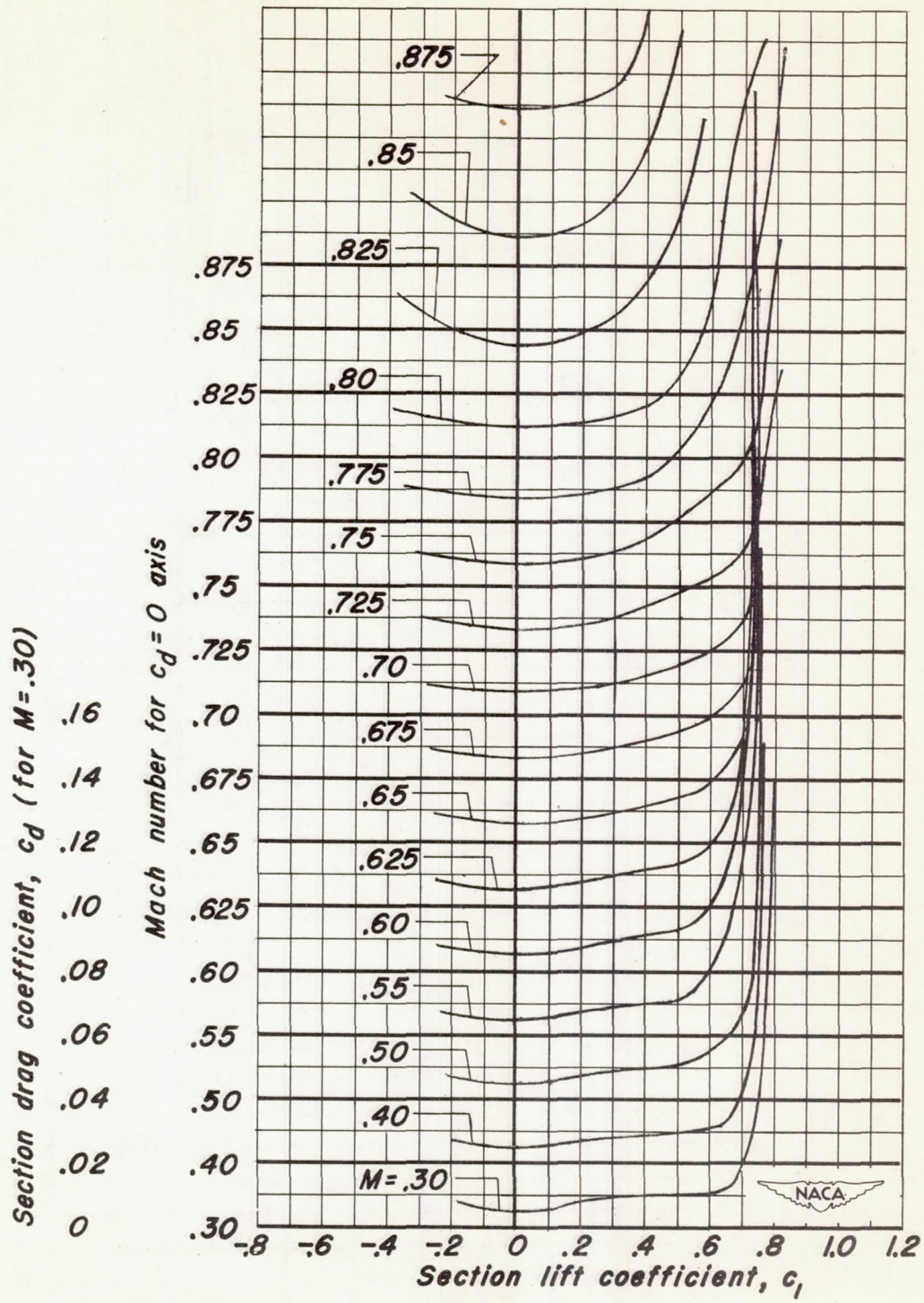

(c) NACA 0010-1.10 40/0.524 airfoil section.

Figure 10.-Continued.

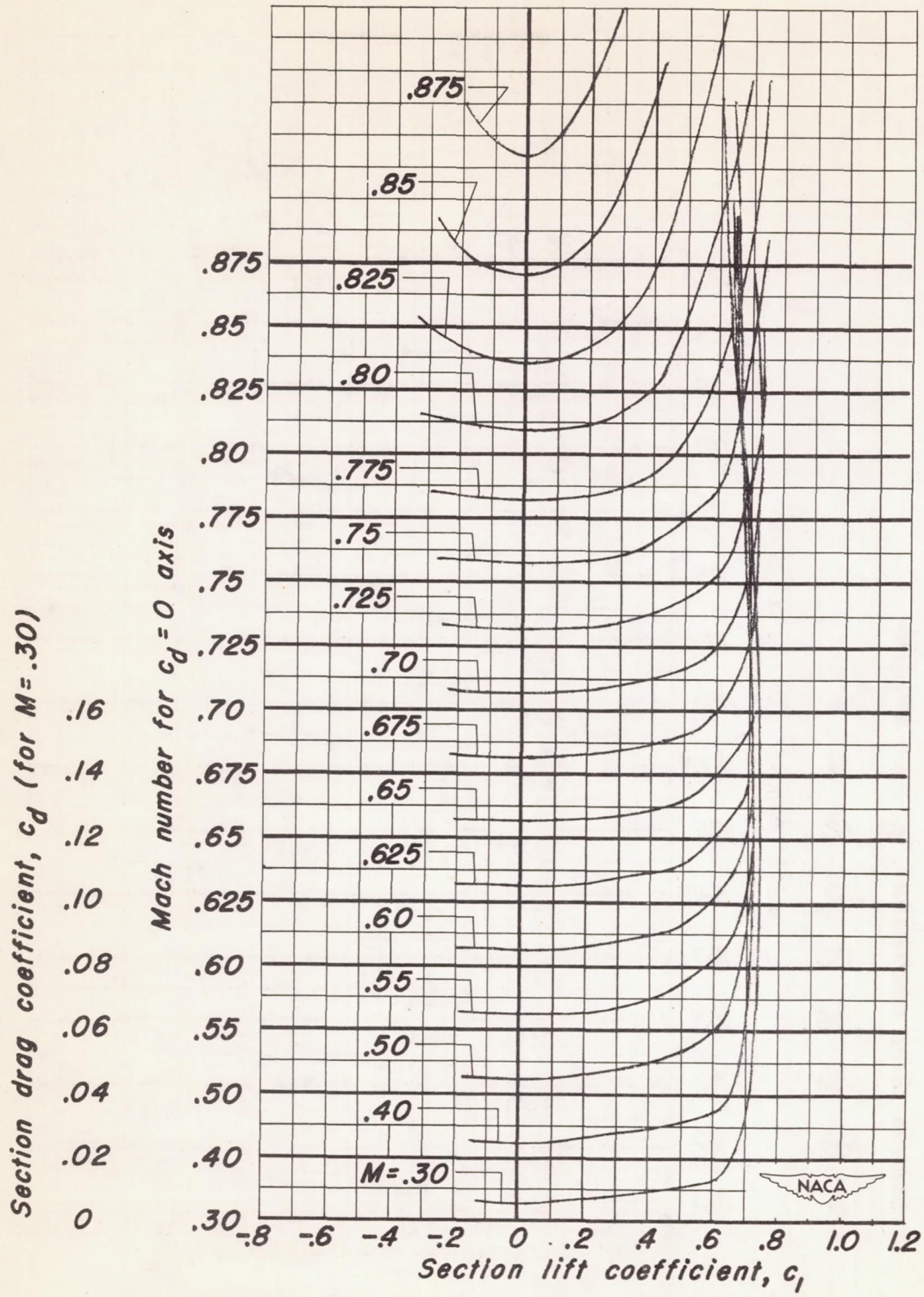

(d) NACA 0010-0.70 40/1.575 airfoil section.

Figure 10.- Continued.

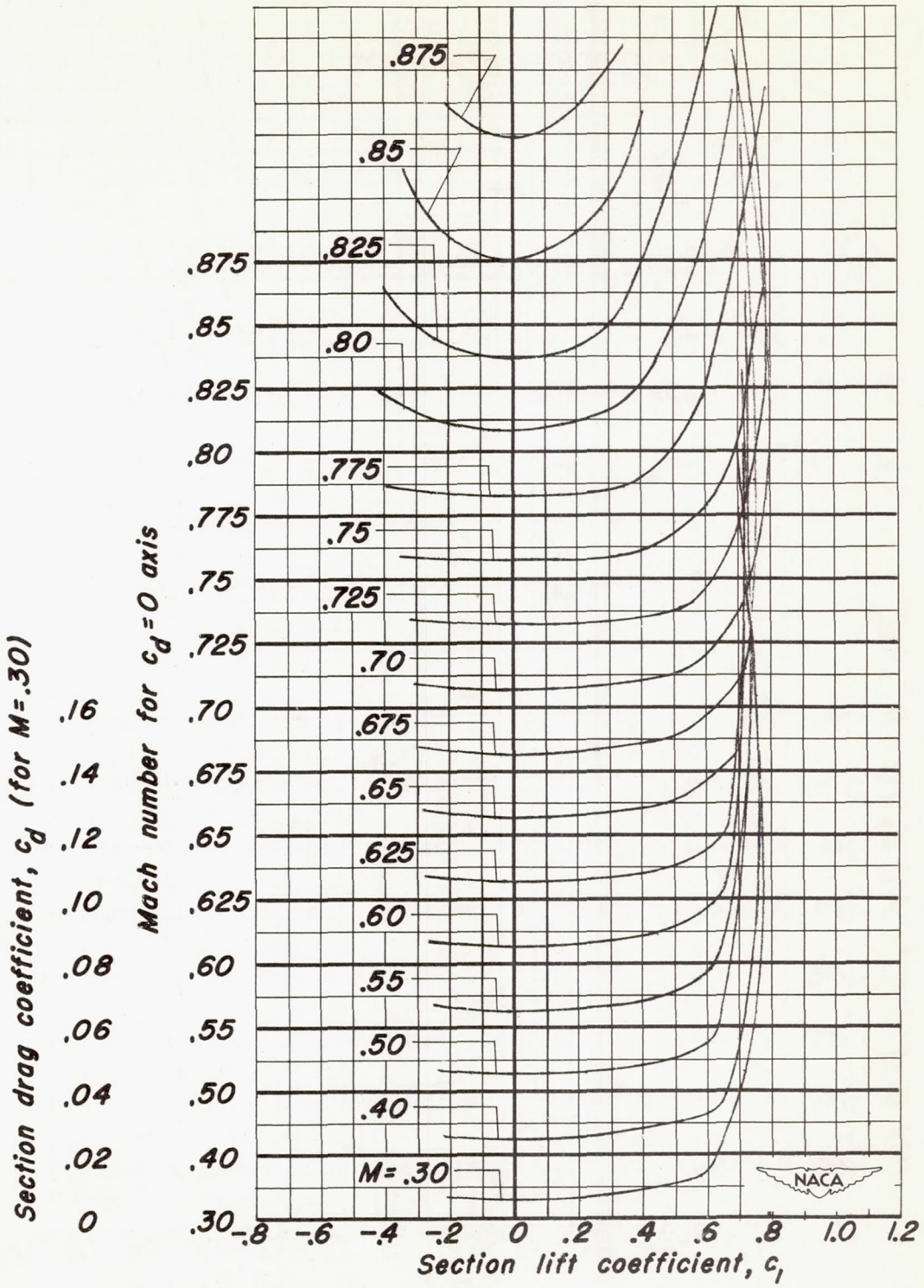

(e) NACA 0010-0.70 40/1.051 airfoil section.

Figure 10.- Continued.

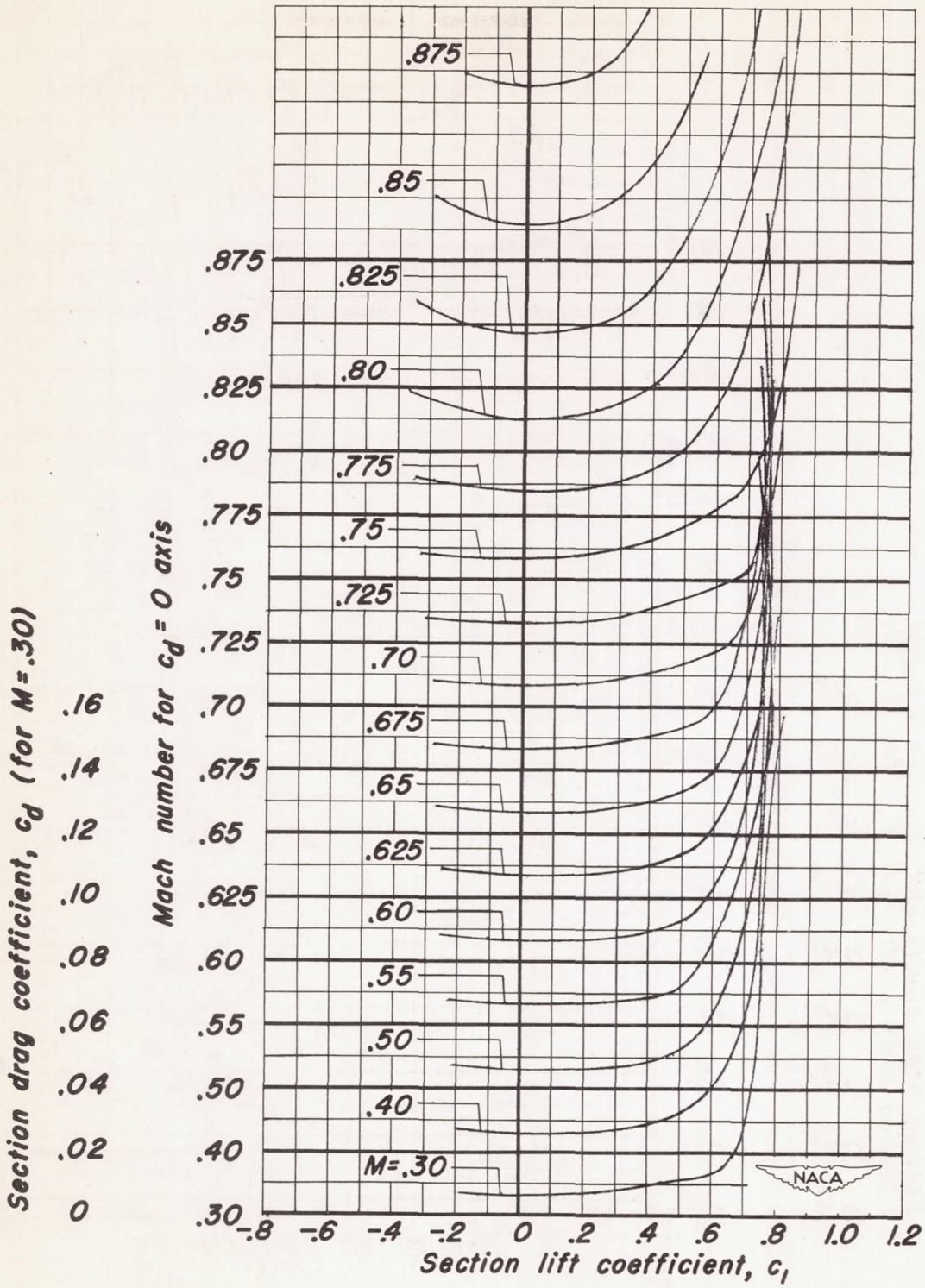

(f) NACA 0010-0.70 40/0.524 airfoil section.

Figure 10.—Continued.

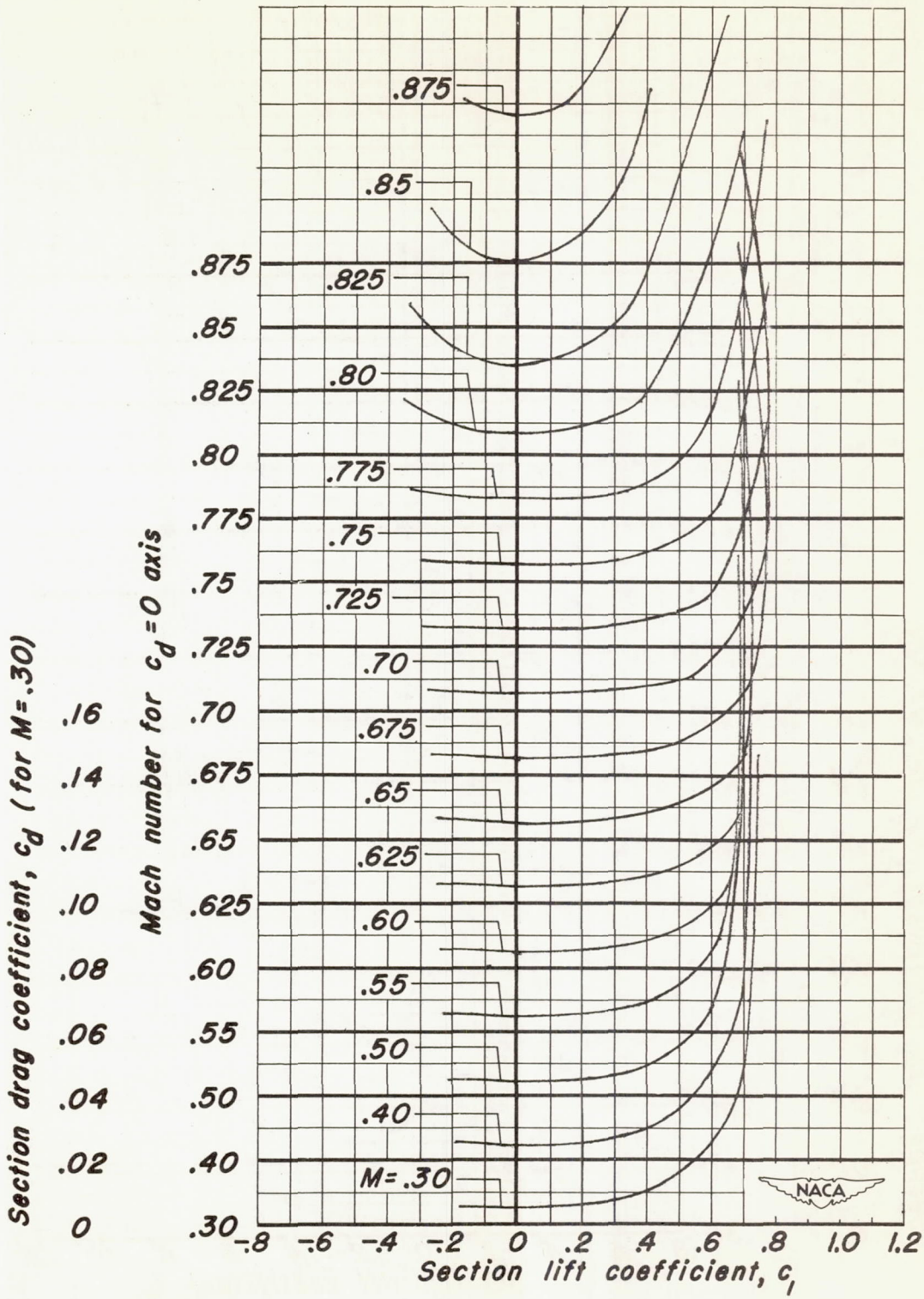

(g) NACA 0010-0.27 40/1.575 airfoil section.

Figure 10.-Continued.

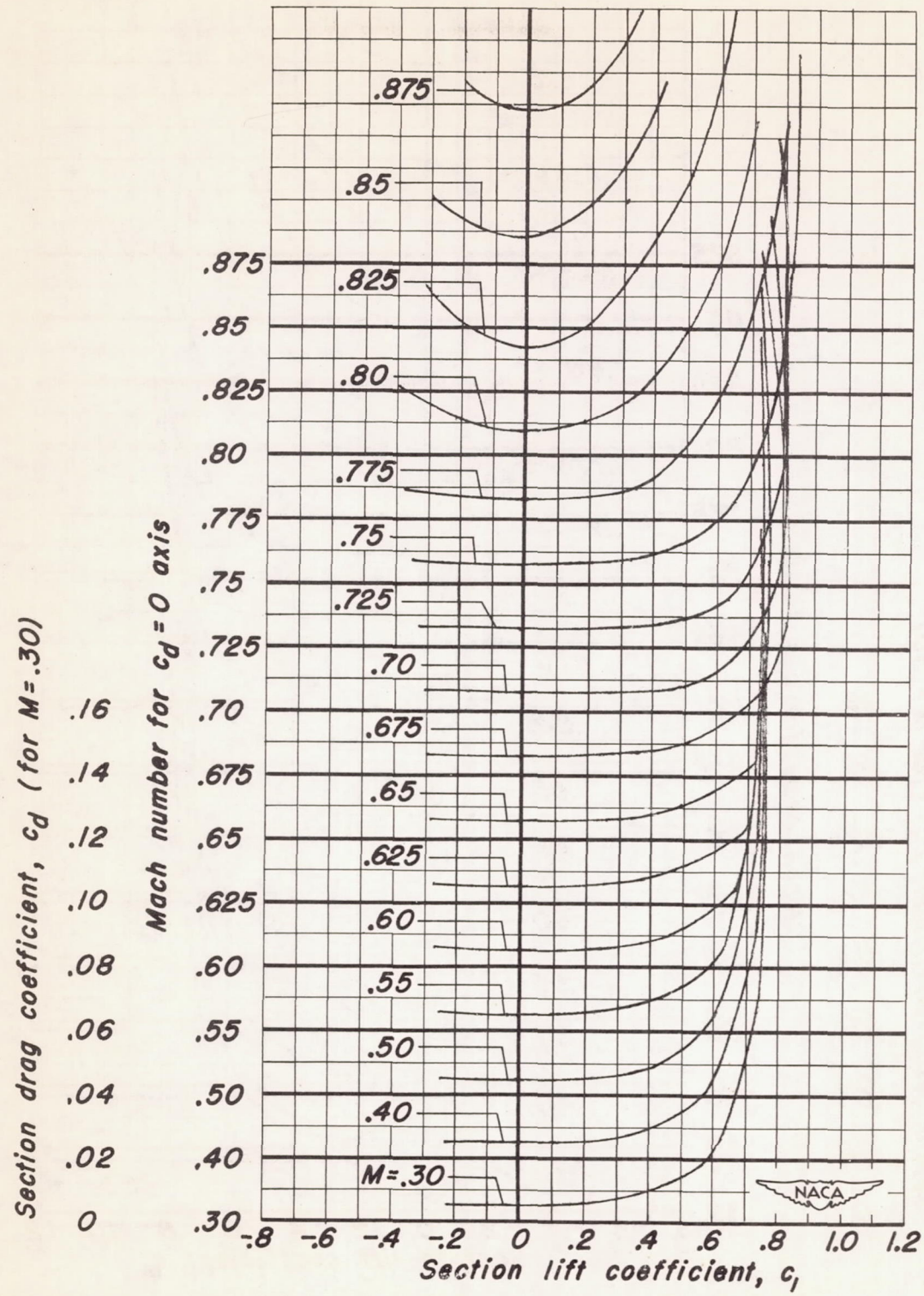

(h) NACA 0010-0.27 40/1.051 airfoil section.

Figure 10.-Continued.

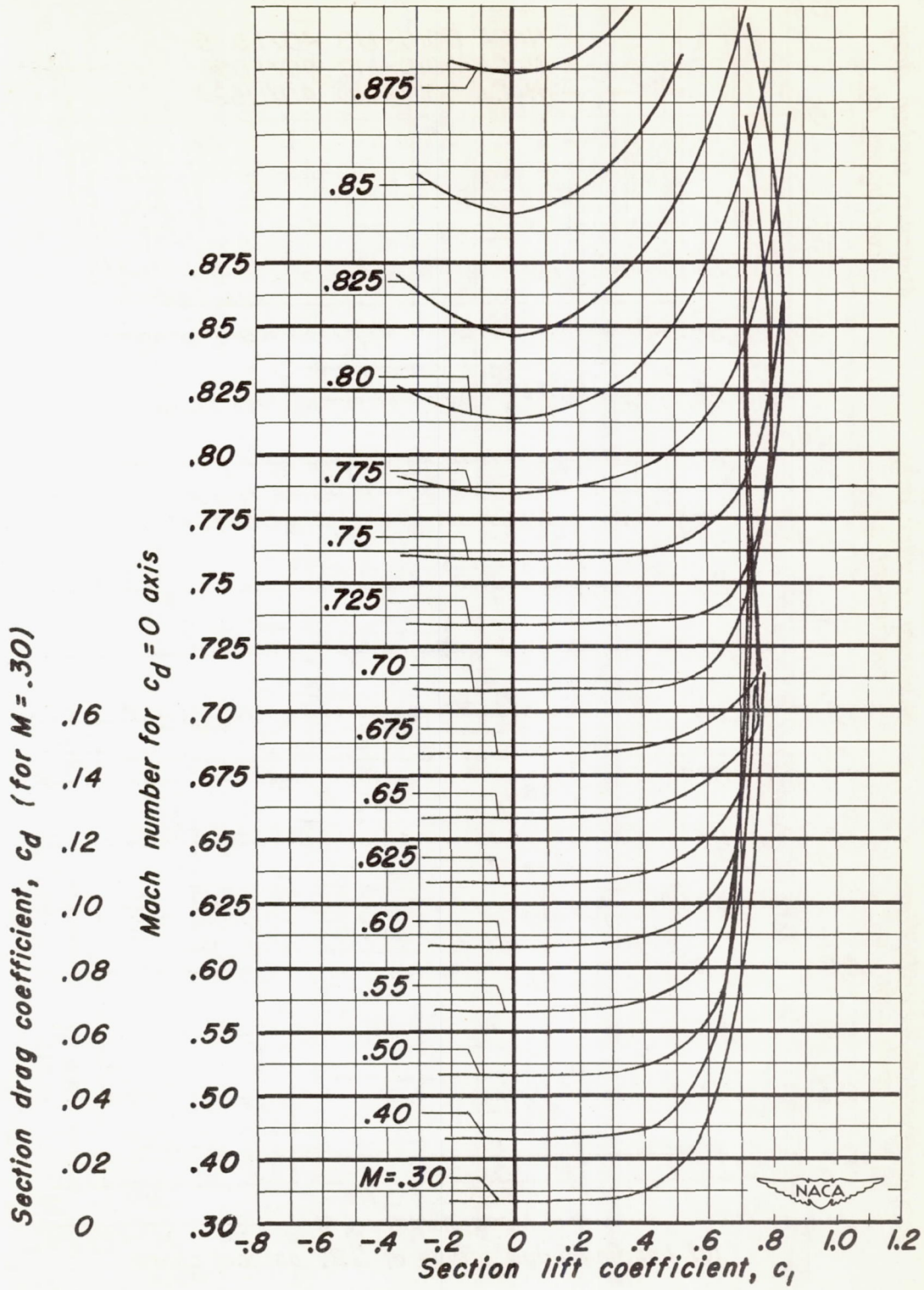

(i) NACA 0010-0.27 40/0.524 airfoil section.

Figure 10.- Concluded.

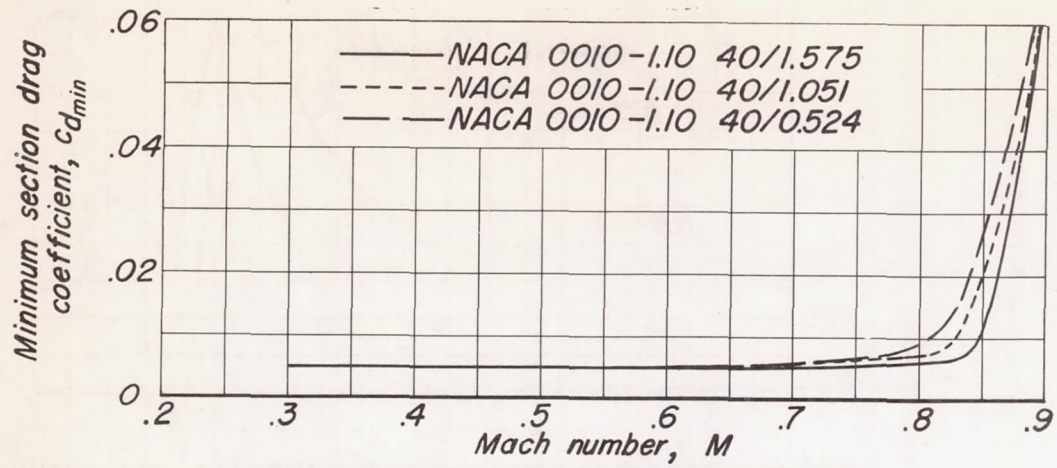

(a) Leading-edge radius of 1.10 percent chord.

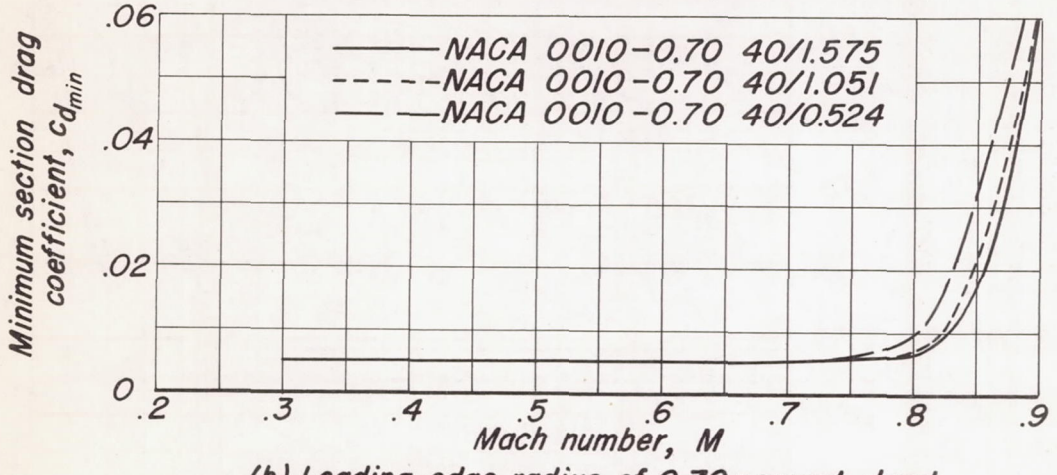

(b) Leading-edge radius of 0.70 percent chord.

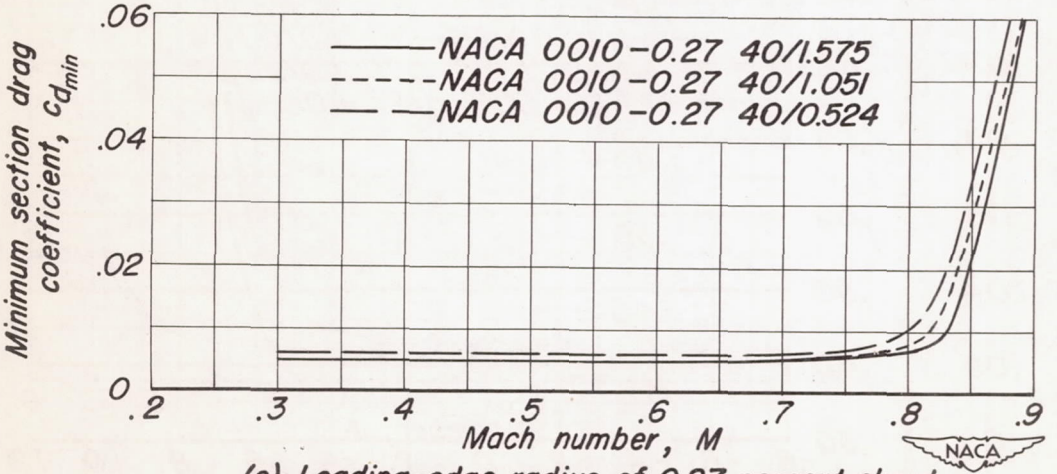

(c) Leading-edge radius of 0.27 percent chord.

Figure 11.- Effect of trailing-edge angle variation on the variation of minimum section drag coefficient with Mach number.

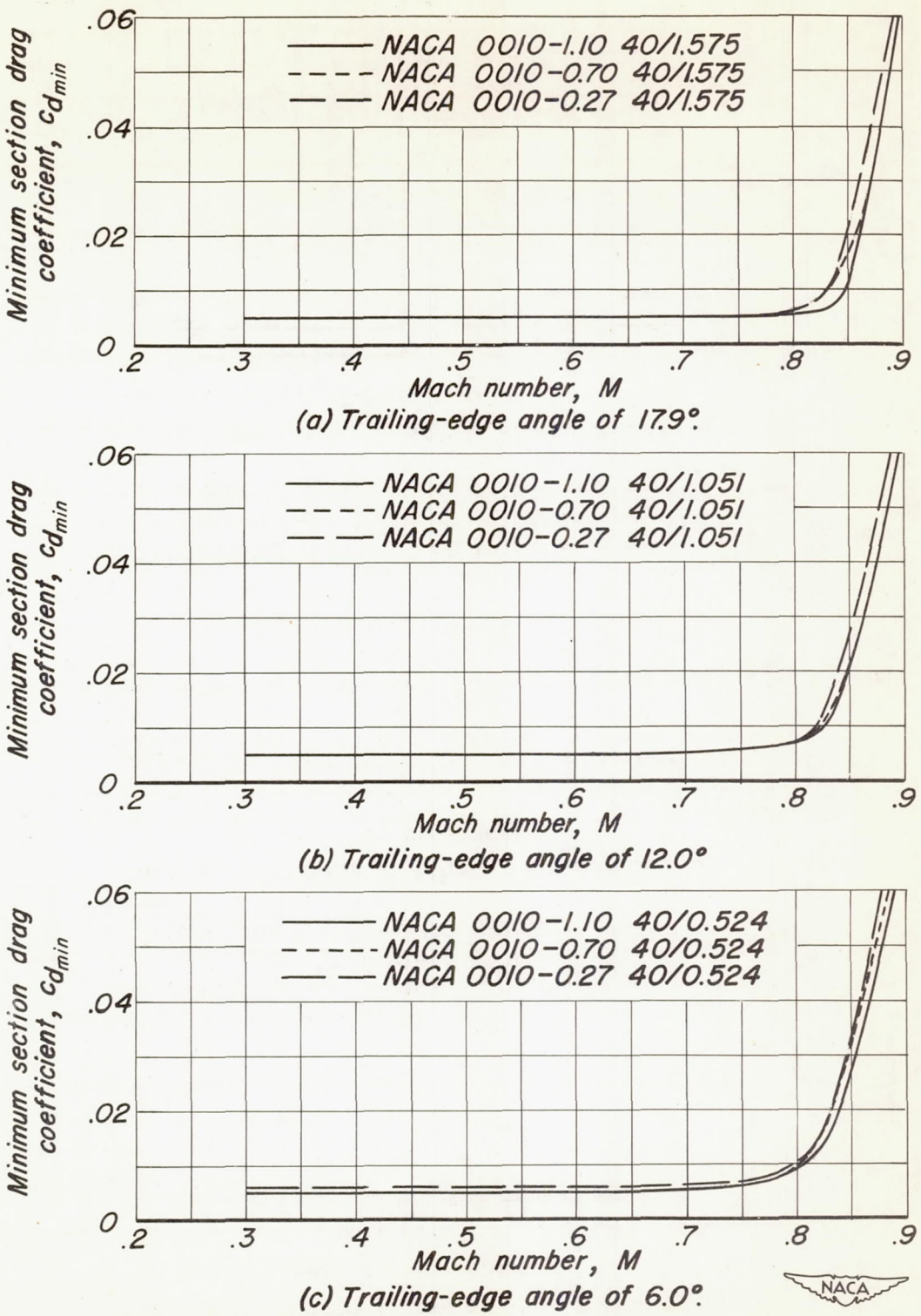

Figure 12.– Effect of leading-edge radius variation on the variation of minimum section drag coefficient with Mach number.

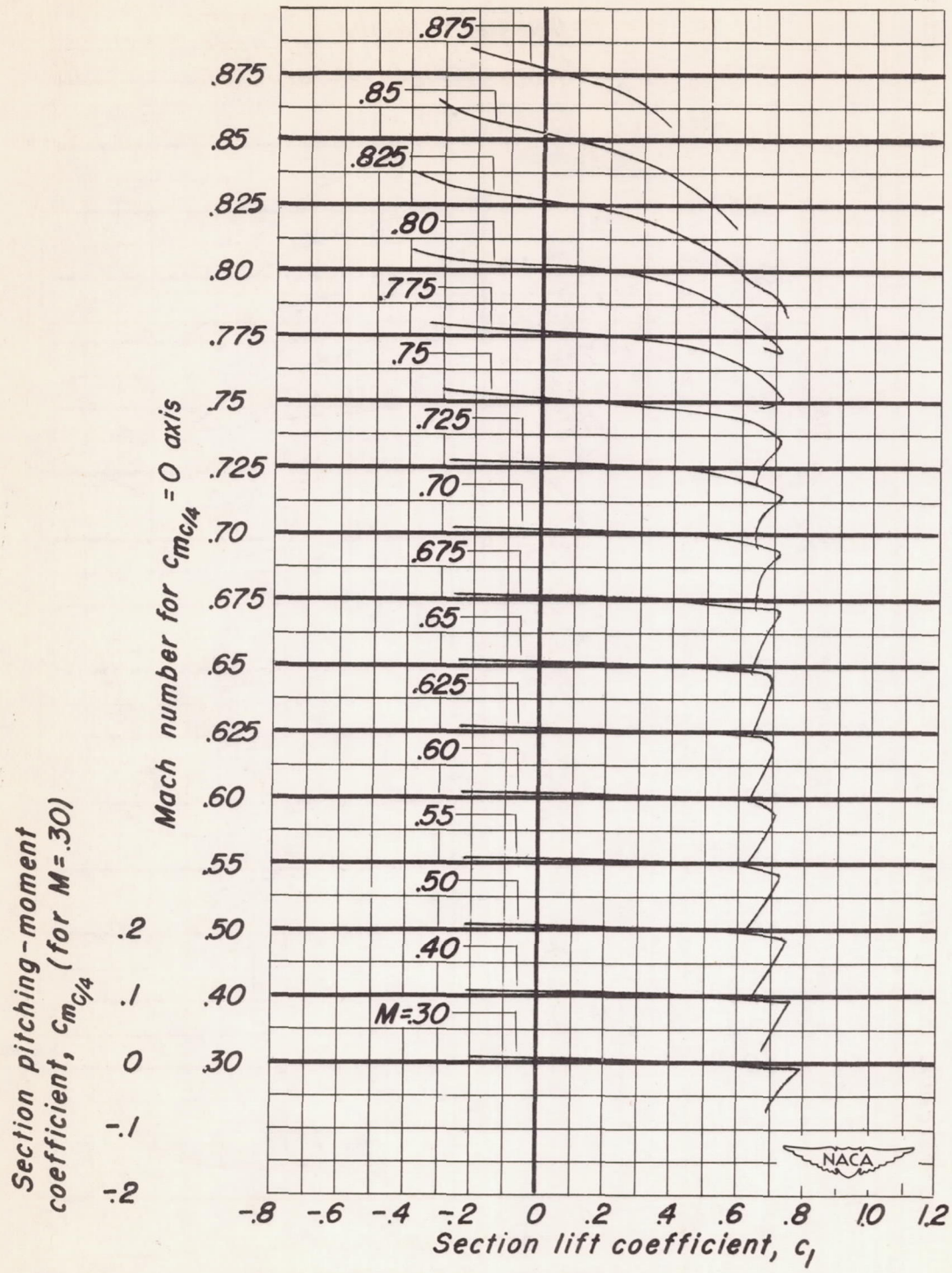

(a) NACA 0010-1.10 40/1.575 airfoil section.

Figure 13.- Variation of section pitching-moment coefficient with section lift coefficient at various Mach numbers.

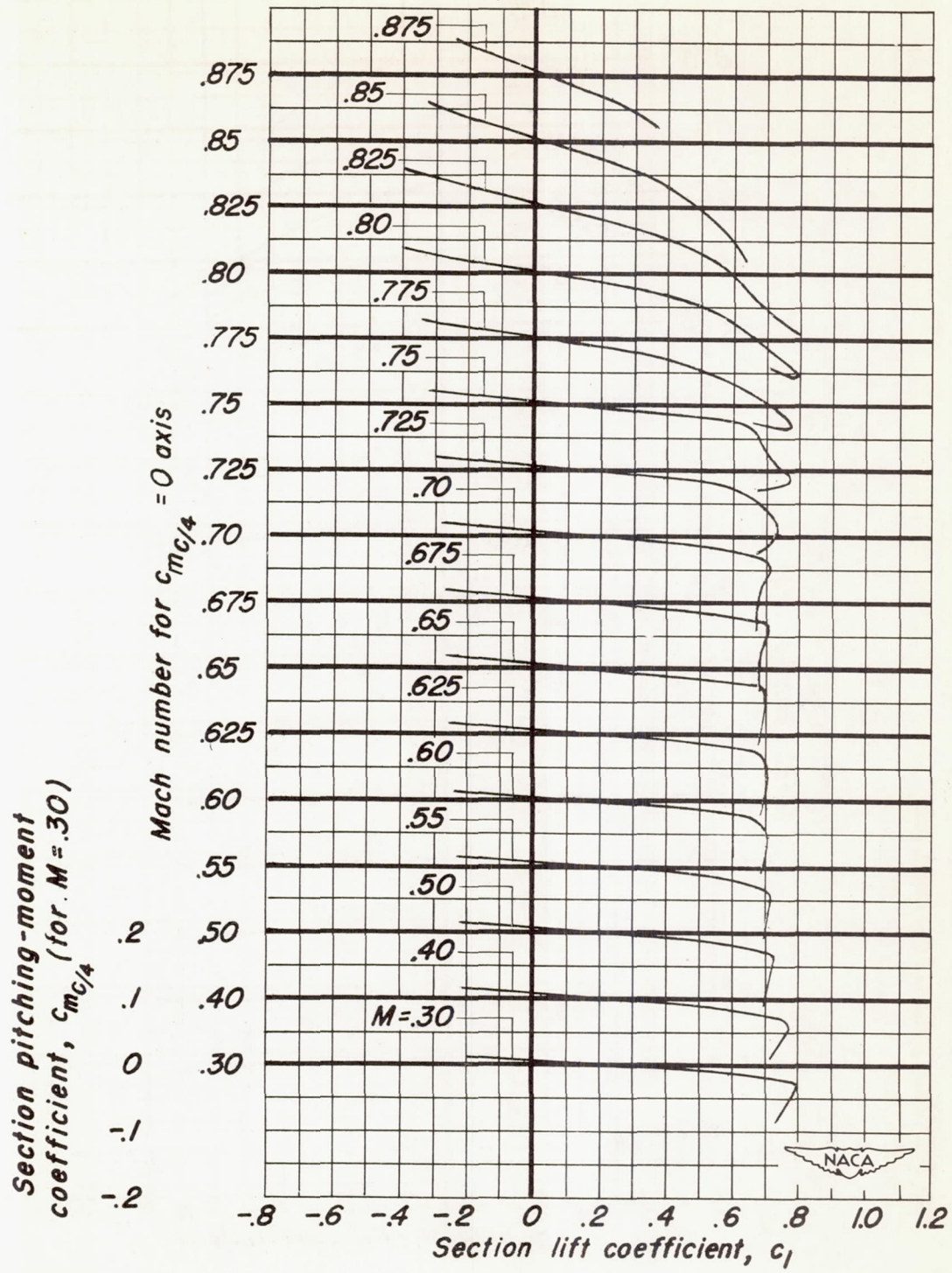

(b) NACA 0010-1.10 40/1.051 airfoil section.

Figure 13.- Continued.

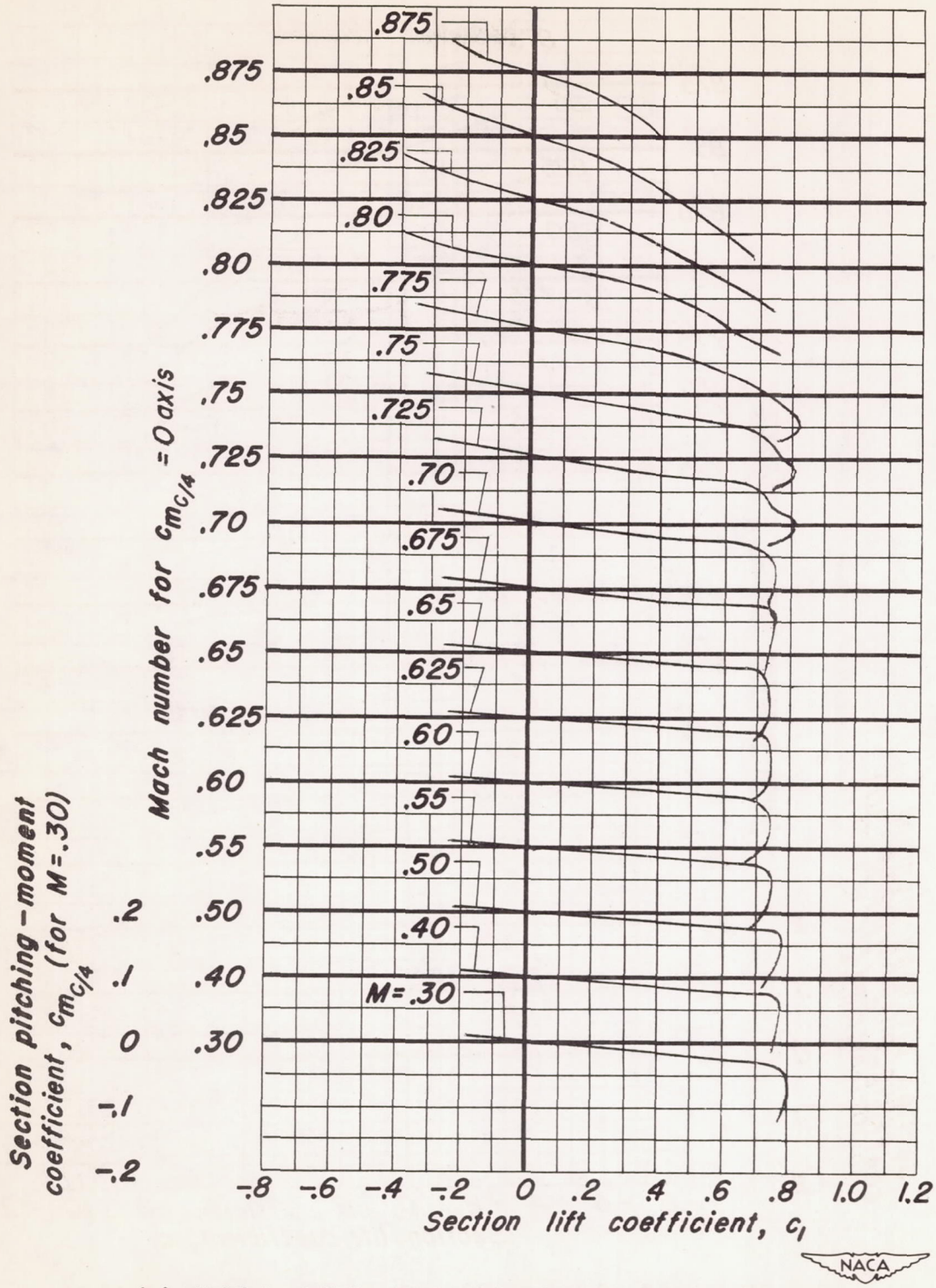

(c) NACA 0010-1.10 40/0.524 airfoil section.

Figure 13.–Continued.

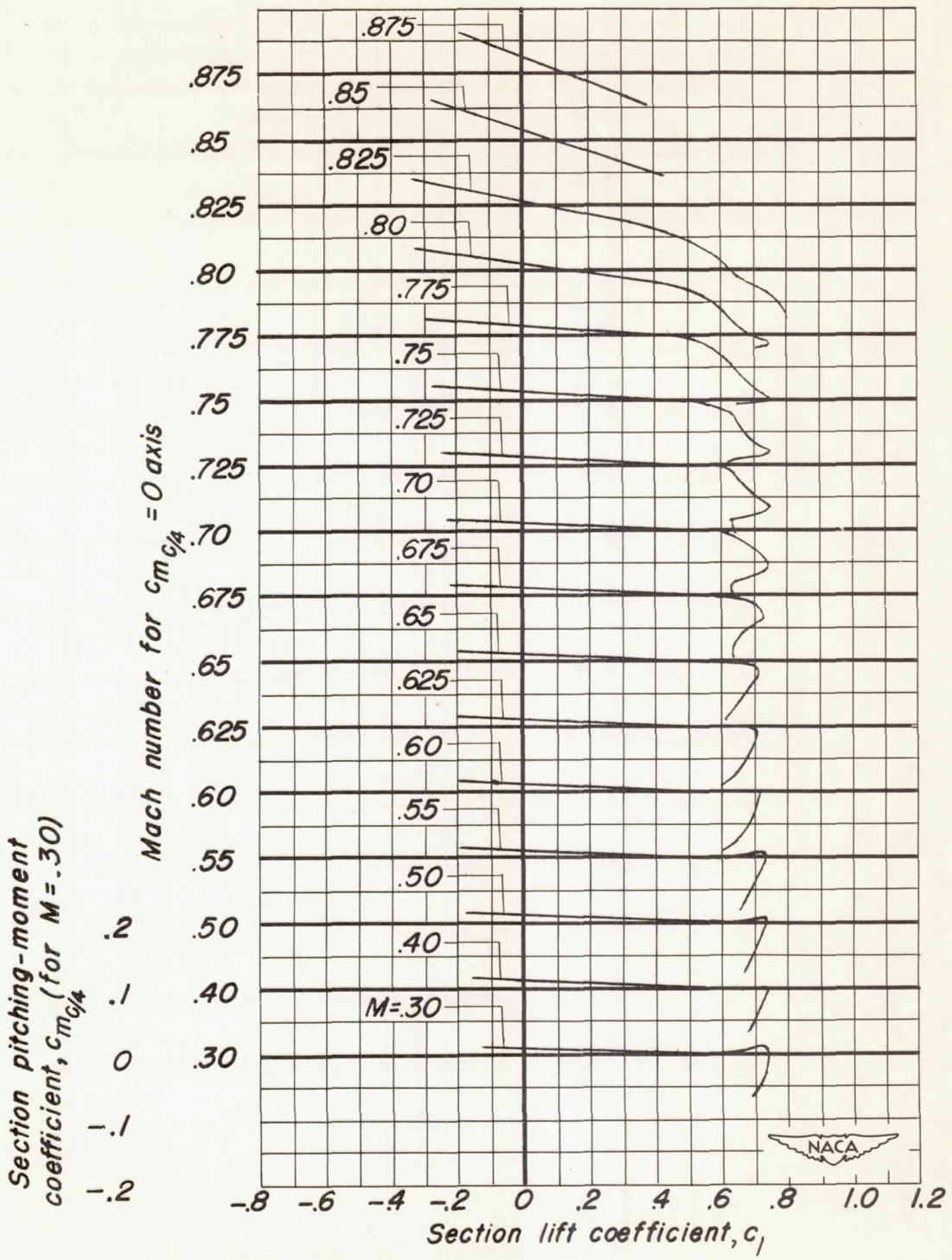

(d) NACA 0010-0.70 40/1.575 airfoil section.

Figure 13.- Continued.

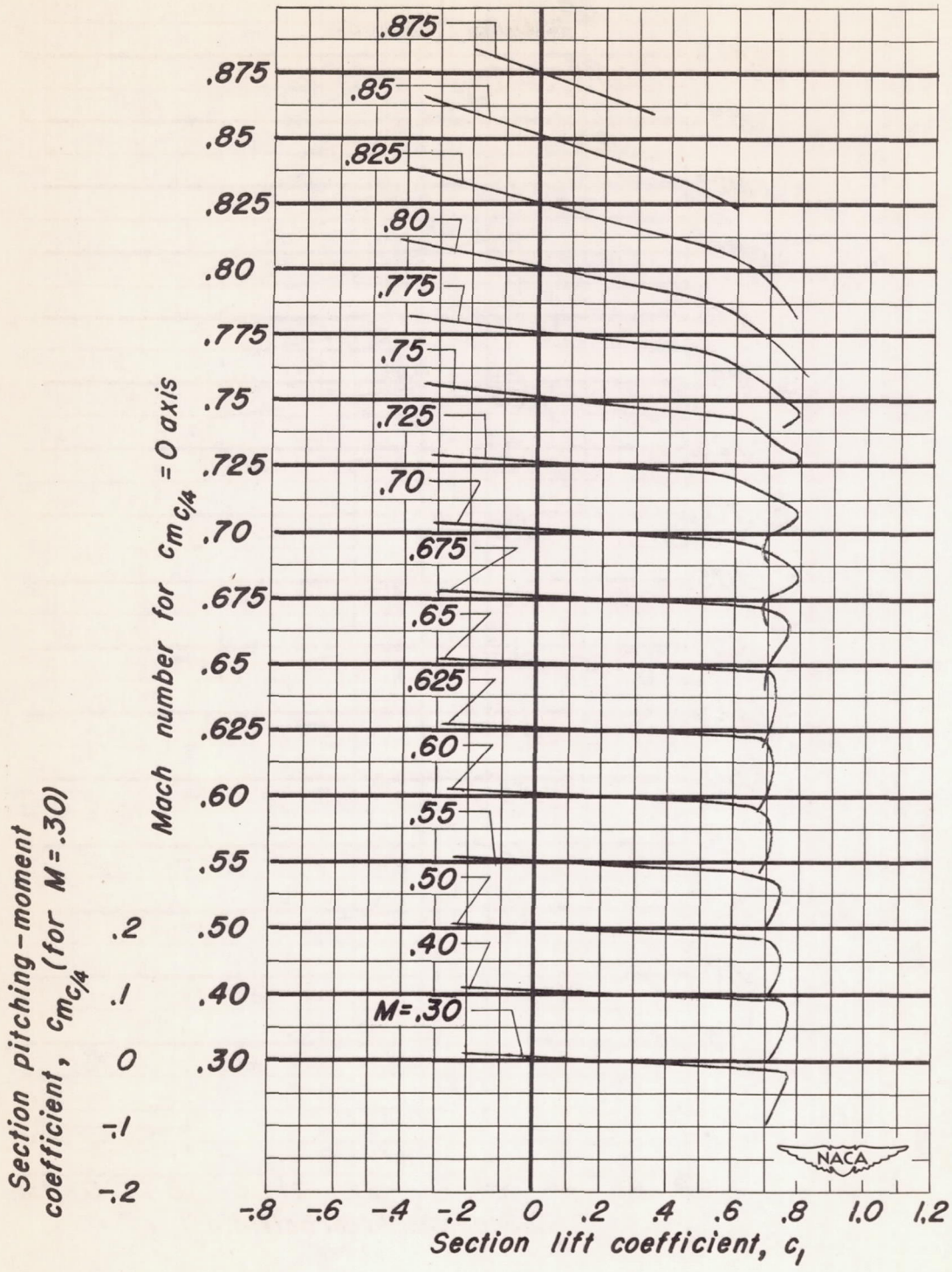

(e) NACA 0010-0.70 40/1.051 airfoil section.

Figure 13.-Continued.

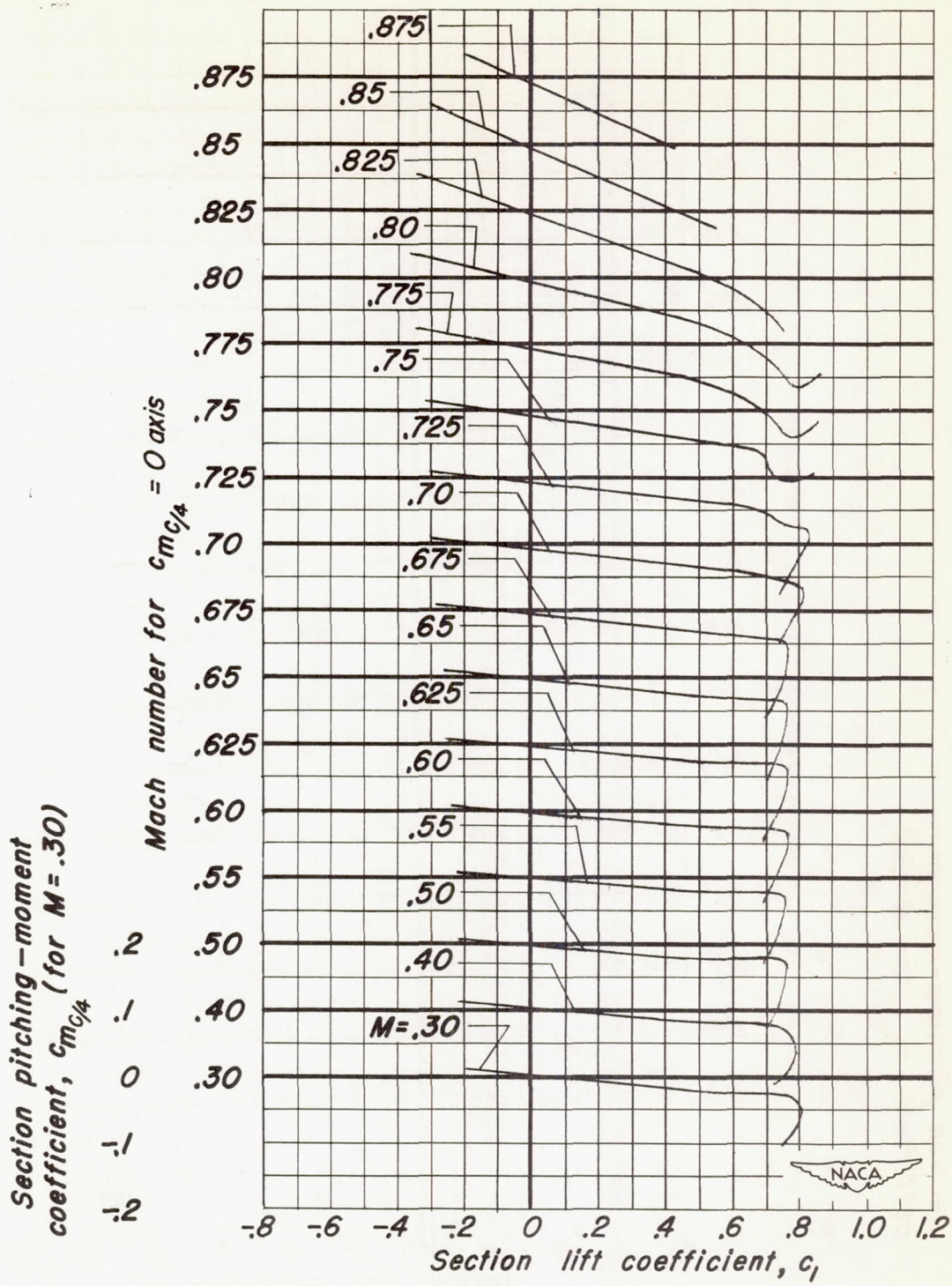

(f) NACA 0010-0.70 40/0.524 airfoil section.

Figure 13.- Continued.

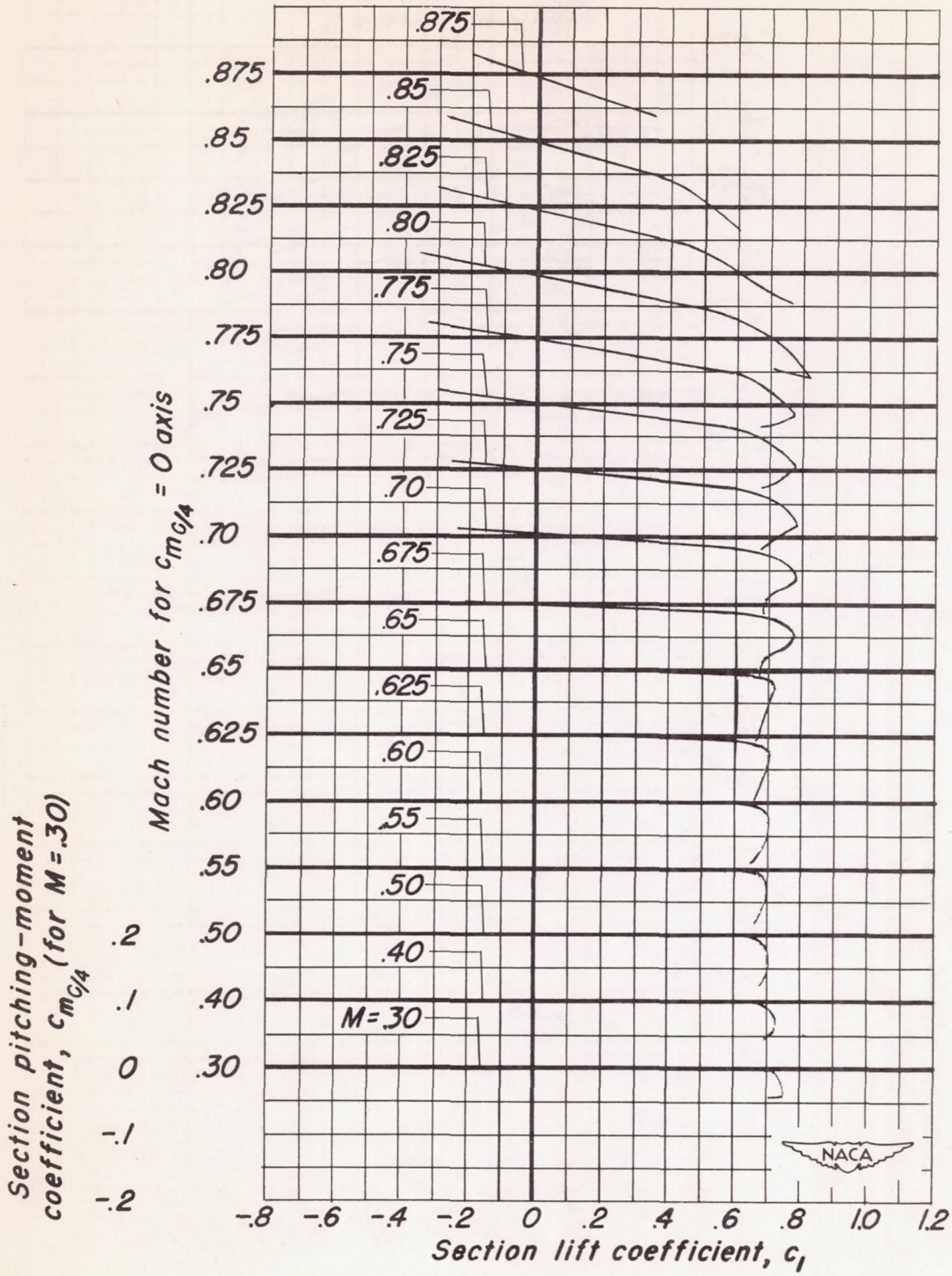

(g) NACA 0010-0.27 40/1.575 airfoil section.

Figure 13.- Continued.

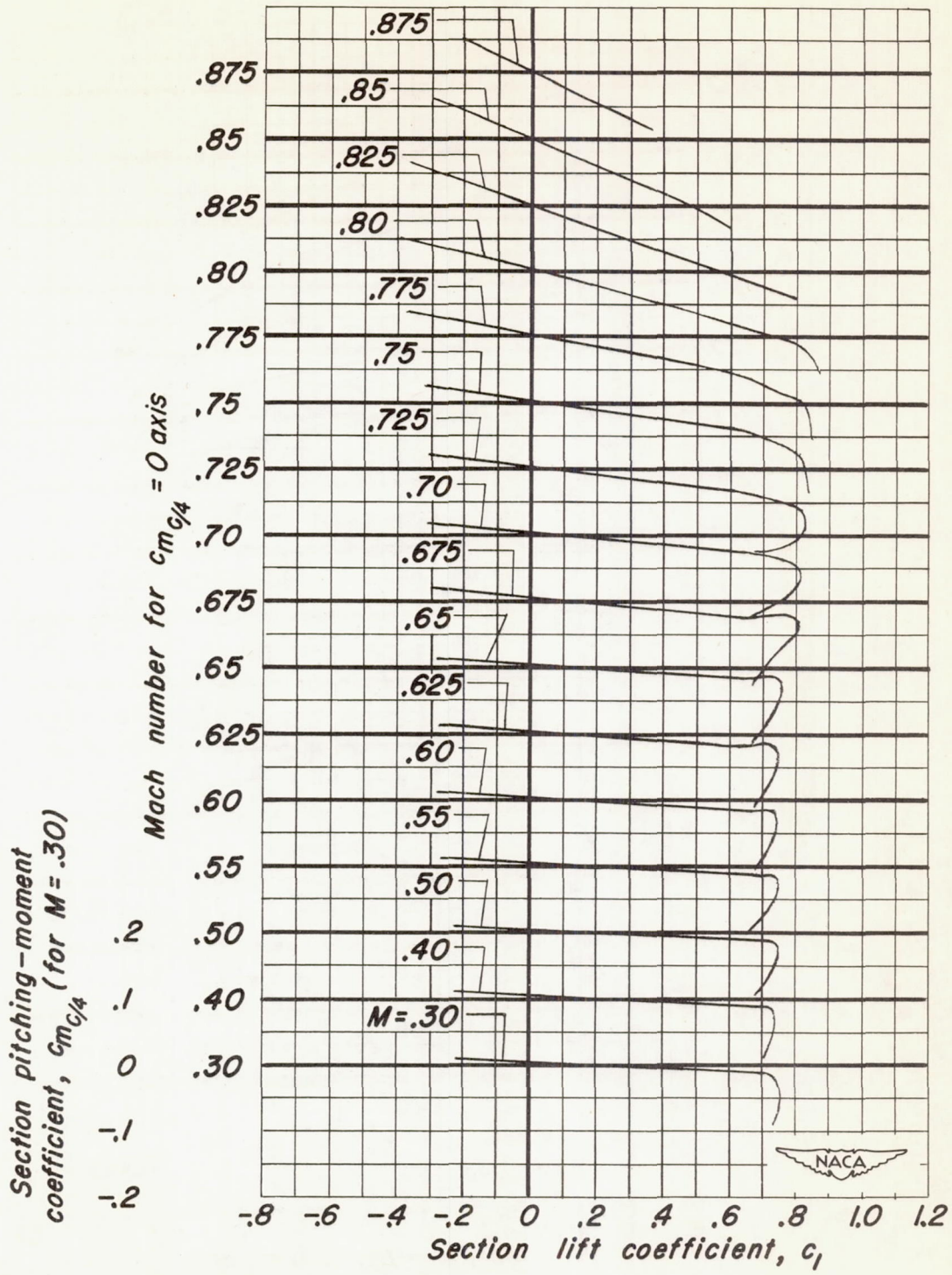

(h) NACA 0010-0.27 40/1.051 airfoil section.

Figure 13.- Continued.

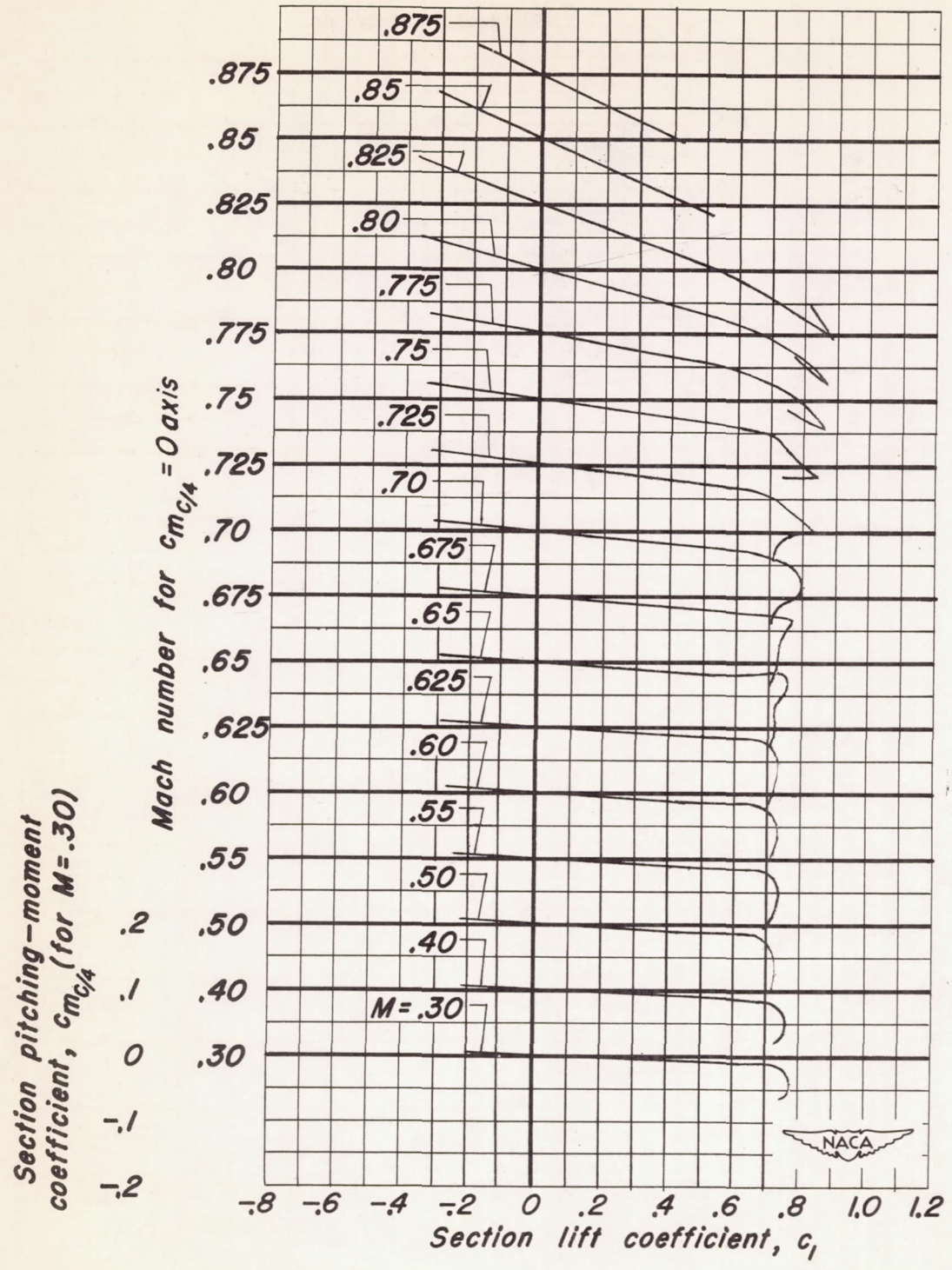

(i) NACA 0010-0.27 40/0.524 airfoil section.

Figure 13.-Concluded.